

HEAT TRANSFER AND PRESSURE DROP FOR FLOW OF
CARBOXYMETHYLCELLULOSE (CMC) SOLUTIONS
ACROSS IDEAL TUBE BANKS

By

DON ADAMS

Bachelor of Science
Oklahoma State University
Stillwater, Oklahoma
1962

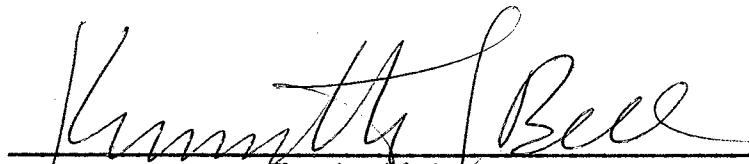
Master of Science
Oklahoma State University
Stillwater, Oklahoma
1964

Submitted to the faculty of the Graduate College
of the Oklahoma State University
in partial fulfillment of the requirements
for the degree of
DOCTOR OF PHILOSOPHY
May, 1968

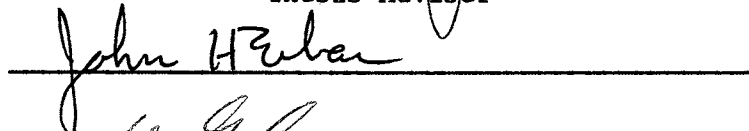
OCT 24 1968

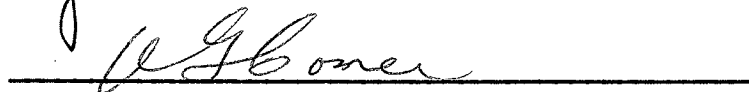
HEAT TRANSFER AND PRESSURE DROP FOR FLOW OF
CARBOXYMETHYLCELLULOSE (CMC) SOLUTIONS
ACROSS IDEAL TUBE BANKS


Thesis Approved:




Thesis Adviser









Dean of the Graduate College

688175

PREFACE

A significant number of chemical plants producing polymers have been built in recent years. The expansion of the existing polymer plants and the construction of new polymer plants are expected in the future. Many of these polymer melts and solutions of these polymers exhibit non-Newtonian fluid behavior. Heat transfer data and pressure drop data for the flow of non-Newtonian fluids across tube banks are needed for the development of more economical and reliable design procedures for heat exchange equipment.

In order to develop heat transfer coefficient and friction factor correlations, heat transfer and pressure drop data for flow of non-Newtonian solutions across three tube banks were obtained. The experimental equipment, experimental procedures, and the results obtained from reduction and correlation of the data are discussed in this dissertation.

I received aid from a number of individuals during the course of this project. Dr. Kenneth J. Bell was very helpful in the formulation and execution of the research program. Messrs. Gene E. McCroskey, Preston Wilson, and Arlin Harris gave many useful suggestions and much aid in the construction of the experimental equipment. Mr. Donald Randolph gave suggestions and experimental assistance relative to the rheological behavior of the non-Newtonian fluid used. I also wish to thank Mr. Kohei Ishihara who assisted me in the construction of the

experimental apparatus and in obtaining the experimental data. I wish to also express my gratitude to my patient wife, Barbara, who typed this dissertation and gave me encouragement.

I am indebted to the Federal Department of Health, Education, and Welfare, the National Science Foundation, Phillips Petroleum Company, and the National Aeronautics and Space Administration for financial assistance during the course of this research project. The Office of Engineering Research of Oklahoma State University and Monsanto Company provided funds for purchasing the experimental equipment. The sodium carboxymethylcellulose powder was provided by Hercules Powder Company through Drilling Specialties, Inc. of Bartlesville, Oklahoma.

TABLE OF CONTENTS

Chapter	Page
I. INTRODUCTION.	1
II. FLUID BEHAVIOR CLASSIFICATION	3
Newtonian Fluids	3
Non-Newtonian Fluids	3
Time-Independent Non-Newtonian Fluids	5
Bingham Plastic.	5
Pseudoplastic.	5
Dilatant Fluid	6
Time-Dependent Non-Newtonian Fluids	6
Viscoelastic Fluids	6
III. LITERATURE SURVEY	8
Newtonian Fluid Flow Across Ideal Tube Banks	8
Non-Newtonian Fluid Pressure Drop and Heat Transfer.	15
IV. THEORETICAL CONSIDERATIONS AND DEVELOPMENT OF CORRELATION PARAMETERS.	20
Theoretical Considerations	20
Pressure Drop	20
Heat Transfer	23
Development of Correlation Parameters.	24
V. EXPERIMENTAL APPARATUS.	28
Tube Banks	28
Tube Bank Headers.	40
Carboxymethylcellulose Solution Flow Equipment	41
Water System Flow Equipment.	44
Temperature Measurement Apparatus.	45
Pressure Drop Measuring Apparatus.	49
Solution Preparation Materials and Equipment	50
Other Equipment.	51
VI. EXPERIMENTAL PROCEDURE.	52
Thermocouple Calibration	52

Chapter	Page
Solution Preparation	53
Flow Rate Determinations	54
CMC Solution Flow Rates	54
Water Flow Rates.	55
Isothermal Pressure Drop Run Procedure	55
High Temperature Isothermal Pressure Drop Run Procedure.	55
Ambient Temperature Isothermal Pressure Drop Run Procedure.	56
Heat Transfer Run Procedure.	57
Heating Run Start-Up Procedure.	58
Cooling Run Start-Up Procedure.	59
Viscometer Operation Procedure	60
Viscometer Spring Calibration Procedure	60
CMC Solution Analysis Procedure	61
VII. PRESENTATION AND DISCUSSION OF RESULTS.	62
VIII. CONCLUSIONS AND RECOMMENDATIONS	77
Conclusions.	77
Recommendations.	77
BIBLIOGRAPHY	79
APPENDIX A. NOMENCLATURE.	82
APPENDIX B. DATA REDUCTION PROCEDURE.	88
APPENDIX C. THERMOCOUPLE CALIBRATION RESULTS.	100
APPENDIX D. RAW DATA FROM HEAT TRANSFER RUNS.	105
APPENDIX E. CALCULATED RESULTS FOR HEAT TRANSFER RUNS	121
APPENDIX F. RAW DATA AND CALCULATED RESULTS FOR ISOTHERMAL PRESSURE DROP RUNS.	154
APPENDIX G. RHEOLOGICAL PROPERTIES CALCULATED FROM FANN VISCOMETER DATA	178
APPENDIX H. COMPUTER PROGRAMS FOR REDUCTION OF HEAT TRANSFER, PRESSURE DROP, AND FANN VISCOMETER DATA	191

LIST OF TABLES

Table	Page
I. Tube Bank Dimensions and Constants.	39
II. Regression Analysis Summary for Log j Versus Log Re	71
III. Regression Analysis Summary for Log f Versus Log Re	72
IV. Regression Analysis Summary for j Versus $Re^{-0.667}$	73
V. Regression Analysis Summary for f Versus $Re^{-1.0}$	74
VI. Sample Fann Viscometer Raw Data and Calculated Rheological Properties.	92
VII. Heat Transfer Run Thermocouple Data	107
VIII. Heat Transfer Run Flow Rate and Manometer Data.	114
IX. Calculated Temperature Data for Heat Transfer Runs.	122
X. Calculated Heat Transfer Coefficients and Pressure Drop for Heat Transfer Runs.	129
XI. Rheological Properties and Reynolds Numbers for Heat Transfer Runs	134
XII. Sieder-Tate Nonisothermal Correction Factors for Heat Transfer Runs	141
XIII. Calculated Dimensionless Groups for Heat Transfer Runs. . .	148
XIV. Raw Data From Isothermal Pressure Drop Runs	155
XV. Calculated Data From Isothermal Pressure Drop Runs.	162
XVI. Rheological Properties for Isothermal Pressure Drop Runs.	168
XVII. Friction Factors and Reynolds Numbers for Isothermal Pressure Drop Runs.	174
XVIII. CMC Solutions' Rheological Properties From Fann Viscometer Data	179

Table

Page

XIX. Regression Coefficients for Calculating Gamma and N Prime as a Function of Temperature.	188
---	-----

LIST OF FIGURES

Figure	Page
1. Shear Diagram for Time-Independent Fluids	4
2. Flow Diagram.	29
3. Test Section Diagram.	30
4. Photograph of Test Section Without Insulation	31
5. Photograph of Test Section With Insulation.	32
6. Tube Bank Model Number 1.	33
7. Tube Bank Model Number 2.	34
8. Tube Bank Model Number 3.	35
9. Tube Bank Model Number 1 Photograph	36
10. Tube Bank Model Number 2 Photograph	37
11. Tube Bank Model Number 3 Photograph	38
12. Tube Bank Shell Side Header Drawing	42
13. Tube Bank Tube Side Header Drawing.	43
14. Drawing of Mixing Orifices.	46
15. Mixing Block Drawing.	47
16. Mixing Block Photograph	48
17. j-Factor Vs. Reynolds Number--Model No. 1	63
18. Friction Factor Vs. Reynolds Number--Model No. 1.	64
19. j-Factor Vs. Reynolds Number--Model No. 2	65
20. Friction Factor Vs. Reynolds Number--Model No. 2.	66
21. j-Factor Vs. Reynolds Number--Model No. 3	67
22. Friction Factor Vs. Reynolds Number--Model No. 3.	68

CHAPTER I

INTRODUCTION

The construction of new plants and expansion of existing plants producing polymers is expected in the future. Non-Newtonian fluid behavior is exhibited by many of the polymer melts and polymer solutions. Shell and tube heat exchangers and pumping equipment constitute a significant portion of the investment for these chemical plants. Development of a reliable means of predicting non-Newtonian fluid shell side heat transfer coefficients and friction factors can decrease the investment and operating expense for the chemical plants producing polymers. A step in the direction of more reliable shell side heat transfer coefficients and friction factors is the accurate determination of heat transfer coefficients and friction factors for flow across ideal tube banks.

The variables affecting the shell side heat transfer coefficient and pressure drop may be divided into two groups, primary and secondary, as follows:

I. Primary Variables

1. Fluid flow rate and physical properties
2. Tube layout configuration
3. Transverse and longitudinal tube spacing
4. Tube diameter
5. Number of tube rows

6. Exchanger length

- II. Secondary Variables

1. Baffle shape, size, and spacing
2. Tube-to-shell clearance leakage
3. Tube-to-baffle clearance leakage
4. Baffle-to-shell clearance leakage

This research project has involved an investigation of the effect of the first two primary variables.

The following goals were set for this project:

1. Construct and operate experimental equipment to obtain heat transfer coefficients and friction factor data for flow of non-Newtonian fluids across three tube banks.
2. Obtain rheological data for the non-Newtonian fluids used in the experimental runs.
3. Using the above data, develop heat transfer coefficient and friction factor correlations as a function of the tube bank geometry, fluid physical and rheological properties, and fluid flow rate.

CHAPTER II

FLUID BEHAVIOR CLASSIFICATION

Newtonian Fluids

The flow behavior of a Newtonian fluid obeys the following equation:

$$\tau = \frac{\mu}{g_c} \frac{du}{dy} \quad (2-1)$$

The proportionality constant, μ , is known as the viscosity and is dependent upon the temperature, pressure, and the fluid under consideration. The velocity gradient, du/dy , is called the shear rate; and τ is called the shear stress. The viscosity of a Newtonian fluid is not a function of the shear rate. The shear stress--shear rate behavior of a Newtonian fluid is presented in Figure 1.

Non-Newtonian Fluids

A non-Newtonian fluid is a fluid whose flow behavior does not obey Equation 1. There are three broad classes of non-Newtonian fluids (31). These classes are as follows:

1. Time-independent
2. Time-dependent
3. Viscoelastic

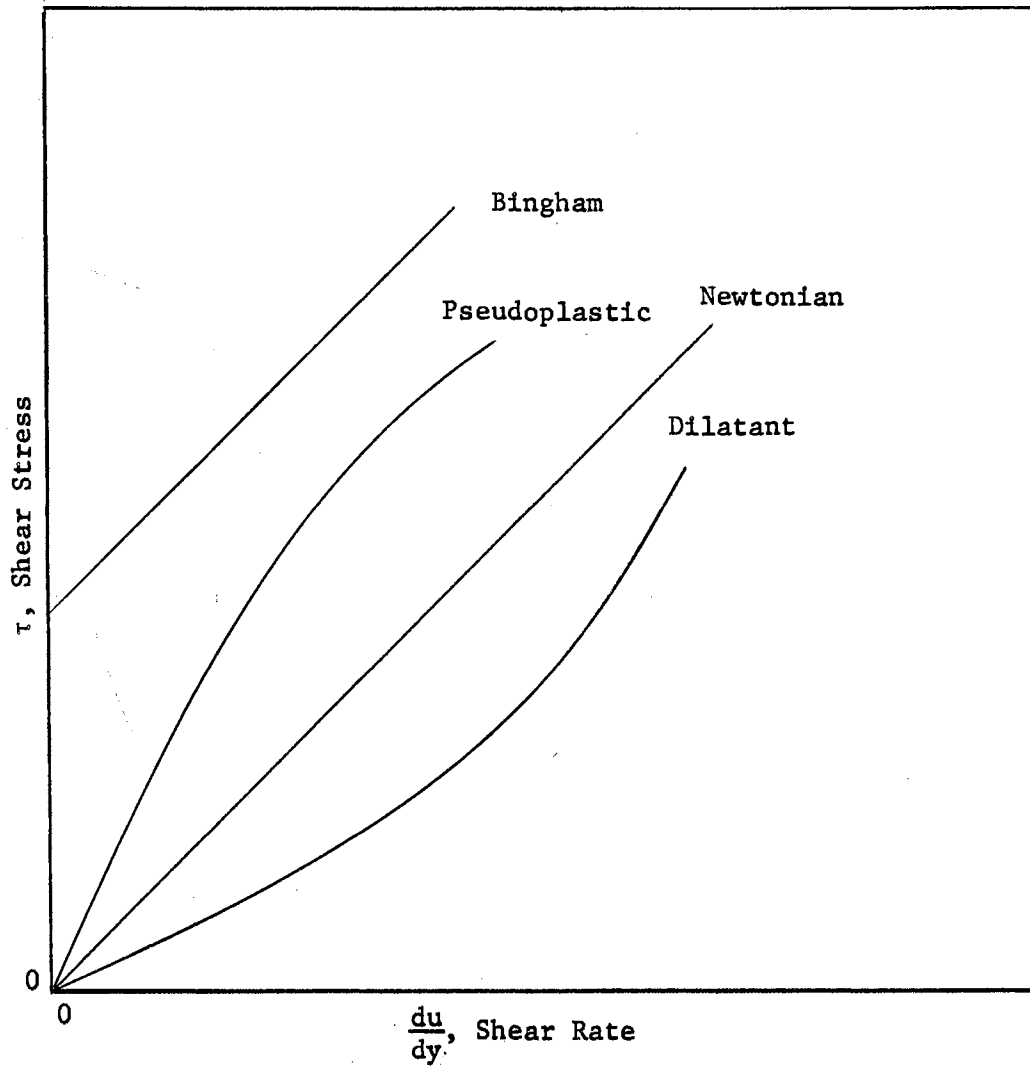


Figure 1. Shear Diagram for Time-Independent Fluids

Time-Independent Non-Newtonian Fluids

The shear stress for these fluids does not depend upon the duration of the shear. These fluids are usually divided into the following three groups:

1. Bingham plastic fluids
2. Pseudoplastic fluids (shear-thinning)
3. Dilatant fluids (shear-thickening)

The shear curve for each of these three types of time-independent non-Newtonian fluids is illustrated in Figure 1.

Bingham Plastic. The Bingham plastic fluid has a linear shear curve; however, an initial shear stress must be exerted on the fluid to make it flow (see Figure 1). This type of fluid behavior is characterized by the following equation (31):

$$\tau - \tau_0 = \mu_B \left(\frac{du}{dy} \right) . \quad (2-2)$$

Some fluids exhibiting this behavior are drilling muds, chalk suspensions, toothpaste, and slurries (31).

Pseudoplastic. The shear stress-shear rate curve for this type of fluid passes through the origin, and its slope decreases with increasing shear rate (see Figure 1). One of the most common behavior models for pseudoplastic fluids is the power law model or Ostwald-de Waele model (31),

$$\tau = K \left(\frac{du}{dy} \right)^n . \quad (2-3)$$

The constant, n , is an indication of the amount of deviation from Newtonian behavior; and K is a measure of the consistency of the fluid.

The constant, n , equals 1.0 for a Newtonian fluid and is less than 1.0 for a pseudoplastic fluid. Some fluids having pseudoplastic behavior are napalm, mayonnaise, and drilling muds (31).

Dilatant Fluid. The shear stress-shear rate curve for this fluid passes through the origin, and its slope increases with increasing shear rate (see Figure 1). Equation 3 is often used to represent the flow behavior of this type of fluid; however, the constant, n , is greater than 1.0 for the dilatant fluid. Some polymer solutions, quicksand, and starch suspensions exhibit this type of flow behavior (31).

Time-Dependent Non-Newtonian Fluids

The apparent viscosity, the ratio of shear stress to shear rate, for time-dependent non-Newtonian fluids depends upon the length of time that the shear has been applied. These fluids are divided into two groups, thixotropic and rheopectic. The thixotropic fluid apparent viscosity decreases with the time of shear, whereas the rheopectic fluid apparent viscosity increases with the time of shear (31).

Viscoelastic Fluids

These fluids exhibit both viscous and elastic properties (31). The energy applied to such a fluid is stored as potential energy in addition to being dissipated as heat by the viscous forces. Equations to describe the behavior of such a fluid should be a combination of Newton's viscosity law for fluids and Hooke's law for elastic materials (31).

It is quite possible that a particular fluid will not fall into a

particular classification for all shear rates and durations of shear. The shear stress-shear rate curve of a fluid may become linear at high shear rates, or the behavior may be time-dependent for a short period of time after application of shear and become time-independent after the shear has been applied for a significant length of time.

More detailed discussions of fluid behavior classification, reasons for types of fluid behavior, and models proposed to describe the types of fluid behavior have been presented by Metzner (19) and Wilkinson (31).

CHAPTER III

LITERATURE SURVEY

No significant heat transfer or pressure drop results for flow of non-Newtonian fluids across tube banks have been published. This chapter will be mostly devoted to the discussion of publications giving results for the following areas of research:

1. Pressure drop and heat transfer for the flow of Newtonian fluids across ideal tube banks.
2. Pressure drop and heat transfer for non-Newtonian fluids flowing inside pipes or tubes.

Publications in these areas of research have provided background material for the development of heat transfer and pressure drop correlations for the flow of non-Newtonian fluids across tube banks. Several publications containing theoretical developments will be discussed in Chapter IV devoted to theoretical considerations.

Newtonian Fluid Flow Across Ideal Tube Banks

In 1933, Chilton and Genereaux (9) attempted to put the meager pressure drop data available at that time covering a few tube spacing arrangements on a basis applicable to design. They proposed the following friction factor correlations:

$$f = \frac{2 \rho g_c \Delta P}{4 G_m^2 N} = 0.264 \left(\frac{D_c G_m}{\mu} \right)^{-0.2} \quad (\text{turbulent flow-in line}) \quad (3-1)$$

$$f = \frac{2 \rho g_c \Delta P}{4 G_m^2 N} = 0.57 \left(\frac{D_c G_m}{\mu} \right)^{-0.2} \quad (\text{turbulent flow-staggered}) \quad (3-2)$$

$$f = \frac{2 \rho g_c \Delta P D_v}{4 G_m^2 L} = 13.2 \left(\frac{D_c G_m}{\mu} \right)^{-1.00} \quad (\text{laminar flow-staggered}) \quad (3-3)$$

No correlation was presented for laminar flow with in-line tube arrangements due to the absence of necessary data. The properties are evaluated at film temperatures given by

$$t_f = t_{AV} - 0.32 \Delta T \quad (\text{laminar flow}) \quad (3-4)$$

$$t_f = t_{AV} \quad (\text{turbulent flow})$$

where

t_{AV} = average bulk temperature

ΔT = logarithmic mean temperature difference between the stream and the tube wall

Pierson (24) obtained convection heat transfer and pressure drop data for the flow of gases across banks of electrically heated tubes. Thirty-eight tube arrangements, including both in-line and staggered tube layouts, were investigated to determine the effect of varying the spacing of tubes of the same size. The heat transfer and pressure drop results are presented in plots of Nusselt number and friction factor versus Reynolds number where

$$Nu = \frac{h_o D_o}{k} \quad (3-5)$$

$$f = \frac{2 g_c \rho \Delta P}{4 N G_m^2} \quad (3-6)$$

$$Re = \frac{D_o G_m}{\mu} \quad (3-7)$$

The Reynolds number range was from 2,000 to 40,000. It was concluded that the spacing of tubes has a significant effect on heat transfer and pressure drop.

Huge (17) presented experimental results to determine the effect of tube size on the heat transfer coefficient and pressure drop for both in-line and staggered tube arrangements. Condensing steam and water passed through the tubes; air flowed across the tubes. The Nusselt number was found to be proportional to the 0.61 power of the Reynolds number. The Reynolds number range was from 2,000 to 70,000. The results are presented in plots of Nusselt number and friction factor versus Reynolds number as defined in Equations 3-1, 3-2, and 3-3. The results are consistent with results obtained by Pierson (24) confirming the validity of the principle of similarity relative to the tube diameter for tube banks.

Grimison (14) carried out an analytical study of the results reported by Huge (17) and Pierson (24) to develop heat transfer coefficient and friction factor correlations suitable for commercial use. Grimison (14) presents graphical correlations of friction factor as a function of Reynolds number, ratio of transverse tube spacing to the tube diameter, and the ratio of longitudinal tube spacing to the tube diameter. The heat transfer coefficient correlation obtained is

$$h_o = 0.284 F_a \left(\frac{D_o G_m}{\mu} \right)^{0.61} \left(\frac{k}{D_o} \right) \quad (3-4)$$

where F_a is an arrangement factor depending upon the tube arrangement, tube spacings, and the Reynolds number.

Gunter and Shaw (15) made an analytical study of friction factor results, both isothermal and non-isothermal presented by Huge (17),

Pierson (24), and others. The purpose of this study was to develop a single correlation for design purposes applicable to all tube layout configurations and spacings. These authors propose the use of volumetric hydraulic diameter, D_v , instead of the tube diameter, D_o . The following correlations are proposed for the laminar and turbulent flow regions, respectively:

$$\frac{f}{2} = \frac{\Delta P G_c D_v \rho}{G_m^2 L} \left(\frac{\mu}{\mu_w}\right)^{0.14} \left(\frac{D_v}{S_T}\right)^{-0.4} \left(\frac{S_L}{S_T}\right)^{-0.6} = 90 \left(\frac{D_v G_m}{\mu}\right)^{-1.0} \quad (3-5)$$

$$\frac{f}{2} = \frac{\Delta P G_c D_v \rho}{G^2 L} \left(\frac{\mu}{\mu_w}\right)^{0.14} \left(\frac{D_v}{S_T}\right)^{-0.4} \left(\frac{S_L}{S_T}\right)^{-0.6} = 0.96 \left(\frac{D_v G_m}{\mu}\right)^{-0.145} \quad (3-6)$$

The transition from laminar to turbulent flow occurs at a Reynolds number of about 200. The range of variables covered by the data used in this study were:

D_o	0.02 to 2 inches
Re	0.01 to 300,000
μ/μ_w	0.015 to 8
S_T/D_v	1.25 to 5
S_L/D_v	1.25 to 5

In 1948, Boucher and Lapple (8) published an excellent critical comparison of the data and proposed correlations for pressure drop of Newtonian fluids flowing across tube banks. They pointed out that the difference between the various proposed correlations was in the definition of the characteristic tube bank dimensions and in the methods of allowing for variations in the tube spacing and tube layout configuration. Only pressure drop data that were essentially isothermal

were considered. The authors recommended the correlations presented by Grimison (14) and Chilton-Genereaux (9) for turbulent and laminar flow, respectively. Boucher and Lapple (8) were somewhat critical of the correlation proposed by Gunter and Shaw (15); and they point out that no equivalent diameter should be expected to correlate data from geometrically different tube banks onto a single curve, because hydrodynamic similarity requires geometrical similarity.

A research program to develop design methods for the shell side of shell and tube heat exchangers was initiated at the University of Delaware in 1946. The first phase of the program involved a study of ideal tube bank heat transfer and pressure drop characteristics followed by a study of non-ideal flow conditions such as bypassing and non-uniform tube layout configuration. The second phase of the program was concerned with baffled exchangers. Numerous theses, dissertations, and publications have resulted from the University of Delaware project. Four of these publications most pertinent to the subject of this dissertation will be discussed.

Bergelin, Davis, and Hull (6) obtained heat transfer data, isothermal pressure drop data, and non-isothermal pressure drop data to compare three tube layout arrangements (staggered square, in-line square, and equilateral triangle. The tube diameter for each tube bank was 3/8 inch, and the pitch-to-diameter ratio was 1.25. Water flowed through the tubes, while a viscous oil flowed across the tubes. The results are reported as j -factors and friction factors versus Reynolds number where

$$j = \frac{h}{C_p G_m} \left(\frac{C_p \mu}{k} \right)^{2/3} \left(\frac{\mu_s}{\mu} \right)^{0.14} \quad (3-7)$$

$$f = \frac{2 g_c \Delta P \rho D_V}{4 G_m^2 L} \left(\frac{\mu}{\mu_s} \right)^{0.56-0.16 Re} \quad (3-8)$$

$$Re = \frac{D_V G_m}{\mu} \quad (3-9)$$

The Reynolds numbers corresponded to the laminar and early transition flow regimes. The effectiveness was represented by plotting heat transfer coefficient versus the power loss per unit heat transfer area. The staggered square and equilateral triangle arrangements are approximately equal in effectiveness, whereas the in-line square arrangement has a lower degree of effectiveness for laminar flow. The performance of the in-line arrangement approaches that of the staggered arrangements in the transition and early turbulent flow regions. Transition was observed to begin at a Reynolds number of about 100.

Bergelin, Brown, Hull, and Sullivan (4) extended the work of Bergelin, Davis, and Hull (6) to four additional tube banks to study the effect of tube size and tube spacing on performance. The results are presented in plots of friction factor and j-factor versus the Reynolds number based on the equivalent hydraulic diameter. The friction factor used in these plots is

$$f = \frac{2 \Delta P \rho g_c}{4 G_m^2 N} \left(\frac{\mu}{\mu_w} \right)^{0.57 Re^{-0.25}} \quad (3-10)$$

where the viscosity correction exponent is for $1 \leq Re \leq 300$. The friction factor results for the in-line tube banks were in good agreement with the correlation proposed by Gunter and Shaw (15); however, the staggered square tube bank friction factors were consistently above the Gunter and Shaw curve. The large tube pressure drop and

heat transfer results agreed well with the small tube diameter results for both in-line and staggered-square tube arrangements. The tube banks having the smallest tube diameter and the smallest pitch gave the best performance.

Bergelin, Brown, and Doberstein (3) extended the University of Delaware (2, 4, 5, 6) work with ideal tube banks to the transition zone. Results for heating, cooling, and isothermal tests covering a Reynolds number range of 25 to 10,000 were presented. Five ideal tube banks with 3/8-inch diameter tubes were used. The results were presented in plots of j factor and friction factor versus the Reynolds number based on the outside tube diameter where

$$j = \frac{h}{C_p G_m} \left(\frac{C_p \mu}{k} \right)^{2/3} \left(\frac{\mu_w}{\mu} \right)^{0.14} \quad (3-11)$$

$$f = \frac{2 \Delta P \rho g_c}{4 G_m^2 N} \left(\frac{\mu}{\mu_w} \right)^{0.14} \quad (3-12)$$

$$Re = \frac{D_o G_m}{\mu} \quad (3-13)$$

The transition zone Reynolds numbers ranged from 200 to 5,000 depending upon the tube bank model under consideration. The transition from laminar to turbulent flow was smooth for staggered tube arrangements; however, the transition for in-line tube arrangements produced a discontinuity in both the j -factor and friction factor curves similar to the behavior existing for flow inside pipes. This difference in transition behavior was attributed to a difference in the mechanisms of turbulence formation. The performances of the staggered tube arrangements based on the heat transfer coefficient for a given power loss were superior to the performances of the in-line arrangements in the

transition zone; however, the superiority decreased as the turbulence increased.

Bergelin, Colburn, and Hull (5) developed a laminar flow region friction factor correlation from the isothermal pressure drop data for seven tube banks.

$$f \left(\frac{P}{D_o} \right)^{1.6} = \frac{2 \Delta P g_c \rho}{4 G_m^2 N} \left(\frac{P}{D_o} \right)^{1.6} = 70 \left(\frac{D_v G_m}{\mu} \right)^{-1.0} \quad (3-14)$$

The correlation given in Equation 3-14 was proposed for Reynolds numbers below 50. Above a Reynolds number of 50, the friction factor-Reynolds number data give four separate curves.

Non-Newtonian Fluid Pressure Drop and Heat Transfer

Metzner and Reed (21) have presented a generalized Reynolds number to be applied to non-Newtonian fluids. The Metzner and Reed (21) Reynolds number development was based on the following shear rate expression derived by Rabinowitsch (25) in 1929 and by Mooney (23) in 1931 for laminar flow in a tube:

$$\left(\frac{du}{dy} \right)_w = 3 \left(\frac{8Q}{\pi D^3} \right) + \frac{D \Delta P}{4L} \frac{d (8Q/\pi D^3)}{d (D \Delta P/4L)} \quad (3-15)$$

Equation 3-15 applies only to time-independent fluids and is independent of fluid properties. Metzner and Reed (21) substituted $v = 4Q/\pi D^2$ and rearranged Equation 3-15 to obtain

$$\left(\frac{du}{dy} \right)_w = \frac{3}{4} \left(\frac{8v}{D} \right) + \frac{1}{4} \left(\frac{8v}{D} \right) \frac{d \ln (8v/D)}{d \ln (D \Delta P/4L)} \quad (3-16)$$

Metzner and Reed (21) then made the following substitution:

$$\frac{1}{n'} = \frac{d \ln (8v/D)}{d \ln (D \Delta P/4L)} \quad (3-17)$$

where n' may be found from the slope of a plot of $\ln (8v/D)$ against $\ln (D \Delta P/4L)$. Substitution of Equation 3-17 into Equation 3-16 and rearrangement gave

$$\left(\frac{du}{dy}\right)_w = \frac{3n' + 1}{4n'} \left(\frac{8v}{D}\right) \quad (3-18)$$

Equation 3-18 is applicable to all time-independent fluids and requires no slip at the tube wall and negligible viscoelastic effects. Integration of Equation 3-18 for constant n' gave

$$\frac{D \Delta P}{4L} = K' \left(\frac{8v}{D}\right)^{n'} \quad (3-19)$$

The constants K' and n' have been found to be constant over a wide range of the quantity $8v/D$ (21). Substitution of the result of Equation 3-19 into the following friction factor equation:

$$f = \frac{\left(\frac{D \Delta P}{4L}\right)}{\left(\frac{\rho v^2}{2 g_c}\right)} \quad (3-20)$$

yielded

$$f = \frac{16 \gamma}{D^{n'} v^{2-n'} \rho} \quad (3-21)$$

where

$$\gamma = g_c 8^{n'-1} K' \quad (3-22)$$

Letting $f = 16/Re$ gave the following generalized Reynolds number:

$$Re = \frac{D^{n'} v^{2-n'} \rho}{\gamma} \quad (3-23)$$

Metzner and Reed (21) found that the Reynolds number defined in Equation 3-23 was quite satisfactory for correlating the friction factor in the laminar, transition, and turbulent flow regions.

Metzner, Vaughn, and Houghton (22) presented theoretical analyses combined with an experimental study of the variables determining the heat transfer coefficient for laminar flow of non-Newtonian fluids in pipes. The theoretical analyses involved a study of limiting cases such as "infinite pseudoplasticity" ($n' = 0$) and "infinite dilatancy" ($n' = \infty$). Theoretical equations were developed for the limiting cases; and methods of interpolation were developed to extend the derived equations to cases of intermediate degrees of non-Newtonian behavior. The experimental data were obtained for the following three non-Newtonian fluids: (1) 1.75 percent solution of Carbopol in water, (2) 3.72 percent solution of sodium carboxymethylcellulose (CMC) in water, and (3) 1.40 percent CMC solution. The value of n' for these solutions ranged from 0.18 to 0.70. For correlations of the heat transfer data, the following generalized dimensionless groups were developed:

$$\text{Prandtl Number} = \text{Pr} = \frac{C_p \gamma}{k} \left(\frac{V}{D}\right)^{n'-1} \quad (3-24)$$

$$\text{Nusselt Number} = \text{Nu} = \frac{hD}{k \Delta^{1/3}} \quad (3-25)$$

$$\text{Stanton Number} = \text{St} = \frac{h}{C_p G \Delta^{1/3}} \quad (3-26)$$

$$\text{Sieder-Tate Factor} = \frac{\gamma_w}{\gamma} \quad (3-27)$$

The heat transfer results are presented in plots of j factor versus the Reed-Metzner Reynolds number where

$$j = \frac{h}{C_p G \Delta^{1/3}} \left[\frac{C_p \gamma}{k} \left(\frac{V}{D} \right)^{n'-1} \right]^{2/3} \left(\frac{\gamma_w}{\gamma} \right)^{0.14} \quad (3-28)$$

$$Re = \frac{D_o^{n'} V^{2-n'} \rho}{\gamma} \quad (3-29)$$

$$\Delta^{1/3} = \frac{\text{Non-Newtonian Fluid Nusselt Number}}{\text{Newtonian Fluid Nusselt Number}} = \left(\frac{3n' + 1}{4n'} \right)^{1/3} \quad (3-30)$$

The quantity Δ represents the ratio of the wall shear rate for non-Newtonian flow to the wall shear rate for Newtonian flow. The following equation was also presented to correlate the heat transfer data:

$$\frac{hD}{k \Delta^{1/3}} = 1.75 \left(\frac{W C_p}{kL} \right)^{1/3} \left(\frac{\gamma}{\gamma_w} \right)^{0.14} \quad (3-31)$$

Heat capacities, thermal conductivities, and densities of the solutions were determined. The heat capacities and densities of the solutions were found to be essentially equal to the heat capacity and density of water. The measured thermal conductivities were as much as 25 percent below the thermal conductivity of water.

Christiansen and Craig (10) used a temperature dependent equation to represent the rheological properties of pseudoplastic fluids. The temperature-dependent rheological equation was used to obtain numerical solutions to the energy flow equation for laminar flow in a pipe having constant wall temperature. Experimental heat transfer coefficients were obtained and compared with the predicted computed coefficients. Good agreement between the experimental and computed heat transfer coefficients was observed.

Shah, Peterson, and Acrivos (27) obtained analytical solutions

and experimental data for heat transfer from a single cylinder to a power law non-Newtonian fluid. The purpose of the work was to determine the feasibility of application of rheological equations of state derived from viscometer data to predict the fluid behavior in laminar boundary-layer flows. The predicted Nusselt numbers were in good agreement with the experimentally determined Nusselt numbers for solutions of sodium carboxymethylcellulose (CMC) in water. The CMC solutions were tested for viscoelastic effects; no viscoelastic effects were observed.

Cruzan (12) obtained isothermal pressure drop data for flow of 1 percent aqueous solutions of sodium carboxymethylcellulose (CMC) across two tube banks having four tube rows and eight tube rows, respectively. The tube layout configuration was a staggered square with a pitch ratio of 1.5 for both tube banks. The experimental runs covered a modified Reed-Metzner Reynolds number range of 14 to 272 where

$$Re = \frac{D_o^{n'} V_m^{2-n'} \rho}{\gamma} \quad (3-32)$$

The results were presented in plots of friction factor versus Reynolds number where

$$f = \frac{2 \Delta P g_c \rho}{4 G_m^2 N} \quad (3-33)$$

The non-Newtonian fluid friction factors determined by Cruzan (12) were in fair agreement with Newtonian fluid friction factors reported by others for the same Reynolds number range. Cruzan (12) also presented equations for obtaining the non-Newtonian fluid rheological constants, K' and n' , from rotational viscometer raw data.

CHAPTER IV

THEORETICAL CONSIDERATIONS AND DEVELOPMENT OF CORRELATION PARAMETERS

Theoretical Considerations

Pressure Drop

The development of theoretical methods of predicting pressure drop for flow in conduits or around objects involves simultaneous solution of the Navier-Stokes equations and the continuity equation. Analytical solutions have been developed for a number of flow situations such as isothermal laminar flow in smooth tubes. Three theoretical methods having limited applicability have been developed to predict the pressure drop for isothermal, steady, incompressible, laminar flow of Newtonian fluids across tube banks. The methods are limited to Stokes or "creeping flow" where the inertial effects are negligible compared to the viscous effects. Elimination of the terms allowing for inertial effects in the Navier-Stokes equations yields

$$\nabla^2 P = 0 \quad (4-1)$$

after some manipulation. Equation 4-1 is applicable up to a Reynolds number on the order of 1 to 10; however, the tube bank boundary conditions for P , the pressure, are not known.

Tamada and Fujikawa (29) have solved Oseen's linearized equations

of motion for the steady, isothermal, incompressible, laminar flow of a Newtonian fluid past an infinite row of equal, regularly spaced, circular cylinders lying in a plane perpendicular to the uniform stream. The solution leads to the following observations:

1. At a fixed velocity, the drag on a cylinder in the infinite row is greater than the drag on the same cylinder when alone in a uniform flow.
2. As the Reynolds number decreases, the drag on the cylinder in the infinite row deviates more from the drag for a single cylinder.
3. The drag is proportional to the velocity at low Reynolds numbers.

The solution is limited to a single row of cylinders because it does not allow for the interaction between transverse rows.

Happel (16) used an "equivalent free surface" model to solve the Navier-Stokes equations for steady incompressible creeping flow past arrays of cylinders. The assumption of creeping flow and use of the stream function defined by

$$v_r = \frac{1}{r} \frac{\partial \psi}{\partial \theta} \quad (4-2)$$

$$v_\theta = - \frac{\partial \psi}{\partial r} \quad (4-3)$$

reduced the Navier-Stokes equations for laminar flow to the biharmonic equation

$$\nabla^4 \psi = 0 \quad (4-4)$$

Assumption of a cylinder surrounded by a unit cell of fluid permits

the establishment of boundary conditions for solution of Equation 4-4. The solution of Equation 4-4 gave values of the Darcy constant, K^* , to be used in the Darcy pressure drop equation,

$$U = - \frac{K^*}{\mu} \frac{dP}{dx} \quad (4-5)$$

The proposed model required a uniform flow pattern around the tubes; therefore, the solution is most applicable to equilateral triangle arrangements. The predicted pressure drops are in good agreement with the pressure drops reported by Bergelin, Brown, Hull, and Sullivan (4) for $Re \leq 5$. Substantial deviations between the predicted and reported pressure drops did not occur until Reynolds numbers over 100 were reached. Differences between the predicted and reported pressure drops were significant for tube arrangements other than equilateral triangle, particularly for the staggered square tube arrangement.

Freidl and Bell (13) used an electrical analog technique to develop analytical solutions for the pressure drop during steady, incompressible, creeping flow across a tube bank. The basic assumption was that the isobars for creeping flow are collinear with the isopotential lines for potential flow in the same geometry. The isopotential lines were found by laying out the tube bank array on conducting paper and applying a voltage difference. The isopotential field was divided into an arbitrary number of flow elements bounded by solid surfaces and two arbitrarily spaced isopotential lines. The pressure drop for each flow element was computed using the solution developed by Graetz for laminar flow through rectangular conduits. The total pressure drop was then found by integrating the pressure gradients for the flow elements along a streamline through the entire

tube bank. Three tube arrays (in-line square, staggered square, and equilateral triangle) were investigated. Friction factors calculated using the proposed method were compared with the friction factors reported by Bergelin, Colburn, and Hull (5). The calculated friction factors were 2 to 14 percent less than the reported experimental friction factors.

Heat Transfer

The development of theoretical methods to predict heat transfer coefficients involves simultaneous solution of (1) the Fourier-Poisson differential equation for heat conduction in a moving fluid, (2) the Navier-Stokes hydrodynamic equations, and (3) the continuity equation. The above equations are so complex that theoretical solutions have been limited to simple geometries and have required simplifying assumptions such as unidirectional flow, potential flow, constant viscosity, or negligible inertial effects. The flow of both Newtonian and non-Newtonian fluids across tube banks is a flow situation much too complex for development of theoretical solutions predicting heat transfer coefficients. The complexity of the tube bank flow situation greatly increases in going from Newtonian fluids to non-Newtonian fluids. The continuous expansion and contraction of the cross-sectional flow area produce varying shear rates which cause the non-Newtonian fluid "viscosity" to change with position in the tube bank. The work by Shah, Petersen, and Acrivos (27) for heat transfer from a single cylinder to a power law non-Newtonian fluid represents the most significant theoretical contribution toward developing theoretical methods of predicting heat transfer coefficients for flow of non-Newtonian

fluids across tube banks. The single cylinder results are not applicable to tube banks of practical interest due to the interaction between tubes. The Nusselt number equation development by Shah, Petersen, and Acrivos (27) was quite complex even though the single cylinder represented a relatively simple geometry.

As a result of the analytical solution difficulties, it is necessary to resort to empirical methods to develop satisfactory heat transfer coefficient and pressure drop relationships for flow of non-Newtonian fluids across tube banks.

Development of Correlation Parameters

The development of empirical relationships for heat transfer coefficients and pressure drop involves establishment of dimensionless groups based on the principle of hydrodynamic similarity. The condition of hydrodynamic similarity is not met by different tube layouts; however, groups based on the principle of similarity have been used with significant success (2, 3, 4, 5, 6) when hydrodynamic similarity does exist.

Comparison of the dimensionless groups proposed by Metzner, Vaughn, and Houghton (22) and the groups developed from the University of Delaware work (2) yields dimensionless groups for application to non-Newtonian fluid flow across tube banks.

Metzner, Vaughn, and Houghton (22) have used the following dimensionless groups to correlate heat transfer data for the flow of non-Newtonian fluids inside tubes:

$$\text{Reynolds Number} = \text{Re} = \frac{D^{n'} V^{2-n'} \rho}{\gamma} \quad (4-6)$$

$$\text{Prandtl Number} = \text{Pr} = \frac{C_p \gamma}{k} \left(\frac{V}{D}\right)^{n'-1} \quad (4-7)$$

$$\text{Stanton Number} = \text{St} = \frac{h_i}{C_p G \Delta^{1/3}} \quad (4-8)$$

$$\text{Nusselt Number} = \text{Nu} = \frac{h_i D}{k} \quad (4-9)$$

$$\text{Sieder-Tate Factor} = \left(\frac{\gamma_w}{\gamma}\right)^{0.14} \quad (4-10)$$

$$j = (\text{St}) (\text{Pr})^{2/3} \left(\frac{\gamma_w}{\gamma}\right)^{0.14} \quad (4-11)$$

The dimensionless groups resulting from the University of Delaware work for flow of Newtonian fluids across tube banks are (2):

$$\text{Re} = \frac{D_o V_m \rho}{\mu} \quad (4-12)$$

$$\text{Pr} = \frac{C_p \mu}{k} \quad (4-13)$$

$$\text{St} = \frac{h_o}{C_p G_m} \quad (4-14)$$

$$\text{Sieder-Tate Factor} = \left(\frac{\mu_w}{\mu}\right)^{0.14} \quad (4-15)$$

$$j = (\text{St}) (\text{Pr})^{2/3} \left(\frac{\mu_w}{\mu}\right)^{0.14} \quad (4-16)$$

$$f = \frac{2 \Delta P g_c \rho}{4 G_m^2 N} \left(\frac{\mu}{\mu_w}\right)^{0.14} \quad (4-17)$$

Comparison of the Reynolds numbers defined in Equations 4-6 and 4-12 yields the following modified Reynolds number for non-Newtonian

flow across tube banks:

$$Re = \frac{D_o^{n'} V_m^{2-n'} \rho}{\gamma} \quad (4-18)$$

Using a procedure similar to that used by Metzner, Vaughn, and Houghton (22), one can derive a Prandtl number for application to non-Newtonian flow across a tube bank.

$$\frac{D_o^{n'} V_m^{2-n'} \rho}{\gamma} = \frac{D_o V_m \rho}{\mu_A} \quad (4-19)$$

$$\mu_A = \gamma \left(\frac{V_m}{D_o} \right)^{n'-1} \quad (4-20)$$

$$Pr = \frac{C_p \mu_A}{k} = \frac{C_p \gamma}{k} \left(\frac{V_m}{D_o} \right)^{n'-1} \quad (4-21)$$

Comparison of Equations 4-8 and 4-14 and Equations 4-10 and 4-15 yields

$$St = \frac{h_o}{C_p G_m \Delta^{1/3}} \quad (4-22)$$

$$\text{Sieder-Tate Factor} = \left(\frac{\gamma_w}{\gamma} \right)^{0.14} \quad (4-23)$$

The friction factor and j-factor based on the derived dimensionless groups for flow of non-Newtonian fluids across tube banks are:

$$f = \frac{2 \Delta P g_c \rho}{4 G_m^2 N} \left(\frac{\gamma}{\gamma_w} \right)^{0.14} \quad (4-24)$$

$$j = \frac{h_o}{C_p G_m \Delta^{1/3}} \left[\frac{C_p \gamma}{k} \left(\frac{V_m}{D_o} \right)^{n'-1} \right]^{2/3} \left(\frac{\gamma_w}{\gamma} \right)^{0.14} \quad (4-25)$$

The proposed Reynolds number, j-factor, and friction factor given in Equations 4-18, 4-24, and 4-25 for non-Newtonian fluid flow across tube banks will reduce to the Reynolds number, j-factor, and friction factor commonly used for Newtonian fluid flow across tube banks when $n' = 1.0$.

CHAPTER V

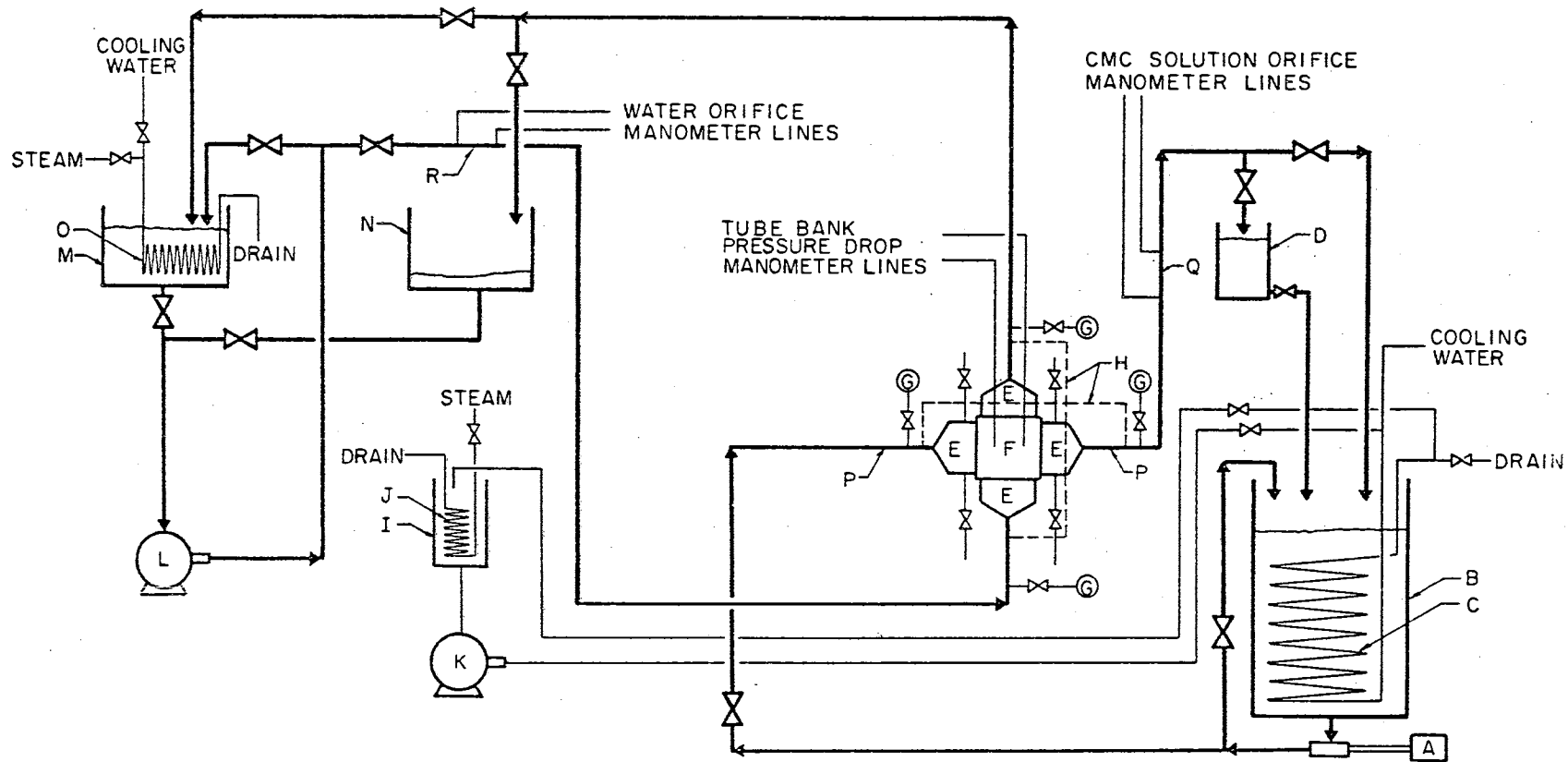
EXPERIMENTAL APPARATUS

The sodium carboxymethylcellulose (CMC) solution was pumped from a holding barrel into a 1 1/2 inch schedule 40 pipe where it flowed through mixing orifices and a mixing block, then through the tube bank, more mixing orifices, another mixing block, an orifice plate, and back into the holding barrel. The water which flowed inside the tubes of the tube bank was pumped from the water storage tank into a 1 1/2 inch schedule 40 pipe where it flowed through an orifice plate, the tube bank, and back into the storage tank. The holding barrel and water storage tank were equipped with coils for heating and cooling the CMC solution and the water. A flow diagram and a diagram of the test section are presented in Figures 2 and 3. Photographs of the test section are presented in Figures 4 and 5.

Tube Banks

Three tube banks having different tube layout arrangements (staggered square, in-line square, and equilateral triangle) were used. Drawings and photographs of the tube banks are presented in Figures 6 through 11. The tube bank dimensions and constants are presented in Table I.

Each tube bank model was designed to represent the center of a baffle section of a shell and tube heat exchanger. Each tube bank



- | | | |
|------------------------------------|-------------------------------|--------------------------------------|
| A - CMC SOLUTION PUMP | G - PRESSURE GAUGE | M - WATER STORAGE TANK |
| B - CMC SOLUTION HOLDING TANK | H - DIFFERENTIAL THERMOCOUPLE | N - WATER FLOW RATE TANK |
| C - CMC SOLUTION HOLDING TANK COIL | I - HOT WATER TANK | O - WATER STORAGE TANK COIL |
| D - CMC SOLUTION FLOW RATE TANK | J - HOT WATER TANK COIL | P - MIXING ORIFICES AND MIXING BLOCK |
| E - TUBE BANK HEADER | K - HOT WATER PUMP | Q - CMC SOLUTION FLOW RATE ORIFICE |
| F - TUBE BANK | L - WATER PUMP | R - WATER FLOW RATE ORIFICE |

Figure 2. Flow Diagram

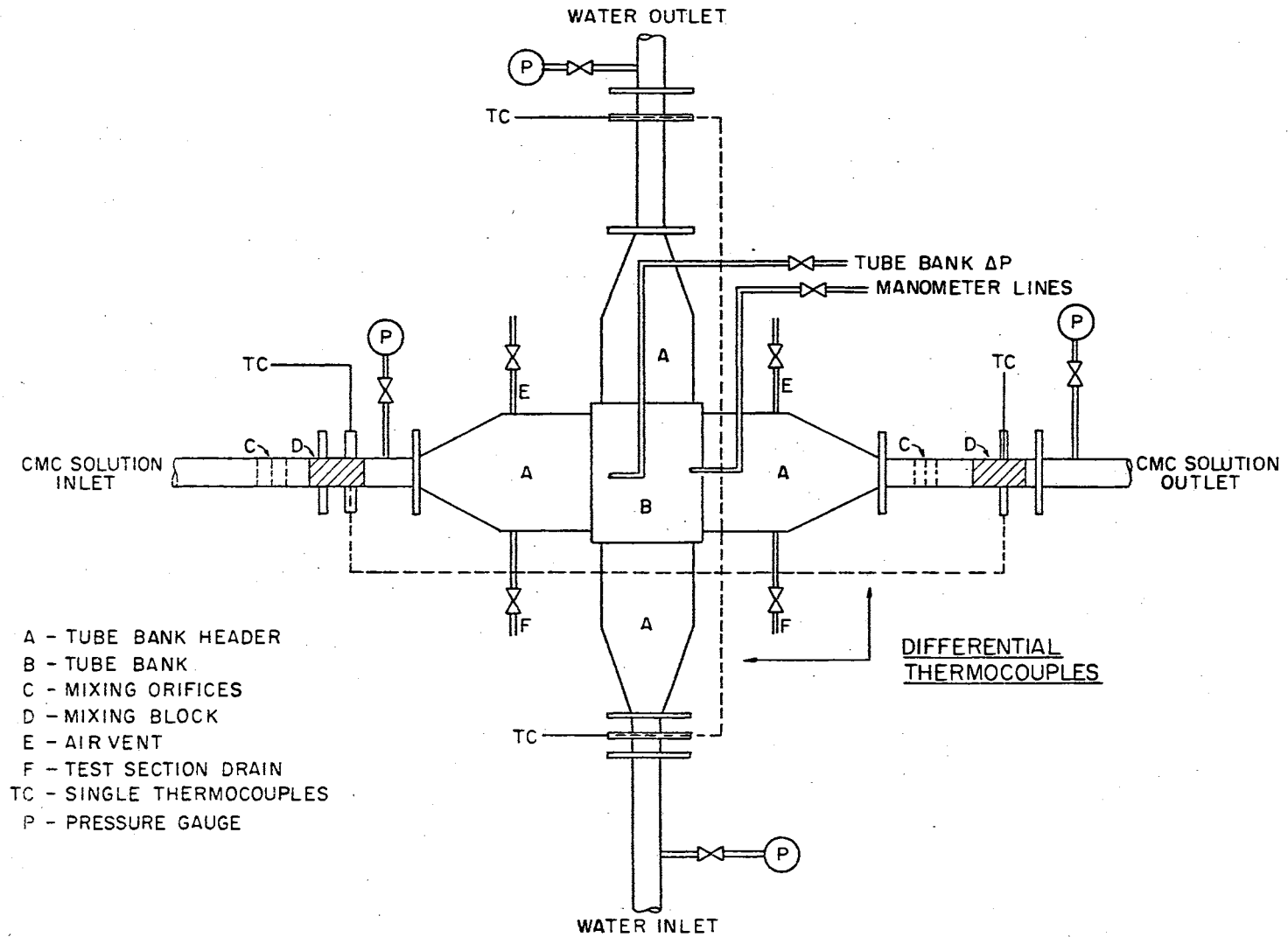


Figure 3. Test Section Diagram

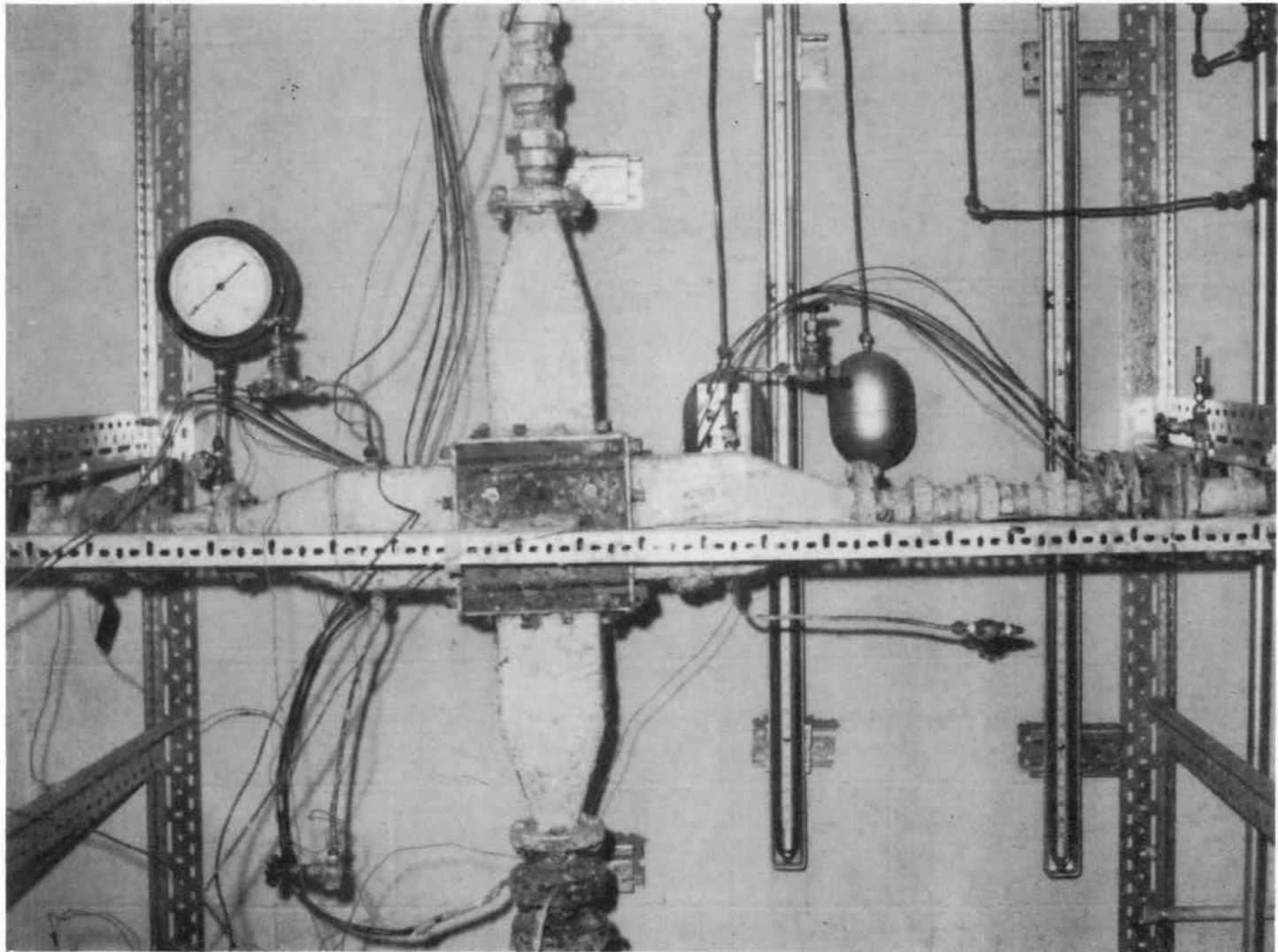


Figure 4. Photograph of Test Section Without Insulation

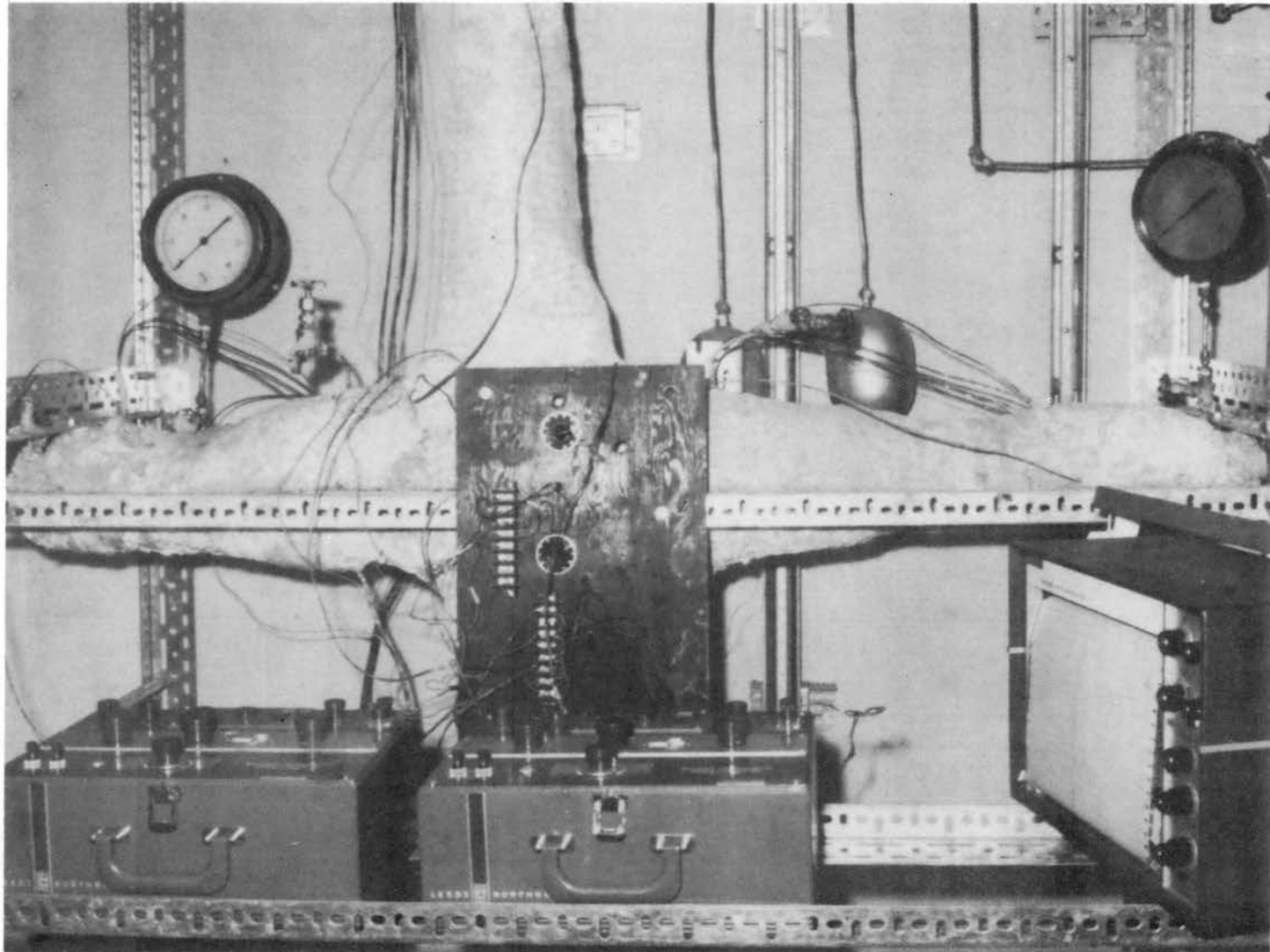


Figure 5. Photograph of Test Section With Insulation

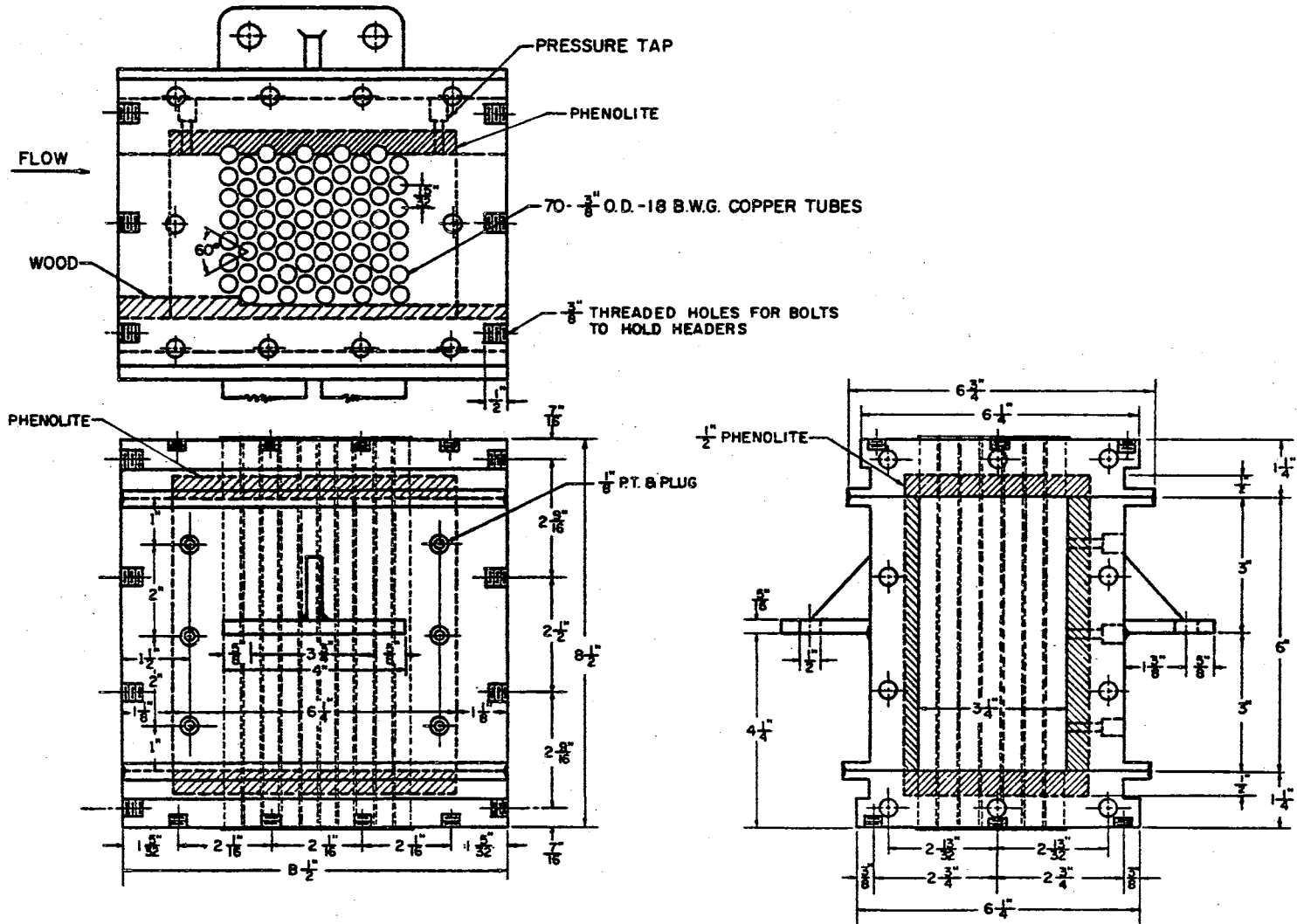


Figure 6. Tube Bank Model Number 1

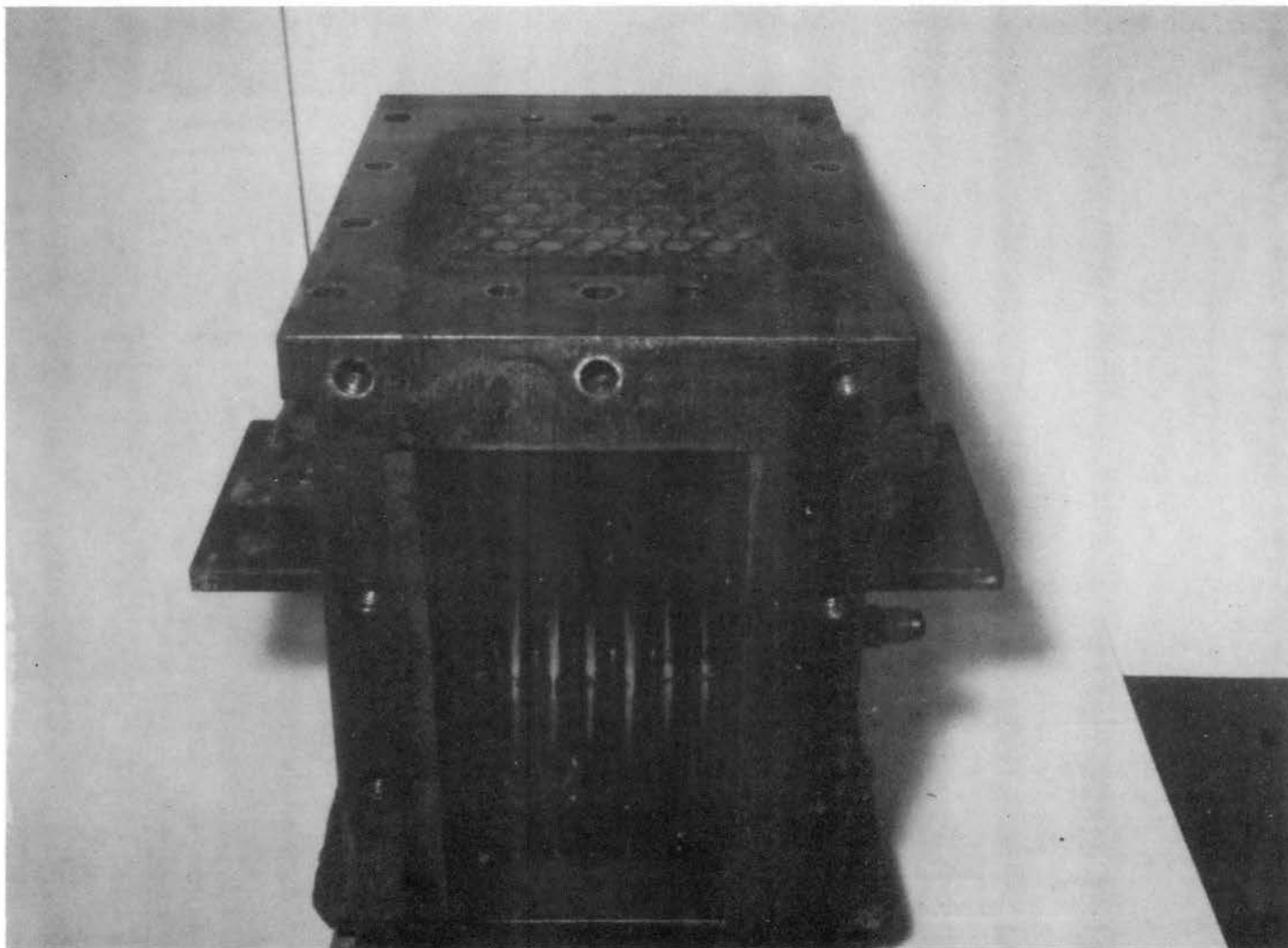


Figure 9. Tube Bank Model Number 1 Photograph

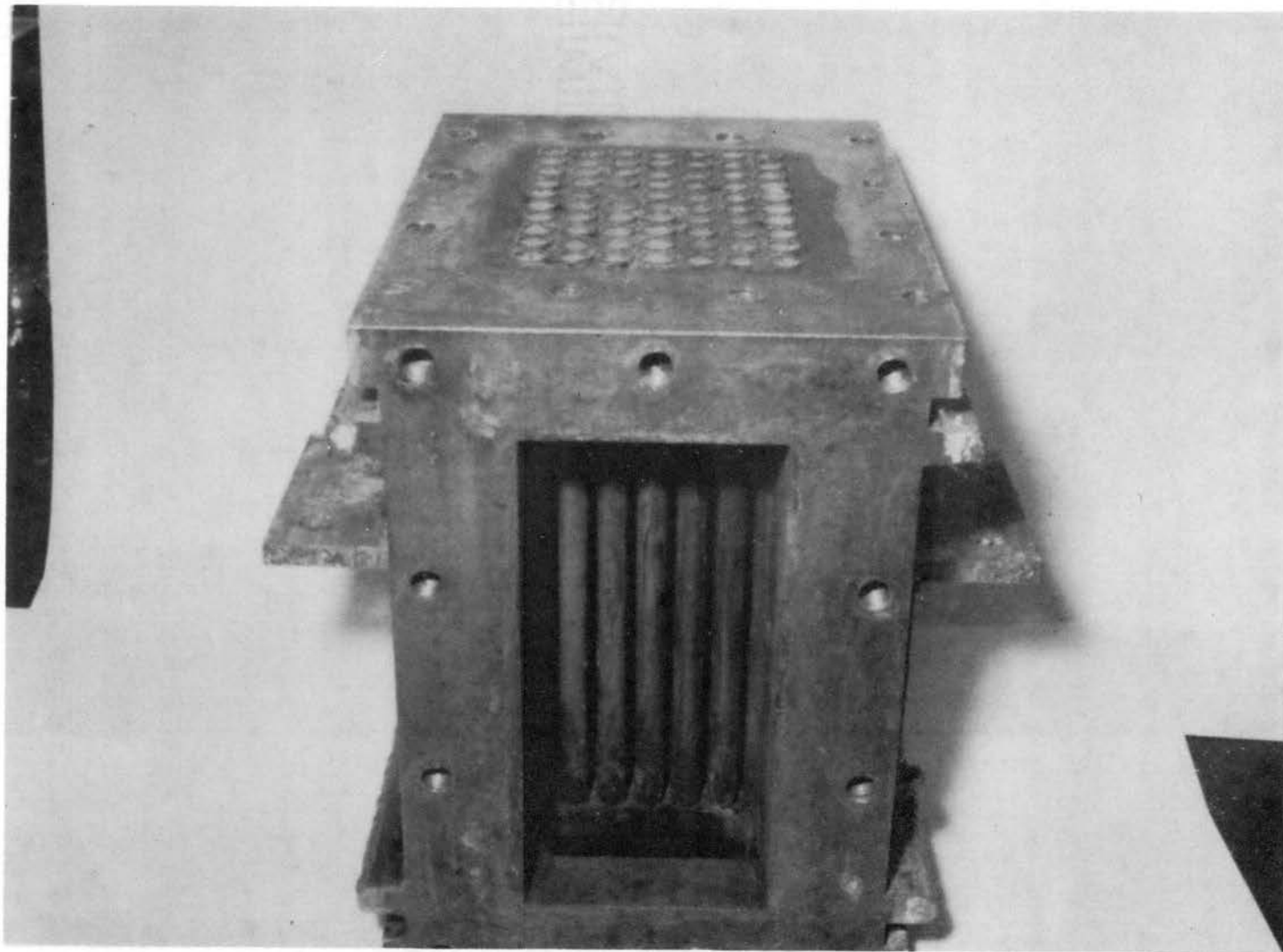


Figure 10. Tube Bank Model Number 2 Photograph

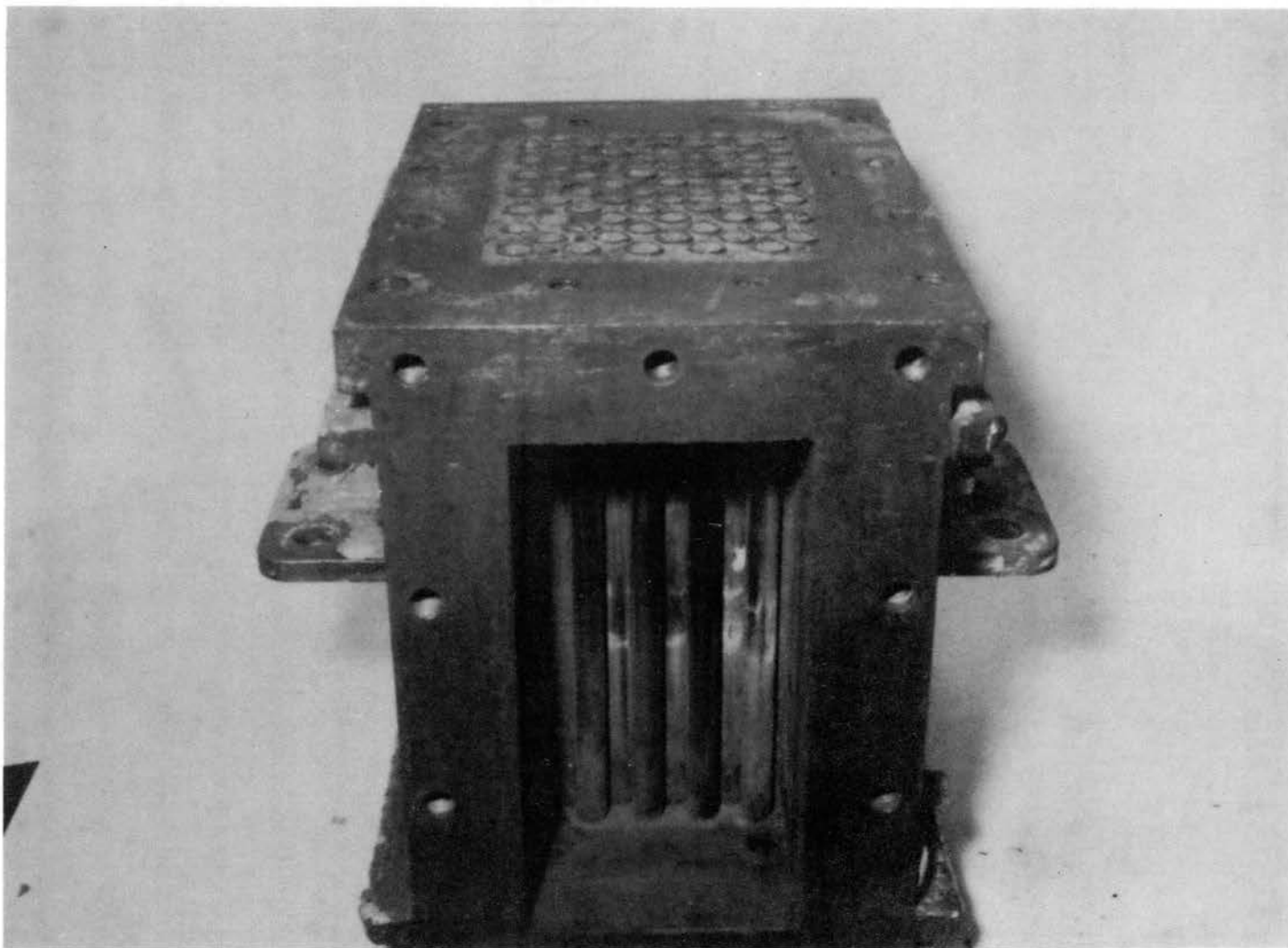


Figure 11. Tube Bank Model Number 3 Photograph

TABLE I
TUBE BANK DIMENSIONS AND CONSTANTS

	<u>Model Number 1</u>	<u>Model Number 2</u>	<u>Model Number 3</u>
Tube Layout	Equilateral Triangle	In-Line Square	Staggered Square
Outside Tube Diameter, In.	0.375	0.375	0.375
Minimum Tube Clearance, In.	0.094	0.094	0.094
Tube Length, In.	6.0	6.0	6.0
Exposed Tubes	67.25	60	63
Volumetric Hydraulic Diameter, Ft.	0.0233	0.0309	0.0309
Minimum Outside Flow Area, Sq. Ft.	0.0254	0.0234	0.0352
Number of Tube Rows	10	10	14
Number of Contractions	10	10	13
Heat Transfer Area, A_o , Sq. Ft.	3.33	2.94	3.09
Pitch Ratio	1.25	1.25	1.25
Inside Tube Diameter, In.	0.277	0.277	0.277
Inside Flow Area, Sq. Ft.	0.0293	0.0293	0.0293
Tube Wall Thickness, In.	0.049	0.049	0.049

consisted of a rectangular shell of 3/4 inch steel containing seventy 3/8-inch O.D., 18-BWG copper tubes with six inches of exposed length. The copper tubes were rolled into two fixed forged steel tube sheets. The tube sheets and walls of the shell were lined with 1/2-inch sheets of laminated phenolite plastic (Phenolite) to reduce heat losses. The tubes nearest the wall were half embedded in the Phenolite to minimize wall effects. The tubes along one wall of Model No. 1 would not be embedded in the plastic due to previous modifications (see Figure 8). Due to the embedding of the tubes along the wall, the effective number of tubes relative to exposed area was less than seventy.

<u>Model</u>	<u>Effective Number of Exposed Tubes</u>
1	67.25
2	60
3	63

The tube banks were installed in a manner to allow the water to pass upward through the tubes while CMC solution passed horizontally across the tube bank.

Each tube bank had 3/16-inch pressure taps located in the side of the shell halfway between the top and the bottom. The first pressure tap was 3/4 inch in front of the leading edge of the first tube row, while the second tap was 3/4 inch behind the trailing edge of the last tube row.

Tube Bank Headers

The headers were constructed of 3/16-inch type 304 stainless steel. One set of headers fits all three tube banks investigated.

Drawings of the headers are presented in Figures 12 and 13. The headers for the shell side had 1/4-inch taps on the top and bottom. The top taps were to allow air to escape from the system; whereas, the bottom taps were for draining the test section. The tube bank headers and the tube bank were covered with an approximately 1/2-inch thick layer of Super Stik-Tite Insulating Cement made by Refractory and Insulation Corporation.

Carboxymethylcellulose Solution Flow Equipment

A Moyno 1L6, type CDQ, positive displacement pump was used to pump the solutions. The pump was driven by a 3-horsepower electric motor with a variable speed drive to control the flow rate.

The solution holding barrel was a 55-gallon barrel containing 250 feet of coiled, 1/2-inch O.D., 14-BWG copper tubing for heating and cooling the solutions. Originally, the copper coil was connected to a cooling water supply and a steam supply. After the runs with the first tube bank model, the steam line was replaced with a hot water line. The steam line was replaced because the steam caused too much permanent decrease in the consistency of the CMC solutions. The hot water tank was a 9.9-gallon cylindrical steel tank containing 50 feet of coiled 1/2-inch O.D., 14-BWG copper coil connected to the steam supply line. The hot water lines to the CMC solution holding barrel were of 3/4-inch schedule 40 pipe covered with a 3/4-inch thick layer of cloth-covered fiberglass insulation. The hot water was circulated by a Gould Model 1L Centrifugal Pump with a 1/4-horsepower Emerson Electric Motor.

Quick-closing 1 1/2 inch gate valves were used to divert the CMC

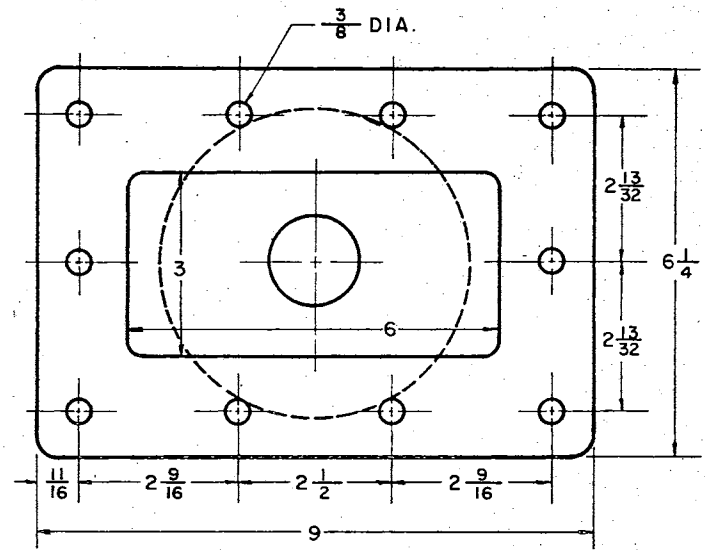
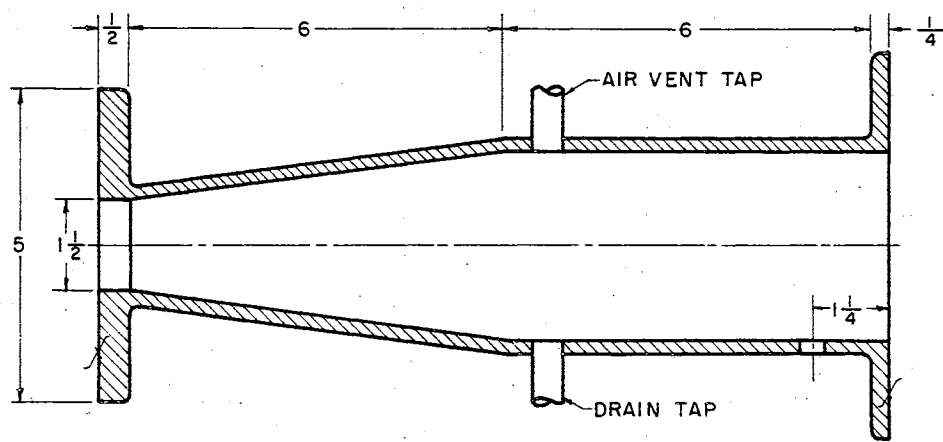


Figure 12. Tube Bank Shell Side Header Drawing

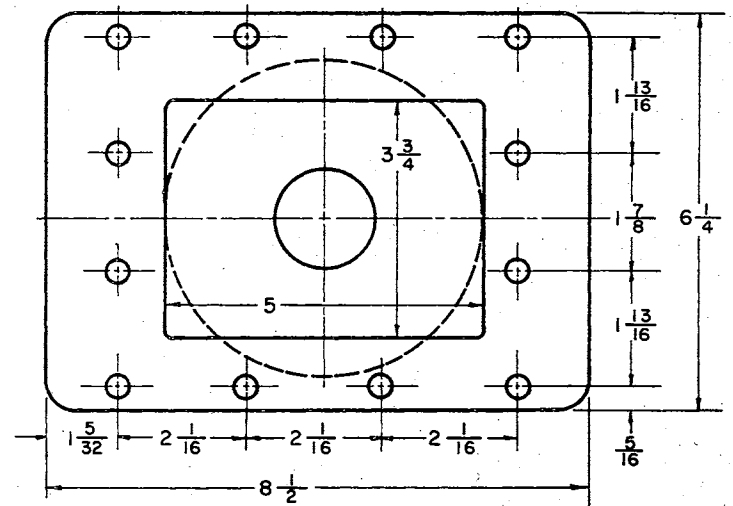
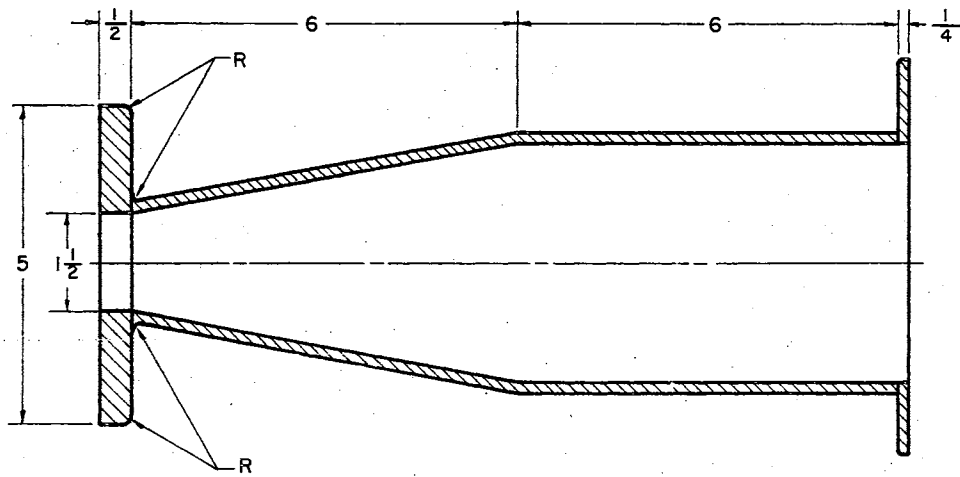


Figure 13. Tube Bank Tube Side Header Drawing

solution from the holding barrel return line to the flow rate determination tank. The CMC solution flow rate determination tank was a 9.9-gallon cylindrical steel tank with a side outlet of flexible 1/2-inch I.D. polyvinyl chloride (Tygon) tubing to return the CMC solution to the solution holding barrel by means of gravity flow. A vertical rod was attached to one wall of the flow rate tank to indicate the amount of CMC solution collected.

The CMC flow rate was monitored using orifice plate with a 23/32-inch diameter orifice. The orifice plate was of 1/8-inch thick brass and was held in place by a 1 1/2 inch pipe union.

Water System Flow Equipment

The water system is shown in Figure 2. The water for flow through the tubes of the tube bank was stored in a steel tank 30 inches deep, 30 inches wide, and 60 inches long. The water storage tank contained a heating and cooling coil, 25 feet long of 1 1/2 inch, 18-BWG copper tubing. The coil was connected to steam and cooling water supply lines.

The water flow rate determination tank had the same dimensions as the water storage tank; however, it was not equipped with a heating and cooling coil.

Three-inch schedule 40 piping led from both water tanks to the water system circulation pump. The water was circulated by a Gould Model 3655 centrifugal pump with a 5-horsepower Westinghouse Electric Motor.

A 7/8-inch diameter sharp-edged orifice of 1/8-inch thick brass was used to monitor the water flow rate to the tubes. The orifice was

held in place by a 1 1/2 inch pipe union.

Temperature Measurement Apparatus

In order to achieve uniform CMC solution temperatures for temperature measurements, mixing orifices and mixing blocks were installed upstream from the CMC solution thermocouples. It was decided that the mixing orifices alone did not provide sufficient mixing; therefore, the mixing blocks were installed downstream from the mixing orifices. The mixing blocks were used for the last eleven runs with Model No. 2 and for all of the runs with Model No. 1.

The mixing orifices, presented in Figure 14, were made from 1/8-inch thick brass and were held in place by 1 1/2 inch pipe unions. The sharp-edged piece of the pipe unions was machined to a flat surface to prevent leakage.

The brass mixing blocks are shown in Figures 15 and 16. A heat-conducting ceramic cement made by Sauereisen was used to cement the thermocouples into the mixing blocks.

Chromel-constantan 20-gauge wire covered with polyvinyl chloride was used for both the single and the differential thermocouples. The chromel-constantan combination was chosen for its high voltage output per degree of temperature. The thermocouple junctions were insulated with Sauereisen ceramic cement. Two complete sets of differential thermocouples and single thermocouples were used during the experimental work. The first set of thermocouples was replaced after the runs with Model No. 3.

The differential thermocouples consisted of five junctions on each side of the tube bank to measure the temperature change of each

DISC OF $\frac{1}{8}$ " THICK BRASS - HELD IN PLACE BY $1\frac{1}{2}$ " PIPE UNIONS

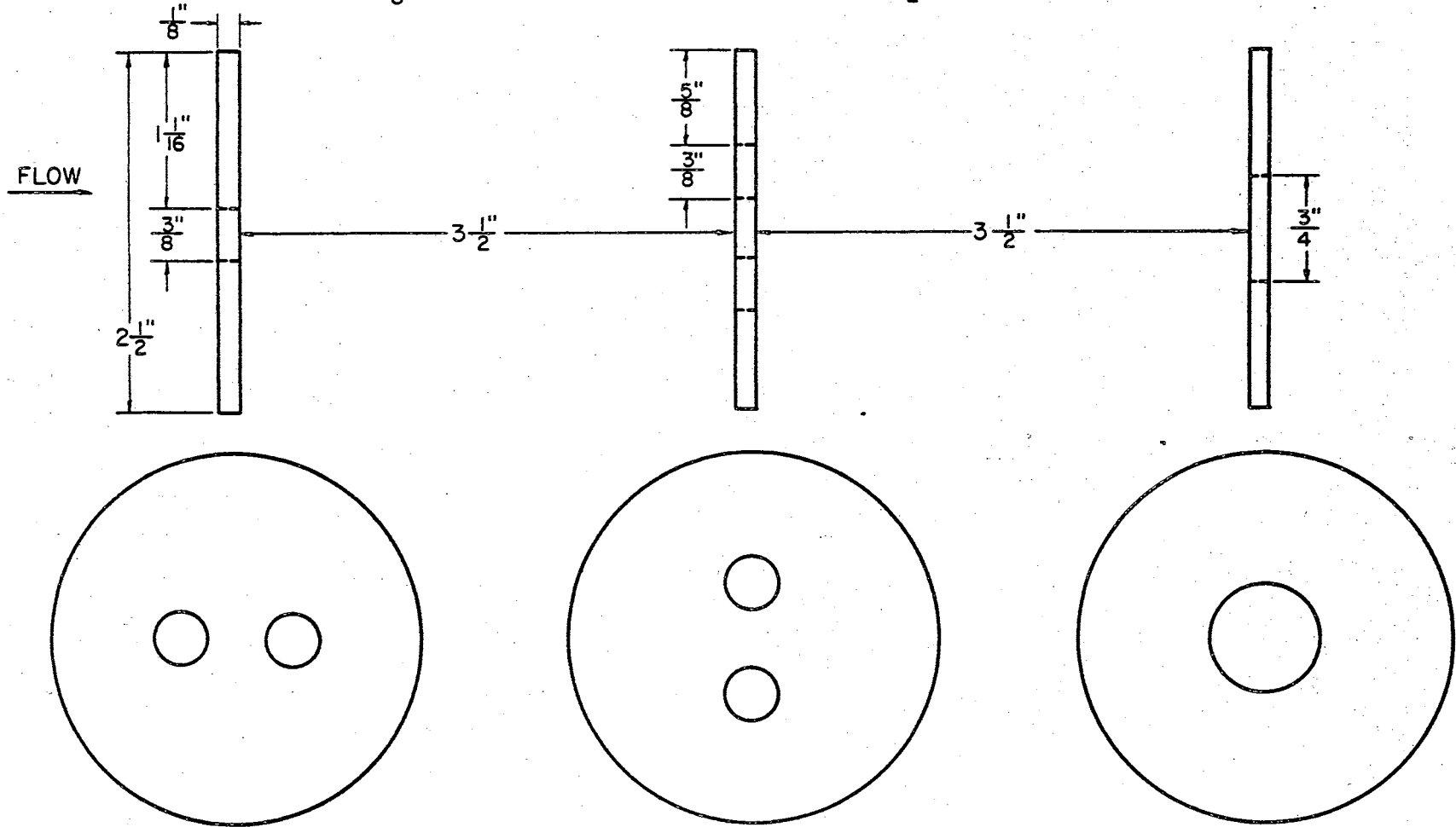


Figure 14. Drawing of Mixing Orifices

19 FLOW CHANNELS
 $2\frac{1}{2}$ " LONG, $\frac{3}{32}$ " DIA.

THERMOCOUPLE SLOT
 $\frac{1}{2}$ " DEEP, $\frac{3}{16}$ " DIA.

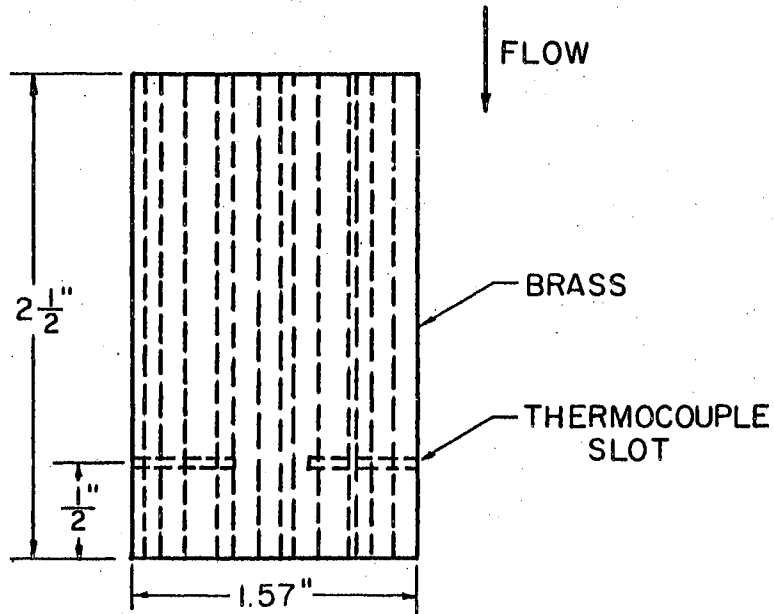
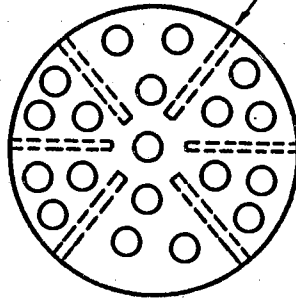


Figure 15. Mixing Block Drawing

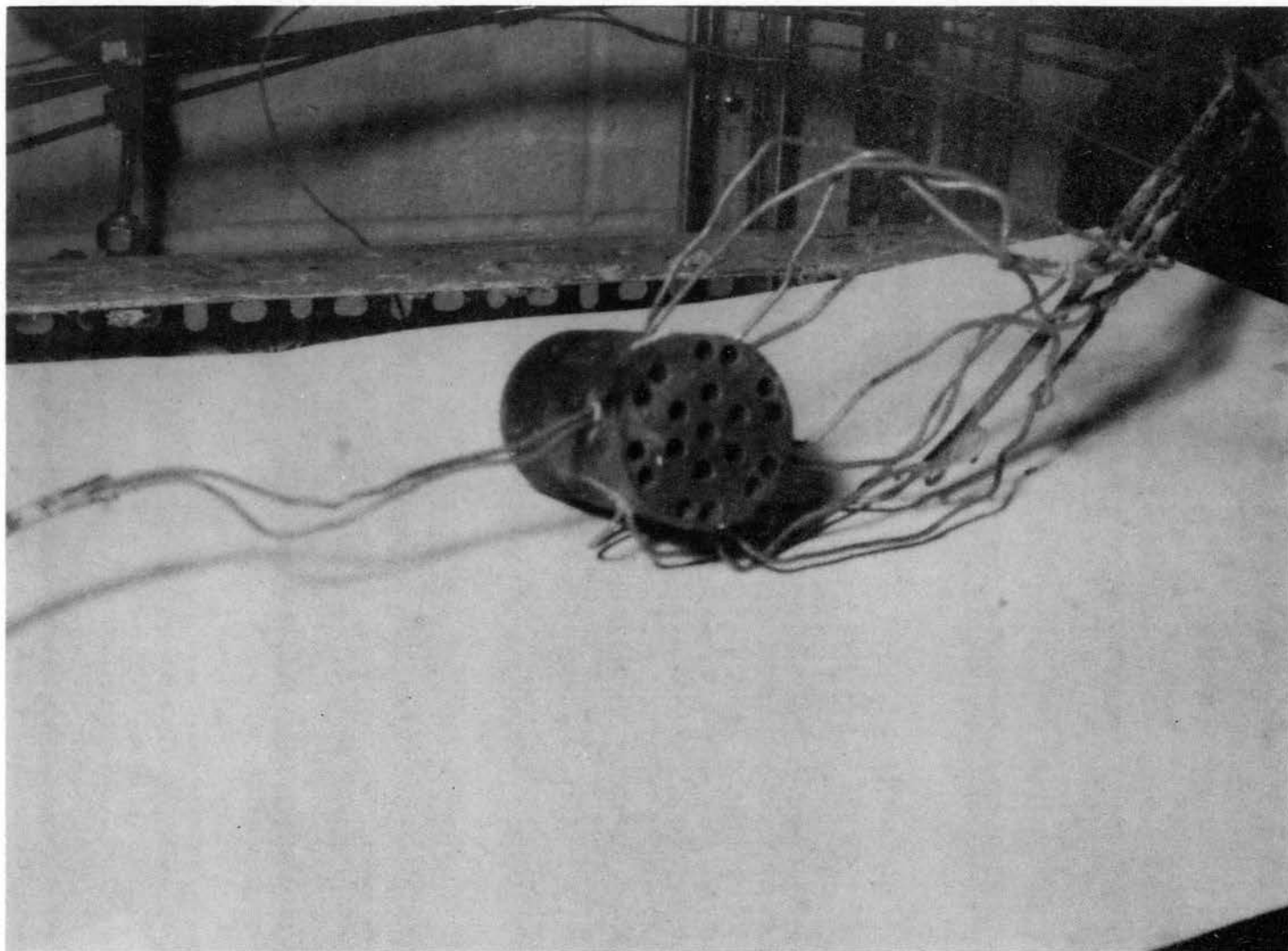


Figure 16. Mixing Block Photograph

steam flowing across the tube bank. The differential thermocouples were calibrated using two constant temperature baths and precision thermometers with 0.02°F subdivisions. The first differential thermocouple set was calibrated before the runs with Model No. 3. The second set was calibrated before the runs with Model No. 2 and was recalibrated before the runs with Model No. 1. The recalibration showed little change in the thermocouple properties. The differential thermocouple calibrations were carried out at temperature levels comparable to the temperatures existing during the experimental runs.

The single thermocouples were used to measure the inlet and outlet water and solution temperatures. The single thermocouple reference junction was ice prepared from distilled water. A constant temperature bath and precision thermometers with 0.02°F subdivision were used to calibrate the single thermocouples.

The single and differential thermocouples were connected to selector switches by means of terminal strips.

Two Leeds and Northrup Model 8686 Millivolt Potentiometers were used to measure the thermocouple responses. A Bush Mark 10 Recorder was used to record the differential thermocouples' output for the last five runs with Model No. 2 and for all of the runs with Model No. 1.

Pressure Drop Measuring Apparatus

The CMC solution flow rate orifice and the water flow rate orifice pressure taps were connected to Merriam 50-Inch U-Tube Manometers with $1/10$ -inch subdivisions. Mercury was used in both orifice manometers. The orifice manometer lines were $1/4$ -inch O.D., 14-BWG copper tubing; and the valves were standard $1/4$ -inch globe valves.

A Merriam 50-Inch U-Tube Manometer with 1/10-inch subdivisions was used for the tube bank pressure drop measurements. Carbon tetrachloride was used in the tube bank manometer during most of the runs. It was necessary to use tetrabromoethane for several runs involving Model No. 3 and a very viscous 1 1/2 percent CMC solution. Iodine was dissolved in both the carbon tetrachloride and the tetrabromoethane to color the fluids for easier manometer reading. The tube bank manometer lines were 1/4-inch O.D., 14-BWG copper tubing; and the valves were standard 1/4-inch globe valves. For the runs with Model No. 1, water displacement bombs filled with 1/2 gallon of water were installed between the tube bank manometer and the test section to prevent CMC solution from entering the manometer. Elimination of CMC solution from the manometer improved the manometer response to pressure changes, and the manometer fluids and tube walls remained cleaner for a longer period of time.

In order to determine the amount of frictional heating taking place between the differential thermocouples, 1/4-inch pressure taps were installed near the flanges holding the differential thermocouples. Pressure gauges were used to measure the pressure at these taps for both the CMC solution and the water.

Solution Preparation Materials and Equipment

The non-Newtonian fluids used were solutions of Hercules Type 7H Sodium Carboxymethylcellulose (CMC) in tap water. A small amount of acetone was used with the CMC powder to facilitate the preparation of the solutions. A mixer with a 1/4-horsepower motor and a 4-inch diameter impeller was used to mix the CMC solutions. A Powerstat was used

to control the speed of the mixer.

Other Equipment

A Brenet No. 65 Stopwatch with a 10-second sweep and 1/10 second subdivisions was used for the flow rate determinations.

A Fann VG Model 35 rotational viscometer was used to obtain shear stress-shear rate data for the CMC solutions. The temperature of the samples being analyzed with the viscometer was controlled by a constant temperature bath circulating water around the outside of the viscometer sample cup. Oils obtained from the National Bureau of Standards were used to calibrate the viscometer springs.

CHAPTER VI

EXPERIMENTAL PROCEDURE

Thermocouple Calibration

During the thermocouple calibrations of both the single and differential thermocouples, the thermocouple circuits were identical to the thermocouple circuits used during the experimental runs. During the thermocouple calibrations and experimental runs, the potentiometers were standardized before each reading.

A constant temperature water bath was used to calibrate the single thermocouples at temperature levels comparable to the levels expected during the experimental runs. The single thermocouples were placed in the constant temperature bath, and a single common reference thermocouple was placed in a thermos containing ice prepared from distilled water. The constant temperature bath temperature was brought to the low end of the temperature range of interest. When the bath temperature reached equilibrium, the bath precision thermometer was read; and the thermocouple response was measured using the potentiometer. For the next calibration point, the bath temperature was increased a small amount (1 to 4°F); and the bath temperature was allowed to reach equilibrium. About one hour was allowed for the temperature to reach equilibrium for each calibration point.

Two constant temperature water baths were used to calibrate the

differential thermocouples at the temperature levels and temperature differences expected during the experimental runs. For each differential thermocouple set, one side of the thermocouple set was designated to be placed at the inlet location. Each side of the differential thermocouple was placed in a water bath, and the bath containing the thermocouple side designated as "inlet" was brought to the desired temperature level. The other bath was operated at temperatures below and above the temperature of the inlet thermocouple bath to allow for both heating and cooling runs. About one hour was allowed between calibration points for the temperatures to reach equilibrium. At each calibration point, both bath temperatures and the thermocouple response were measured and recorded.

Solution Preparation

Two kilograms of sodium carboxymethylcellulose (CMC) powder were required to prepare one barrel of one percent CMC solution. Previous experience has shown that direct addition of CMC powder to water causes the formation of large lumps. These lumps have CMC gel around the outside and dry CMC powder inside and are very difficult to dissolve. To prevent the lump formation, a thick slurry of the CMC powder in acetone was prepared for addition to the water. The mixer impeller was placed in a bucket of water, and the mixer was started at a moderate speed. Some of the CMC-acetone slurry was gradually added; and, as the CMC dissolved, the mixer power was increased. When the CMC was sufficiently dissolved, the bucket of solution was transferred to the holding barrel. This procedure was continued until all of the measured amount of CMC powder was dissolved in the water. Water was then added

to the holding barrel to bring the solution to the desired level in the holding barrel. The solution was then pumped around the bypass loop for several hours to complete the mixing process.

Flow Rate Determinations

CMC Solution Flow Rates

During the course of the experimental runs, two methods were used to determine the CMC solution flow rates.

The first method was used for the experimental runs with Tube Bank Model No. 3 using the one percent CMC solution. A level gauge attached to the side of the CMC solution flow rate tank was calibrated to give the volume of solution in the flow rate determination tank. The flow rate was determined from the change in level gauge reading during a measured length of time. The stopwatch was started when the solution flow was diverted from the CMC solution holding barrel return line to the flow rate tank by means of quick-closing valves and was stopped when the valves were returned to the normal position.

The second flow rate determination method was used for the remainder of experimental runs with Model No. 3 and for all of the runs with Model No. 2 and Model No. 1. A rod with two marks was attached to one side of the inside of the flow rate determination tank. The volume of fluid represented by the space between the two marks was determined using a graduated cylinder. The CMC solution flow rate was determined by diverting the solution flow from the solution holding barrel return line to the flow rate determination tank. The time required for the solution level in the flow rate tank to go from the first mark to the second mark was measured with a stopwatch. The times measured during

these flow rate determinations ranged from 14 seconds to 62 seconds.

Water Flow Rates

The water flow was diverted from the water storage tank return line to the water flow rate determination tank. The time required for the water level in the tank to pass from one level mark to another level mark was measured with a stopwatch. The volume represented by the distance between the level marks on the side of the tank was calculated from the tank dimensions and the distance between the marks.

Isothermal Pressure Drop Run Procedure

The isothermal pressure drop experimental runs can be separated into two groups: (1) pressure drop runs at temperature levels comparable to the temperature levels existing during the heat transfer runs and (2) pressure drop runs at a temperature level determined by the cooling water temperature and ambient room temperature.

At the start of all pressure drop runs, valves located above the tube bank pressure drop manometer were opened to bleed the air from the manometer lines. These valves were closed when no more air could be forced to leave the manometer system. The air-vent valves were opened periodically during the runs to make sure that all air had been removed from the manometer system.

High Temperature Isothermal Pressure Drop Run Procedure

The air in the manometer system was removed, and the flow rate was established by means of the CMC solution pump variable speed drive. The CMC solution was heated to the desired temperature level with steam for the runs with Model No. 3. Hot water was used to heat the

CMC solution for the runs with Model No. 2 and Model No. 1. The steam or hot water circulation was stopped when the CMC solution reached the desired temperature level. The CMC solution then slowly cooled due to heat loss to the room. The CMC solution inlet and outlet thermocouple response readings and tube bank pressure drop manometer readings were observed and recorded at intervals of several minutes until equilibrium appeared to be established, and the temperature level of the CMC solution fell below the temperature level of interest. Each isothermal pressure drop run required an average time of about one hour. When the temperature and pressure drop measurements for a pressure drop run were completed, the CMC solution flow rate was determined. The CMC solution differential thermocouple response was observed and recorded during all of the isothermal runs with Model No. 3 and during part of the runs with Model No. 2. The differential thermocouple response was measured to determine the amount of heat loss and frictional heating incurred by the CMC solution crossing the tube bank; however, this method was determined to be unreliable because the temperature changes to be measured were too small for accurate measurement using the thermocouples.

Ambient Temperature Isothermal Pressure Drop Run Procedure

Cooling water was circulated through the CMC solution holding tank coil during isothermal pressure drop runs for Tube Bank Models No. 3 and No. 2. Cooling water was not used during the pressure drop runs with Model No. 1 because the runs were made during the winter, and the cooling water would cool the solutions below the desired temperature range.

The air in the manometer system was removed, and the flow rate was established. The CMC solution inlet and outlet thermocouple response readings and tube bank pressure drop readings were observed and recorded until equilibrium appeared to be established. Each of these pressure drop runs required time of about one hour. The CMC solution flow rate was determined after the temperature measurements and pressure drop measurements for each run were completed.

Heat Transfer Run Procedure

The heat transfer runs may be divided into two groups: (1) heating runs where the CMC solution was heated during flow across the tube bank and (2) cooling runs where the CMC solution was cooled during flow across the tube bank. The experimental procedures for the heating and cooling runs were the same after the equipment start-up was achieved.

Sets of data during each heat transfer run were taken at 10- to 20-minute intervals for about an hour. Each set of data consisted of the following measurements:

1. CMC solution inlet and outlet thermocouple response
2. Water inlet and outlet thermocouple responses
3. CMC solution differential thermocouple response
4. Water differential thermocouple response
5. CMC solution orifice manometer reading
6. Water orifice manometer reading
7. Tube bank pressure drop manometer reading

The CMC solution flow rate determinations were made after the first and last sets of data were taken for each run. After the first set of

data, pressure gauges were used to measure the pressure at the thermocouple holding flanges to determine the amount of frictional heating incurred by the CMC solution and water flowing through the test section.

A new CMC solution flow rate was established by changing the pump speed after the temperature, pressure and flow rate measurements for a run were completed. The millivolt recorder output showed that a time period of 20 minutes was quite sufficient for the thermocouple readings to reach equilibrium at the new flow rate. After start-up was achieved, five runs at different CMC solution flow rates were usually made before the equipment was shutdown. Eight to ten hours were required to complete the five runs. For the runs with Models No. 2 and No. 1, the CMC solution pump was set at its lowest speed for the first run; and the flow rate was increased for each of the succeeding runs. For the last run, the CMC solution rate was returned to the lowest rate to try to reproduce the results of the first run after start-up.

Samples of the CMC solutions were collected during the runs for rheological analysis at a later time. The frequency of the CMC solution sample collection was determined by the age of the CMC solution and by the amount of heating undergone by the CMC solution. The fresh CMC solution properties were more time dependent than the properties of older solutions.

Heating Run Start-Up Procedure

The CMC solution pump was started and set at the speed necessary to provide the desired CMC solution flow rate. The cooling water valve for the CMC solution holding tank coil was opened to allow the

maximum cooling water flow rate throughout the heating runs.

The water circulation pump was started to establish the circulation of water through the tube bank tubes. For runs where only part of the water circulation pump output was sent through the tube bank, the bypass water line valve was opened to allow approximately half of the water pump output to return directly to the storage tank without passing through the tube bank. For runs where the water bypass line valve was closed, the water circulation pump provided a water flow rate of 27,000 pounds per hour. A steam valve was opened to allow steam to flow through the water storage tank coil. The steam flow rate was later decreased to maintain constant temperature when the water tube bank inlet temperature response reached 4.1 millivolts (about 150°F). It was necessary during runs to make slight changes in the steam flow rate to the water storage tank coil in order to keep the water temperature within the desired temperature range.

Cooling Run Start-Up Procedure

The CMC solution pump was started at the speed necessary to give the desired flow rate. For the runs with Model No. 3, a steam valve was opened allowing steam to pass through the CMC solution holding tank coil to heat the CMC solution to the desired temperature level (about 120°F). For the runs with Models No. 2 and No. 1, the pump used to circulate hot water (at about 190°F) through the CMC solution holding tank coil was started. The steam valve for the line to the hot water tank coil was opened to heat the water for circulation through the solution tank coil. The steam flow rate to the hot water tank coil was slightly changed during the runs to keep the hot water

at 190°F.

The water circulation pump was started to establish water flow through the tube bank tubes. The total water pump output was circulated through the tube bank during the cooling runs. The cooling water valve was opened providing cooling water for the water storage tank coil. During the runs, minor changes in the cooling water rate were necessary to keep the water temperature within the desired temperature range.

While the water and CMC solution were being circulated to reach the desired temperatures and equilibrium, the air was removed from the manometer systems by opening valves located above the manometers. The potentiometers and millivolt recorder were also prepared for operation during this time. The recorder chart speed was set at 20 inches per hour, and the recorder output was set at 0.5 millivolts per inch.

Viscometer Operation Procedure

Viscometer Spring Calibration Procedure

Two methods were used to make necessary periodic calibrations of the viscometer springs.

The first method consisted of using the viscometer with an oil having a known viscosity. The viscometer spring constant was calculated from the observed rotor speed, deflection reading, and the known oil viscosity.

For the second method, a string was attached to the viscometer bob and passed over a pulley. A weight of known mass was attached to the string, and the resulting viscometer deflection was observed. The spring constant was calculated from the observed deflection, bob

radius, and the mass of the weight attached to the string.

Spring constants obtained using the weight were about 5 percent greater than the spring constants obtained using the viscosity standards. These differences may be attributed to (1) temperature control and measurement difficulties and (2) change of the viscosity standards' viscosity due to aging. Spring constants based on the weight calibration data were used to reduce the CMC solution viscometer data.

CMC Solution Analysis Procedure

The appropriate bob, rotor, and spring were installed on the viscometer. The water circulating constant temperature bath was started and set at the desired temperature. The water from the temperature bath was circulated around the outside of the sample cup. The appropriate amount of CMC solution was poured into the sample cup, and the cup was placed on the viscometer with the rotor and bob immersed in the CMC solution sample. The proper depth for immersion was indicated by a mark on the viscometer rotor. While waiting for the CMC solution to reach the desired equilibrium temperature level, the viscometer motor was started; and the rotor speed was set at 600 revolutions per minute to mix the CMC solution sample. When the equilibrium temperature level was established, the temperature of the CMC solution sample was observed and recorded; viscometer deflection readings were taken at rotor speeds of 600, 300, 200, and 100 revolutions per minute. The solution temperature was again measured after the last reading. For an acceptable viscometer run, the initial and final solution temperatures could not differ by more than 0.1°F. Viscometer runs for most samples were made at three temperature levels.

CHAPTER VII

PRESENTATION AND DISCUSSION OF RESULTS

The raw data and calculated results for the heat transfer runs are tabulated in Appendices D and E. Appendix F contains tabulated raw data and calculated results for the isothermal pressure drop runs. Rheological properties calculated from the Fann Viscometer data are presented in Appendix G.

The resulting j -factors and friction factors obtained for the three tube bank models are presented in Figures 17 through 22 as a function of the modified Reynolds number. Examination of Figures 17 through 22 yields the following statements:

1. The use of the proposed modified Reed-Metzner Reynolds number brings the j -factors and friction factors for the CMC solutions having different rheological properties into reasonable agreement.
2. The application of the modified Reed-Metzner Reynolds number to the pressure drop data gives CMC solution friction factors which are in fair agreement with the accepted friction factors for Newtonian fluids.
3. The j -factor versus modified Reed-Metzner Reynolds number curves are approximately parallel to and below the accepted Newtonian fluid j -factor versus Reynolds number curves. The CMC solution j -factors are about one-half the value of the

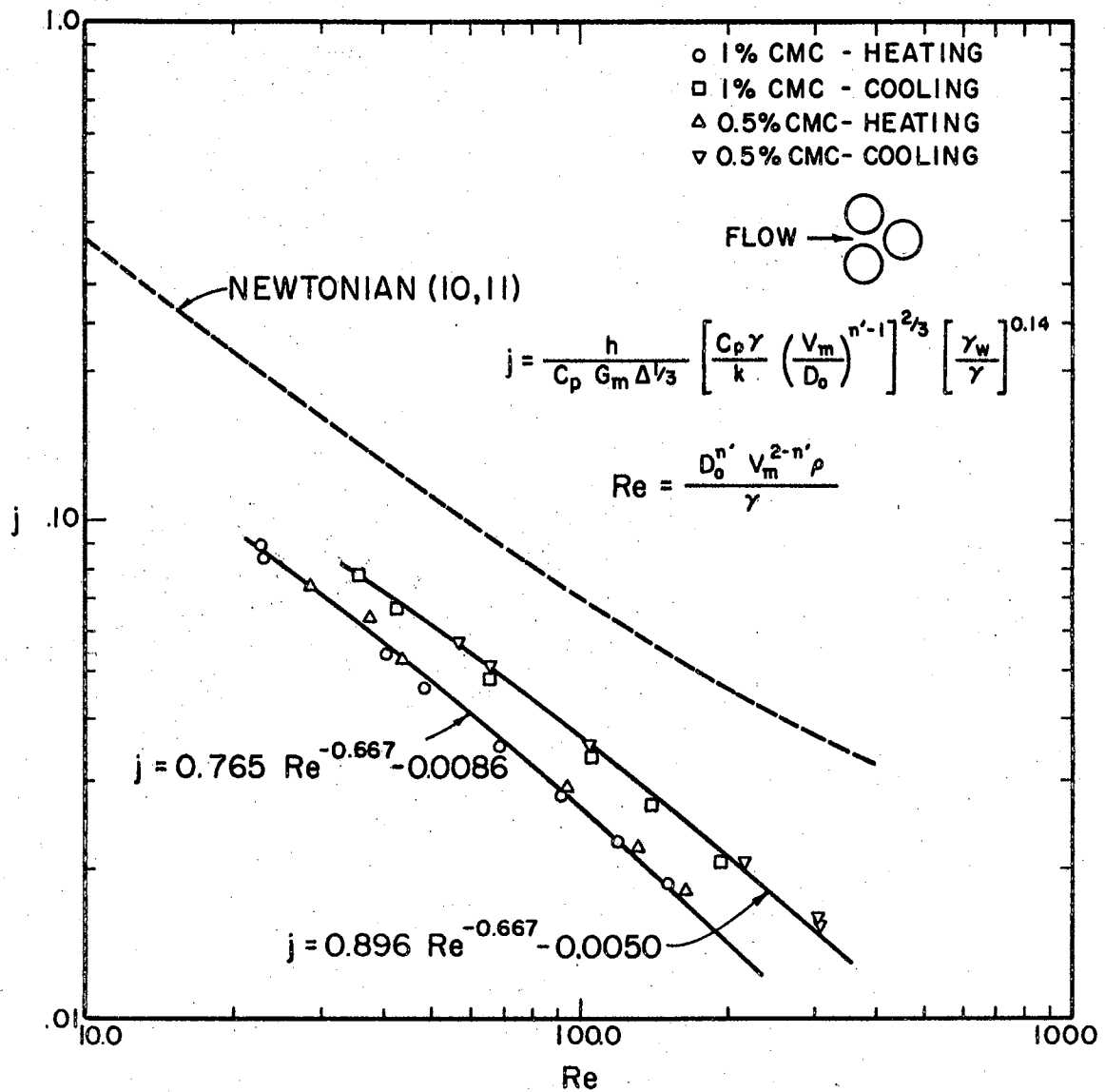


Figure 17. j-Factor Vs. Reynolds Number--Model No. 1

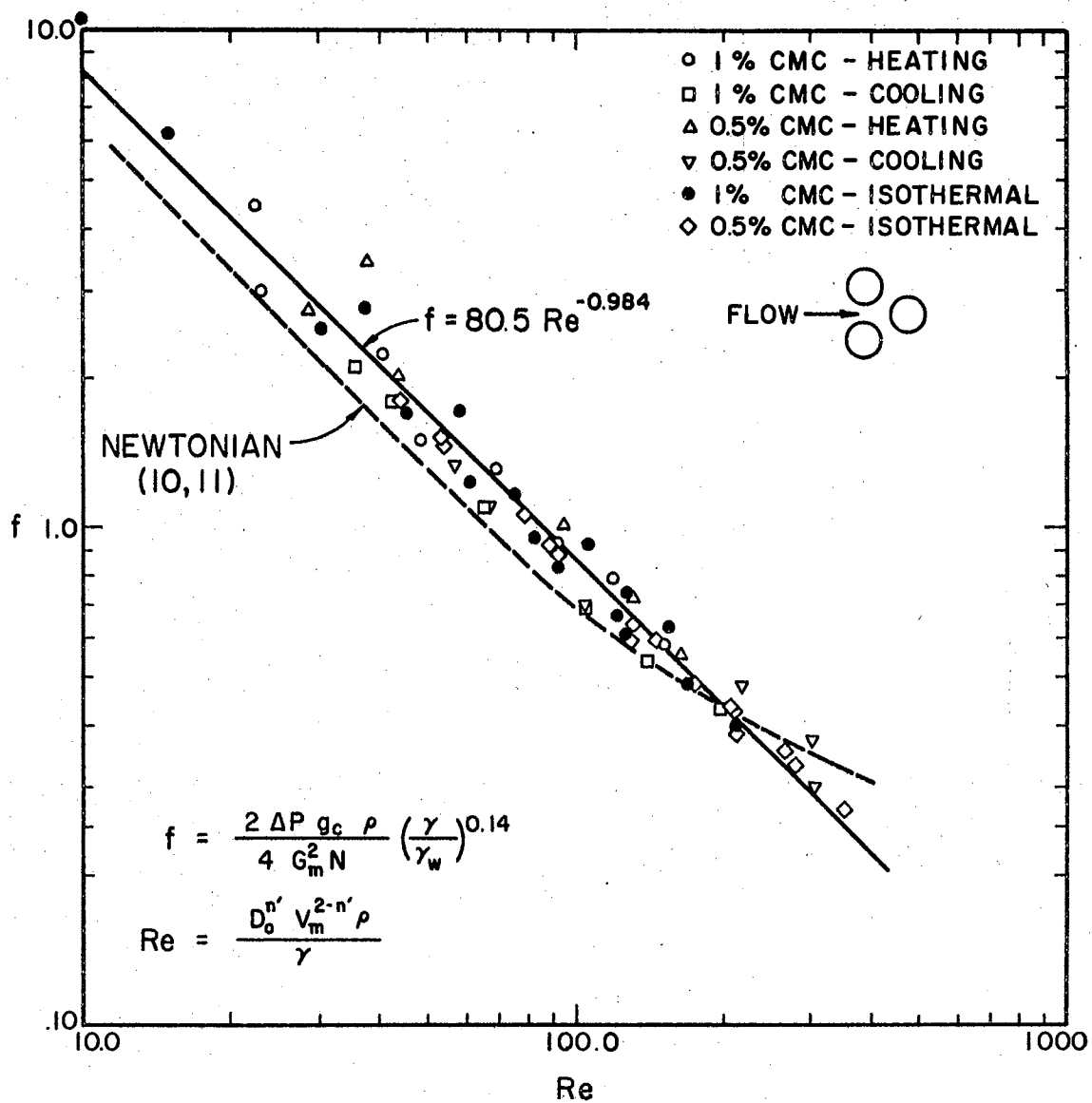


Figure 18. Friction Factor Vs. Reynolds Number--Model No. 1

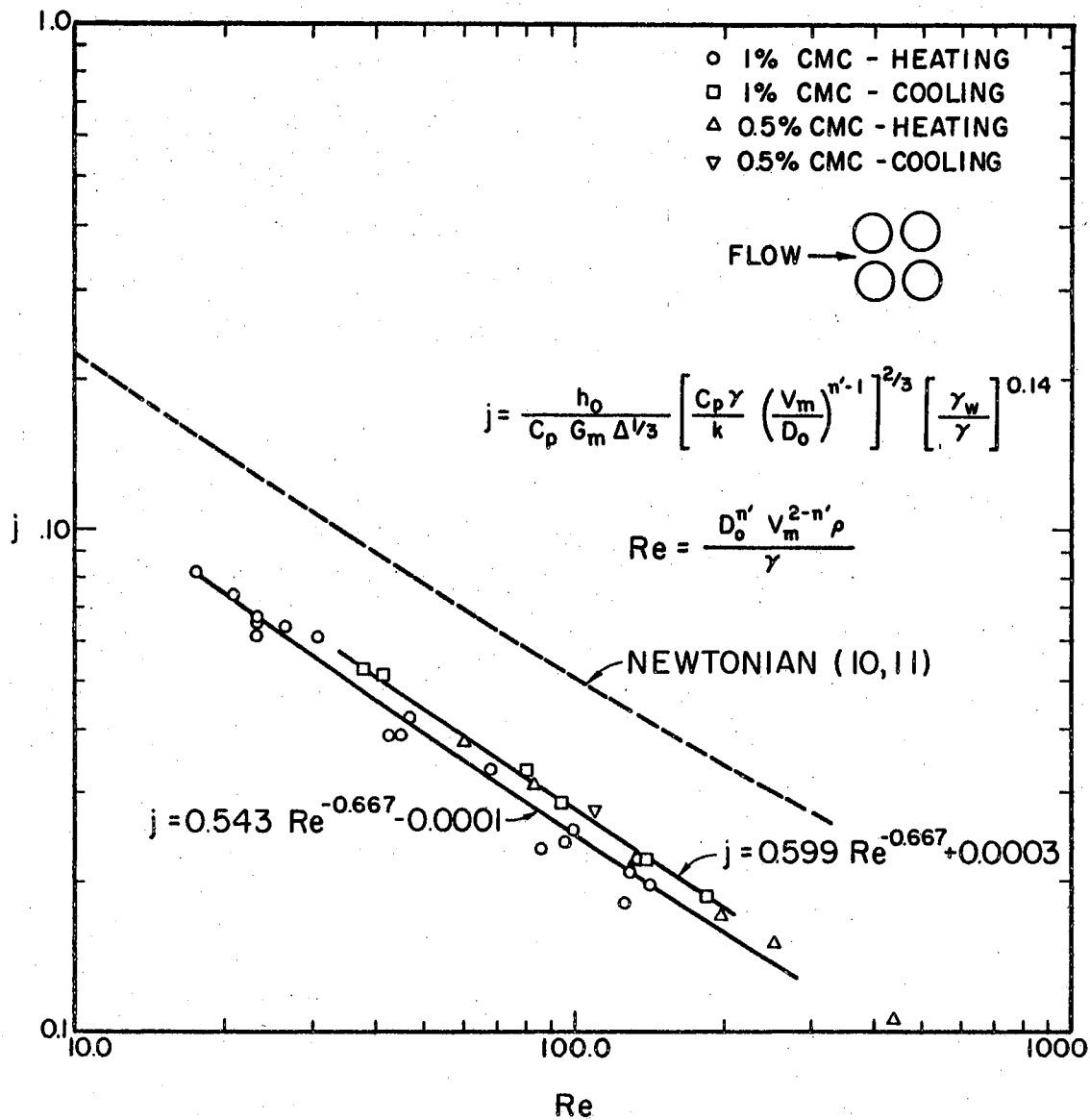


Figure 19. j-Factor Vs. Reynolds Number--Model No. 2

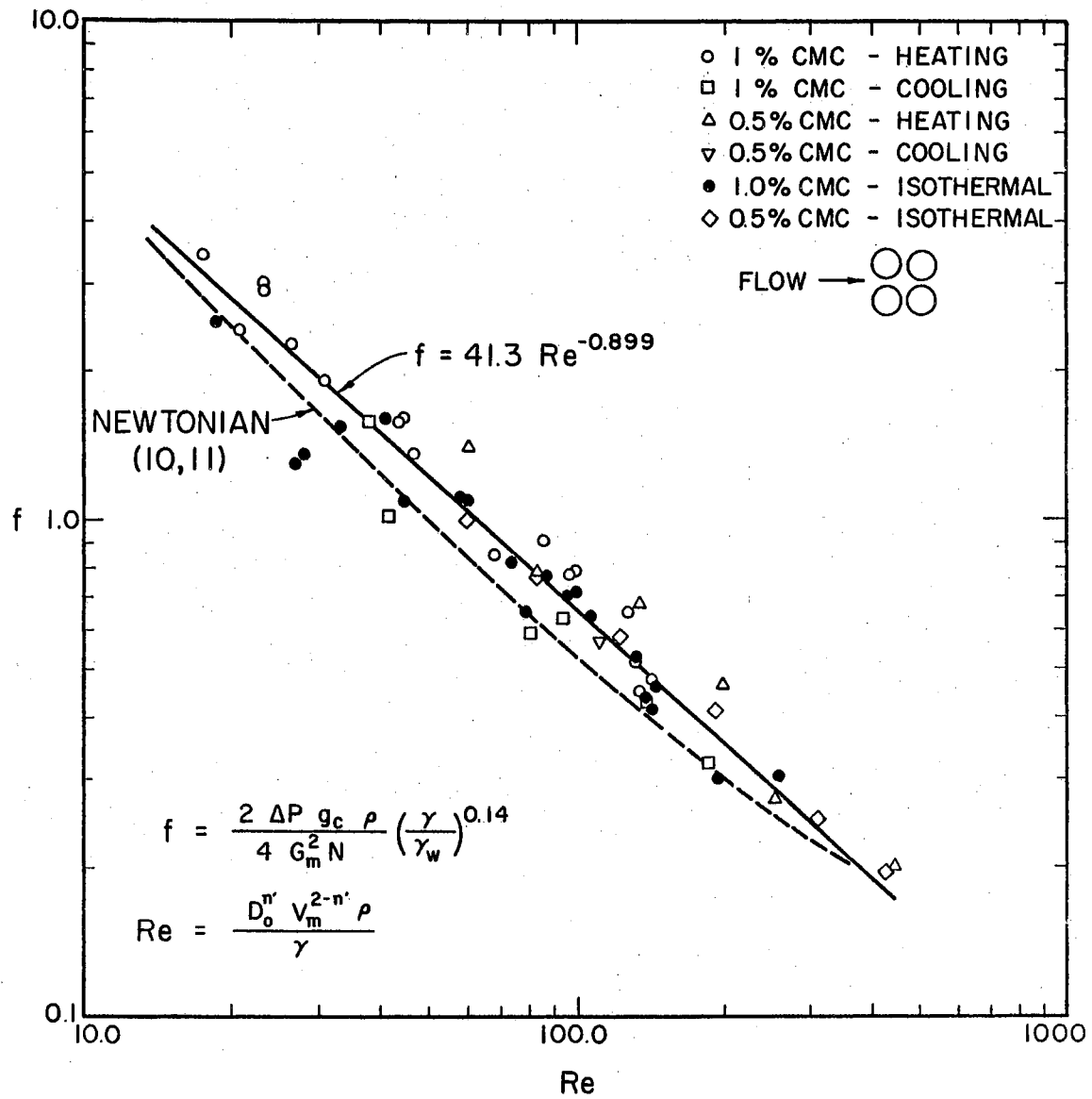


Figure 20. Friction Factor Vs. Reynolds Number--Model No. 2

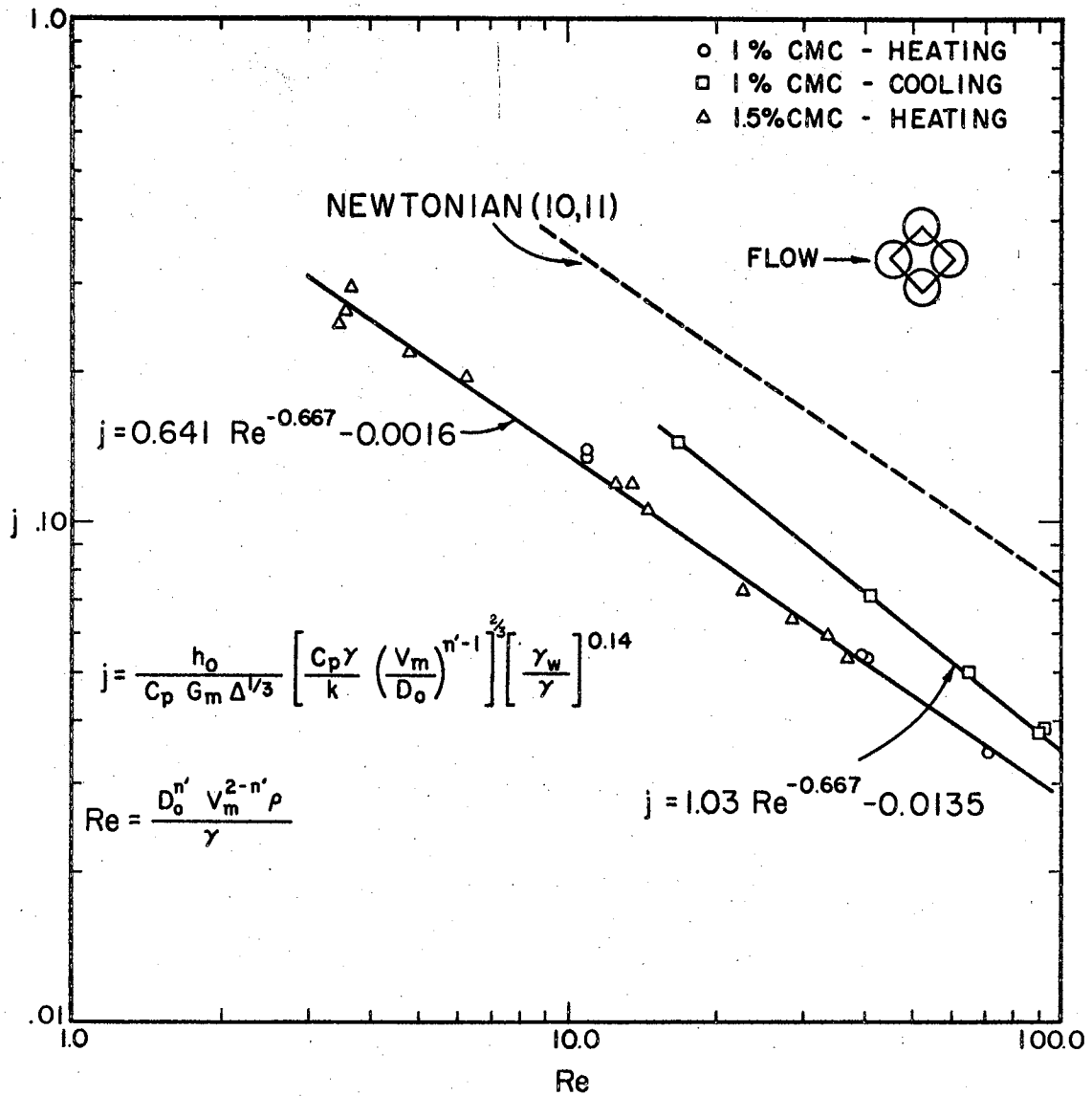


Figure 21. j -Factor Vs. Reynolds Number--Model No. 3

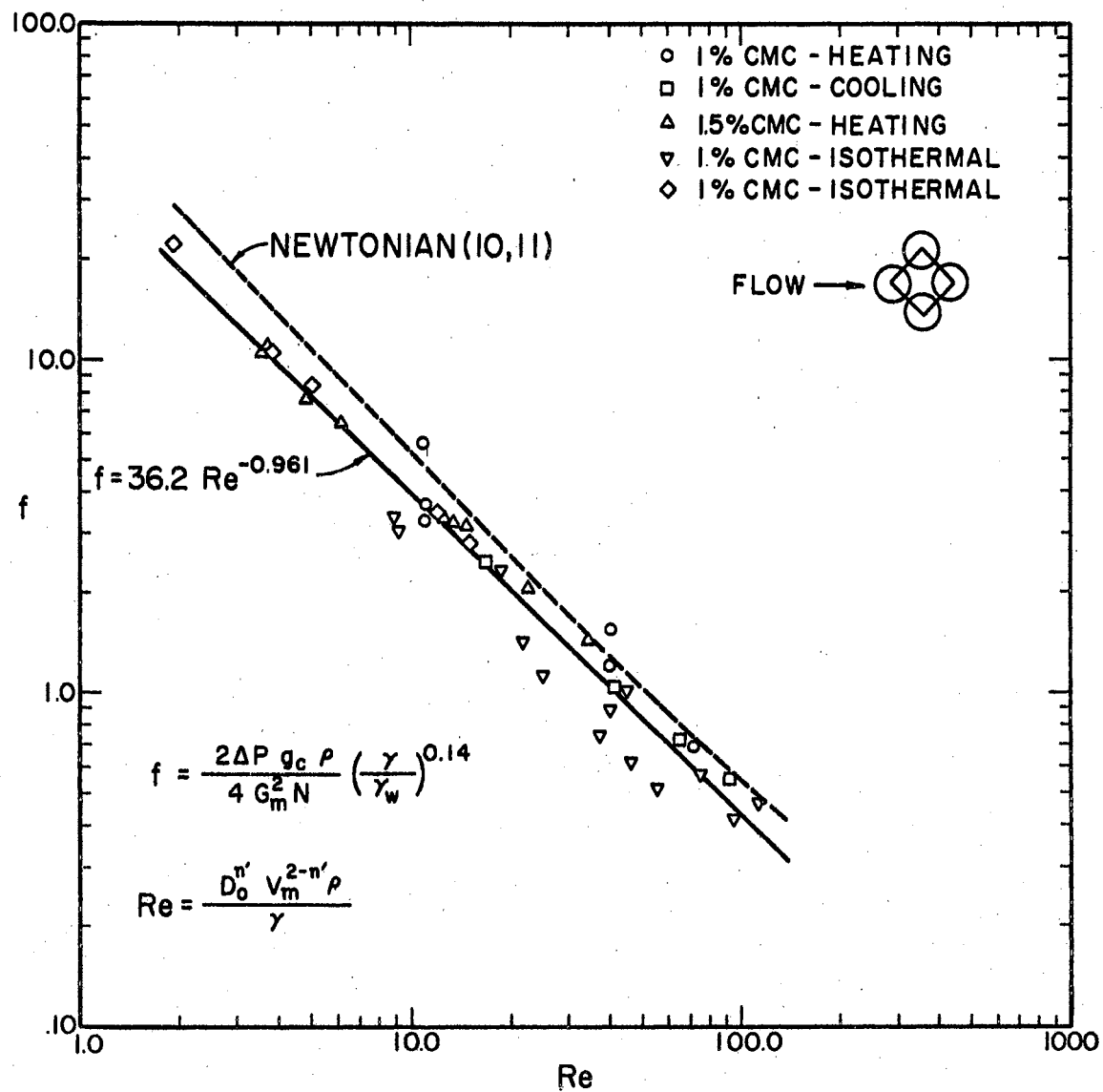


Figure 22. Friction Factor Vs. Reynolds Number--Model No. 3

Newtonian fluid j -factors.

4. The heat transfer results for Tube Bank Models No. 1 and No. 3 yield significantly different j -factor versus modified Reynolds number curves for heating and cooling runs. This effect is only slightly evident in the j -factor-Reynolds number curves for Tube Bank Model No. 2. More data at various values of (γ_w/γ) are needed to develop a single curve to represent both heating and cooling heat transfer data.

The difference pointed out in statement 3 between the calculated non-Newtonian fluid j -factors and the accepted Newtonian fluid j -factors may be attributed to one or both of the following: (1) fouling resistance to heat transfer and (2) CMC solution rheological behavior, i.e., the increase in apparent viscosity with decreasing shear rate.

Examination of the tubes after removal of the tube bank headers showed deposition of scale both inside and outside of the tubes. The scale deposit was not thick enough to alter the dimensions for flow (thus producing no pressure drop change due to fouling); however, the deposits could have presented a significant resistance to heat transfer. At the end of each series of runs, the first run was replicated to check for fouling buildup during the time required to make the series of runs (approximately seven hours were required to make a series of runs). The results of series of runs made several days apart are also in reasonable agreement and do not indicate any significant fouling increase with time.

There exists the possibility that the fouling occurred soon after installation of the tube banks, before the data were taken. This

fouling would be expected to significantly dampen the variation of the fouled j -factor with Reynolds number. However, the observed non-Newtonian j -factor versus Re curves are approximately parallel to the established Newtonian curves.

Due to the existence of varying cross-sectional area within a tube bank for flow across the tube bank, the shear rate is a function of position in the tube bank. This variation of the shear rate with position causes the apparent viscosity of the CMC solution to also be a function of position. Since the region behind each tube is a region of relatively low shear rate, the fluid behind the tube is more viscous than the fluid in the main flow. The existence of this more viscous fluid behind the tube decreases the heat transfer rate from the rear of the tube to the fluid behind the tube. This region of higher viscosity does not exist for Newtonian fluid flow; therefore, the non-Newtonian fluid j -factors can be expected to be less than the Newtonian fluid j -factors. One method of evaluating this effect of the apparent viscosity dependence upon the shear rate would be to obtain heat transfer data for a dilatant fluid. If the apparent viscosity dependence upon the shear rate is significant, one would expect the dilatant fluid j -factors to exceed the Newtonian fluid j -factors.

There are not sufficient data to positively attribute the relatively low non-Newtonian j -factors to either fouling or to the fluid behavior.

In order to obtain some quantitative evaluation of the spread in the data, two types of regression analyses were applied to the j -factors and friction factors. The results of the regression analyses are presented in Tables II through V. A regression analysis was

TABLE II

REGRESSION ANALYSIS SUMMARY FOR LOG j VERSUS LOG Re

<u>Tube Bank Model</u>	<u>Calculated Relationships</u>	<u>Heating or Cooling</u>	<u>Number of Points</u>	<u>Minimum Reynolds Number</u>	<u>Maximum Reynolds Number</u>	<u>Maximum Percent Difference</u>	<u>Average* Absolute Percent Difference</u>
1	$j = 0.827 \text{ Re}^{-0.711}$	H + C	26	22.3	307	-25.9	12.7
1	$j = 1.10 \text{ Re}^{-0.809}$	H	14	22.3	164	8.8	2.88
1	$j = 1.17 \text{ Re}^{-0.757}$	C	12	35.7	307	-6.0	2.96
2	$j = 0.499 \text{ Re}^{-0.642}$	H + C	31	20.6	439	-25.4	7.00
2	$j = 0.499 \text{ Re}^{-0.645}$	H	24	20.6	439	-22.2	6.97
2	$j = 0.605 \text{ Re}^{-0.667}$	C	7	37.7	183	5.3	2.44
3	$j = 0.607 \text{ Re}^{-0.636}$	H + C**	23	3.46	91.8	-30.3	10.1
3	$j = 0.678 \text{ Re}^{-0.698}$	H	18	3.46	70.9	-17.0	5.2
3	$j = 0.747 \text{ Re}^{-0.790}$	C	5	16.7	91.8	-2.3	1.0

* Average Absolute Percent Difference = $\frac{\Sigma \text{ABS (Percent Difference)}}{\text{Number of Points}}$

** Regression Analysis includes points for both heating and cooling runs.

TABLE III

REGRESSION ANALYSIS SUMMARY FOR LOG f VERSUS LOG Re

Tube Bank Model	Calculated Relationship	Heating, Cooling, or Isothermal	Number of Points	Minimum Reynolds Number	Maximum Reynolds Number	Maximum Percent Difference	Average* Absolute Percent Difference
1	$f = 80.5 \text{ Re}^{-0.984}$	H + C + I	59	10.1	351	34.5	9.93
1	$f = 78.0 \text{ Re}^{-0.969}$	H	14	22.3	164	31.9	9.17
1	$f = 39.7 \text{ Re}^{-0.845}$	C	12	42.6	307	15.0	9.00
1	$f = 90.0 \text{ Re}^{-1.011}$	I	33	10.1	351	19.2	8.38
2	$f = 41.3 \text{ Re}^{-0.899}$	H + C + I	58	17.5	439	-42.9	11.5
2	$f = 44.3 \text{ Re}^{-0.894}$	H	23	17.5	439	-22.8	10.6
2	$f = 31.3 \text{ Re}^{-0.873}$	C	7	37.7	183	-19.3	10.1
2	$f = 36.7 \text{ Re}^{-0.880}$	I	28	18.7	425	-20.6	9.76
3	$f = 36.2 \text{ Re}^{-0.961}$	H + C + I **	39	1.92	113	-51.7	16.0
3	$f = 33.7 \text{ Re}^{-0.894}$	H	15	3.58	70.9	28.8	8.15
3	$f = 31.5 \text{ Re}^{-0.910}$	C	5	16.7	91.8	4.65	2.89
3	$f = 34.2 \text{ Re}^{-0.974}$	I	19	1.92	113	-36.6	21.0

* Average absolute percent difference = $\frac{\Sigma \text{ABS (Percent Difference)}}{\text{Number of Points}}$.

** H + C + I indicates that data points for heating, cooling, and isothermal pressure drop runs were used in the regression analysis.

TABLE IV

REGRESSION ANALYSIS SUMMARY FOR j VERSUS $Re^{-0.667}$

Tube Bank Model	Calculated Relationship	Heating or Cooling	Number of Points	Minimum Reynolds Number	Maximum Reynolds Number	Maximum Percent Difference	Average Absolute Percent Difference
1	$j = 0.738 Re^{-0.667} - 0.0023$	H + C	26	22.3	307	-27.6	13.0
1	$j = 0.765 Re^{-0.667} - 0.0086$	H	14	22.3	164	7.59	3.50
1	$j = 0.896 Re^{-0.667} - 0.0050$	C	12	22.3	307	7.72	3.86
2	$j = 0.540 Re^{-0.667} + 0.0009$	H + C	31	20.6	439	-24.9	6.84
2	$j = 0.543 Re^{-0.667} - 0.0001$	H	24	20.6	439	-20.0	7.03
2	$j = 0.599 Re^{-0.667} + 0.0003$	C	7	37.7	183	5.07	2.59
3	$j = 0.622 Re^{-0.667} + 0.0060$	H + C	23	3.46	91.8	-32.0	10.0
3	$j = 0.641 Re^{-0.667} - 0.0016$	H	18	3.46	70.9	-20.4	5.29
3	$j = 1.03 Re^{-0.667} - 0.0135$	C	5	16.7	91.8	3.40	1.33

TABLE V
REGRESSION ANALYSIS SUMMARY FOR f VERSUS $Re^{-1.0}$

<u>Tube Bank Model</u>	<u>Calculated Relationship</u>	<u>Heating, Cooling, or Isothermal</u>	<u>Number of Points</u>	<u>Minimum Reynolds Number</u>	<u>Maximum Reynolds Number</u>	<u>Maximum Percent Difference</u>	<u>Average Absolute Percent Difference</u>
1	$f = 99.2 Re^{-1.0} - 0.18$	H + C + I	59	10.1	351	63.1	18.3
1	$f = 84.8 Re^{-1.0} + 0.08$	H	14	22.3	164	31.7	10.3
1	$f = 71.6 Re^{-1.0} + 0.07$	C	12	42.6	307	18.9	6.7
1	$f = 103.6 Re^{-1.0} - 0.21$	I	33	10.1	351	19.6	18.5
2	$f = 56.7 Re^{-1.0} - 0.09$	H + C + I	58	17.5	439	-43.2	11.6
2	$f = 58.4 Re^{-1.0} + 0.14$	H	23	17.5	439	-35.6	12.7
2	$f = 49.0 Re^{-1.0} + 0.06$	C	7	37.7	183	-22.8	10.6
2	$f = 52.2 Re^{-1.0} + 0.11$	I	28	18.7	425	-27.3	10.9
3	$f = 41.1 Re^{-1.0} - 0.050$	H + C + I	39	1.92	113	-43.0	17.5
3	$f = 37.9 Re^{-1.0} + 0.42$	H	15	3.58	70.9	-39.7	10.4
3	$f = 39.7 Re^{-1.0} + 0.09$	C	5	16.7	91.8	-4.88	2.49
3	$f = 42.3 Re^{-1.0} - 0.29$	I	19	1.92	113	82.2	27.1

applied to the logarithm of the j -factors, friction factors, and modified Reynolds number to obtain relationships of the form

$$j = (AJ) \text{Re}^{BJ} \quad (7-1)$$

$$f = (AF) \text{Re}^{BF} \quad (7-2)$$

where AJ , BJ , AF , and BF are regression coefficients.

Results of laminar flow studies for flow inside tubes have indicated the j -factor is a linear function of $\text{Re}^{-2/3}$ and f is a linear function of Re^{-1} (20, 28). The results of the regression analyses based on Equations 7-1 and 7-2 indicate the existence of a similar linear relationship between j and $\text{Re}^{-2/3}$ and between f and Re^{-1} for non-Newtonian flow across ideal tube banks. Thus relationships of the form

$$j = \frac{C_1}{\text{Re}^{2/3}} + C_2 \quad (7-3)$$

$$f = \frac{D_1}{\text{Re}} + D_2 \quad (7-4)$$

where C_1 , C_2 , D_1 , and D_2 are regression coefficients were used in the second group of regression analysis. The constants C_2 and D_2 become increasingly significant as the Reynolds number approaches the transition flow regime, and the constants should be positive. The regression analyses gave negative values for C_2 and D_2 in some cases, and the negative values should not be used for extrapolation. The scatter in the experimental data makes it quite difficult to calculate reliable values for C_2 and D_2 .

The regression analyses based on Equations 7-1 and 7-3 gave

comparable results for the observed j -factors as a function of Reynolds number. The j -factor regression analyses also indicate that separate curves should be used for heating and cooling the CMC solutions. The curves based upon j as a function of $Re^{2/3}$ are presented in Figures 17, 19, and 21.

Examination of Tables III and V indicates that the regression analyses based upon $\log f$ versus $\log Re$ do a better job of fitting the observed data. The results of the analyses also indicate that the heating, cooling, and isothermal friction factors for a given tube bank may be represented by a single curve. Friction factor versus Reynolds number based upon the log-log regression analyses are presented in Figures 18, 20, and 22.

CHAPTER VIII

CONCLUSIONS AND RECOMMENDATIONS

Conclusions

The proposed modified Reed-Metzner Reynolds number successfully brings the j -factors and friction factors for CMC solutions having different rheological properties into agreement.

The determined curves for the friction factor versus the modified Reynolds number are in fair agreement with the accepted friction factor-Reynolds number curves for flow of Newtonian fluids across tube banks.

The experimental non-Newtonian fluid j -factor versus Reynolds number curves fall significantly below the accepted j -factor versus Reynolds number curves. This phenomenon is attributed to fouling and to increase in apparent viscosity with decreasing shear rate.

Different j -factor versus modified Reynolds number curves are obtained depending upon whether the CMC solution was being heated or cooled.

Recommendations

Heat transfer data and pressure drop data are needed for a wider range of Reynolds numbers. The behavior of other non-Newtonian fluids besides CMC solutions should also be investigated.

The installation of thermocouples at various locations on the surfaces of the tubes could provide useful information relative to the variation of the heat transfer rate with radial tube position.

The replacement of manometers with strain gauge pressure transducers for the pressure drop measurements should also be considered. A more rapid and more accurate response can be expected from the pressure transducers.

BIBLIOGRAPHY

1. Albertson, M. L., et al. Fluid Mechanics for Engineers. New Jersey: Prentice-Hall (1960), 562.
2. Bell, K. J. "Final Report--Cooperative Research Program on Shell and Tube Heat Exchangers," University of Delaware Experiment Station Bulletin No. 5 (1963).
3. Bergelin, O. P., G. A. Brown, and S. C. Doberstein. "Heat Transfer and Fluid Friction During Flow Across Banks of Tubes--IV; A Study of the Transition Zone Between Viscous and Turbulent Flow." Transactions A.S.M.E. 74 (1952), 953-960.
4. Bergelin, O. P., G. A. Brown, H. L. Hull, and F. W. Sullivan. "Heat Transfer and Fluid Friction During Viscous Flow Across Banks of Tubes--III; A Study of Tube Spacing and Tube Size." Transactions A.S.M.E. 72 (1950), 881-888.
5. Bergelin, O. P., A. P. Colburn, and H. L. Hull. "Heat Transfer and Fluid Friction During Flow Across Banks of Tubes," University of Delaware Engineering Experiment Station Bulletin No. 2 (1950).
6. Bergelin, O. P., E. S. Davis, and H. L. Hull. "A Study of Heat Transfer and Fluid Friction Across Banks of Tubes." Transactions A.S.M.E. 71 (1949), 369-374.
7. Boggs, J. H. and W. L. Sibbitt. "Thermal Conductivity Measurements of Viscous Liquids." Ind. Eng. Chem. 47 (1955), 288-293.
8. Boucher, D. F. and C. F. Lapple. "Pressure Drop Across Tube Banks: A Critical Comparison of Available Data and the Proposed Method of Comparison." Chem. Engr. Prog. 44 (1948), 117-134.
9. Chilton, T. H. and R. P. Genereaux. "Pressure Drop Across Tube Banks." Transactions A.I.Ch.E. 29 (1933), 161-173.
10. Christiansen, E. B. and S. E. Craig. "Heat Transfer to Pseudoplastic Fluids in Laminar Flow." A.I.Ch.E. Journal. 8 (1962), 154-160.
11. Clarke, L. and R. L. Davidson. Manual for Process Engineering Calculations. New York: McGraw-Hill (1962), 42.

12. Cruzan, C. G. "Non-Newtonian Fluid Flow Through a Staggered Square Tube Bank." M.S. Thesis, Oklahoma State University (1964).
13. Friedl, P. J. and K. J. Bell. "Approximate Solution for Creeping Flow in Complex Geometries: Flow Across Banks of Tubes." presented at December, 1960, meeting of American Institute of Chemical Engineers, Washington, D. C.
14. Grimison, E. D. "Correlation and Utilization of New Data on Flow Resistance and Heat Transfer for Cross Flow of Gases Over Tube Banks." Transactions A.S.M.E. 59 (1937), 583-594.
15. Gunter, A. Y. and W. A. Shaw. "A General Correlation of Friction Factors for Various Types of Surfaces in Cross Flow." Transactions A.S.M.E. 67 (1945), 643-660.
16. Happel, J. "Viscous Flow Relative to Arrays of Cylinders." A.I.Ch.E. Journal. 5 (1959), 174-177.
17. Huger, E. C. "Experimental Investigation of Effects of Equipment Size on Convection Heat Transfer and Flow Resistance in Cross Flow of Gases Over Tube Banks." Transactions A.S.M.E. 59 (1937), 573-581.
18. Lawrence, A. E. and T. K. Sherwood. "Heat Transmission to Water Flowing in Pipes." Ind. Eng. Chem. 23 (1931), 301-309.
19. Metzner, A. B. "Non-Newtonian Technology." Advances in Chemical Engineering--Volume I, New York: Academic Press (1956).
20. Metzner, A. B. "Heat Transfer in Non-Newtonian Fluids." Advances in Heat Transfer--Volume II, New York: Academic Press (1965).
21. Metzner, A. B. and J. C. Reed. "Flow of Non-Newtonian Fluids--Correlation of the Laminar, Transition, and Turbulent Flow Regions." A.I.Ch.E. Journal. 1 (1955), 434-440.
22. Metzner, A. B., R. D. Vaughn, and G. L. Houghton. "Heat Transfer to Non-Newtonian Fluids." A.I.Ch.E. Journal. 3 (1957), 92-100.
23. Mooney, M. Journal of Rheology. 2 (1931), 210.
24. Pierson, O. L. "Experimental Investigation of the Influence of Tube Arrangement on Convection Heat Transfer and Flow Resistance in Cross Flow of Gases Over Tube Banks." Transactions A.S.M.E. 59 (1937), 563-572.
25. Rabinowitsch, B. "Über die Viskosität und Elastizität von Solew." Z. Physik. Chem. 1 (1929), 145A.

26. Randolph, D. D. "A Capillary Viscometer for Non-Newtonian Fluids." M.S. Thesis, Oklahoma State University (1966).
27. Shah, M. N., E. E. Petersen, and A. Acrivos. "Heat Transfer From a Cylinder to a Power-Law Non-Newtonian Fluid." A.I.Ch.E. Journal. 8 (1962), 542-549.
28. Sieder, E. N. and G. E. Tate. "Heat Transfer and Pressure Drop of Liquids in Tubes." Ind. Eng. Chem. 28 (1936), 1429-1435.
29. Tamada, K. and H. Fujikawa. "The Steady Two Dimensional Flow of Viscous Fluid at Low Reynolds Numbers Passing Through an Infinite Row of Equal Parallel Circular Cylinders." Quart. Journ. Mech. and Applied Math. 10 (1957), 425-432.
30. Van Wazer, J. R., J. W. Lyons, K. Y. Kim, and R. E. Colwell. Viscosity and Flow Measurement. New York: Interscience Publishers (1963), 66-67.
31. Wilkinson, W. L. Non-Newtonian Fluids. New York: Pergamon Press (1960).

APPENDIX A
NOMENCLATURE

NOMENCLATURE

- A_m - Minimum cross-sectional area for flow across the tube bank
- A_o - Heat transfer area based upon the outside area of the tubes
- ADT - Regression coefficient for temperature difference as a function of differential thermocouple response
- AGAM - Regression coefficient for gamma as a function of temperature
- AK - Regression coefficient for water thermal conductivity as a function of temperature
- APR - Regression coefficient for water Prandtl number as a function of temperature
- AR - Regression coefficient for water Reynolds number properties as a function of temperature
- BGAM - Regression coefficient for gamma as a function of temperature
- BK - Regression coefficient for water thermal conductivity as a function of temperature
- BPR - Regression coefficient for water Prandtl number as a function of temperature
- BR - Regression coefficient for water Reynolds number properties as a function of temperature

- C_p - Heat capacity
 CNP - Regression coefficient for n prime as a function of temperature
 CPR - Regression coefficient for water Prandtl number as a function of temperature
 CR - Regression coefficient for water Reynolds number properties as a function of temperature
 D_c - Minimum clearance between tubes
 D_i - Inside tube diameter
 D_o, D_t - Outside tube diameter
 D_v - Volumetric hydraulic diameter
 DNP - Regression coefficient for n prime as a function of temperature
 $(du/du)_1$ - Shear rate at the wall
 $(du/dy)_{APP}$ - Apparent shear rate for flow across tube bank
 $(du/dy)_T$ - True shear rate for flow across tube bank
 E - Single thermocouple response
 F_a - Arrangement factor
 f - Friction factor
 G_m - Mass velocity at minimum cross-sectional flow area
 g_c - Conversion factor, 4.17×10^8 (lb._m-ft.)/(lb._f-hr.²)
 h_i - Heat transfer coefficient for flow inside tube
 h_o - Heat transfer coefficient for flow outside tubes
 J - Mechanical equivalent of heat, 778 lb._f-ft./Btu
 j - j -factor for heat transfer
 K - Power law consistency index
 K' - Reed-Metzner generalized power law consistency index

- K^* - Darcy law constant
 K_S - Viscometer spring constant
 k - Thermal conductivity
 L - Length of flow across tube bank
 M - Viscometer deflection reading
 N - Number of major restrictions encountered in flow through the tube bank
 Nu - Nusselt number
 n - Power law fluid behavior index
 n' - Reed-Metzner generalized power law behavior index
 P - Pitch, minimum center-to-center distance between adjacent tubes
 p - Pressure
 Pr - Prandtl number
 Q_{CMC}^* - Apparent amount of heat transferred to the CMC solution
 Q_w^* - Apparent amount of heat transferred to the water
 Q_{CCMC} - CMC solution heat gain correction accounting for frictional heating
 Q_{cw} - Water heat gain correction accounting for frictional heating
 Q_{CMC} - Net amount of heat transferred to the CMC solution
 Q_w - New amount of heat transferred to the water
 R_i - Tube inside radius
 R_o - Tube outside radius
 Re - Reynolds number
 r - Distance from axis of cylinder
 r_1 - Radius of viscometer bob

- r_2 - Inside radius of the rotating cylinder of the viscometer
 S_L - Longitudinal pitch, same as P
 S_T - Transverse pitch, center-to-center distance from tube to tube in one transverse tube row
 St - Stanton number
 R - Temperature
 T^* - Absolute temperature
 TA - Regression coefficient for temperature as a function of single thermocouple response
 TE - Regression coefficient for temperature as a function of single thermocouple response
 U_o - Overall heat transfer coefficient based on the outside heat transfer area
 V_r - Velocity in the radial direction
 V_θ - Angular velocity
 W - Mass flow rate
 γ - Reed-Metzner generalized viscosity coefficient
 γ_w - Value of γ at the wall temperature
 Δ - Ratio of non-Newtonian shear rate to the Newtonian shear rate
 ∇^2 - Laplacian operator
 ∇^4 - Biharmonic operator
 ΔE - Differential thermocouple response
 ΔP - Pressure drop
 $(\Delta T)_{CMC}$ - Temperature change for CMC solution flowing across the test section
 $(\Delta T)_w$ - Temperature change for water flowing across the test

section

- $(\Delta T)_{lm}$ - Log mean temperature difference
- ΔZ - Manometer differential
- θ - Angular distance
- μ - Newtonian fluid viscosity
- μ_A - Apparent viscosity
- μ_B - Bingham plastic viscosity
- ρ - Density
- τ - Shear stress
- τ_1 - Shear stress at the wall
- τ_0 - Bingham plastic yield stress
- ψ - Stream function
- Ω - Viscometer rotor speed

APPENDIX B

DATA REDUCTION PROCEDURE

DATA REDUCTION PROCEDURE

Reduction of Thermocouple Calibration Data

Differential Thermocouples

A linear regression analysis was applied to the differential thermocouple response data to obtain relationships of the form

$$T = (ADT) (\Delta E) \quad (B-1)$$

where

T = temperature change, °F

ΔE = thermocouple response, millivolts

ADT = linear regression coefficient, °F/millivolt

Single Thermocouples

The single thermocouple calibration data were analyzed using a linear regression analysis to obtain relationships of the form

$$T = (TA) (E) + TB \quad (B-2)$$

where

T = temperature, °F

E = thermocouple response, millivolts

TA and TB = regression coefficients

Reduction of Viscometer Data

The computer program used to reduce the viscometer data is given

in Appendix H.

The value of n , the flow behavior index, was determined by applying a linear regression analysis to the deflection and rotor speed data to obtain the relationship

$$\log M = (n) \log \Omega \quad (\text{B-3})$$

where

M = viscometer deflection reading, degrees

Ω = rotor speed, rpm

Van Wazer, et al., (30) and Cruzan (12) have presented equations for calculating the shear stress and the shear rate at the viscometer bob for a power law fluid. The equations are

$$\tau_1 = \frac{K_s M}{2\pi r_1^2 L} \quad (\text{B-4})$$

$$\left(\frac{du}{dy}\right)_1 = \frac{2 r_1^{2/n} \Omega^*}{n (r_1^{2/n} - r_1^{2/n})} \quad (\text{B-5})$$

where

τ_1 = shear stress at viscometer bob, dyne/cm.²

K_s = viscometer spring constant, dyne/cm.-deg.

M = viscometer deflection reading, deg.

r_1 = radius of viscometer bob, cm.

r_2 = radius of outer viscometer cylinder, cm.

L = length of viscometer bob, cm.

$\left(\frac{du}{dy}\right)_1$ = shear rate at viscometer bob, sec.⁻¹

Ω^* = viscometer rotor speed, radians/sec.

n = flow behavior index from Equation B-3

The value of K , the power law consistency index, was then found from

$$K = \frac{\tau_1}{\left(\frac{du}{dy}\right)_1^n} \quad (\text{B-6})$$

where

$$K = \text{power law consistency index, dyne-sec.}^n/\text{cm.}^2$$

The constants, K and n , obtained from the rotational viscometer data were then used to calculate the constants, K' and n' , for the generalized Reed-Metzner power law. The constants are related by the following equations:

$$n' = n \quad (\text{B-7})$$

$$K' = \left(\frac{3n+1}{4n}\right)^n K \quad (\text{B-8})$$

The generalized viscosity coefficient was calculated using the relationship given by Metzner and Reed (21):

$$\gamma = g_c 8^{n'-1} K' \quad (\text{B-9})$$

where

$$\gamma = \text{generalized viscosity coefficient, gm.-sec.}^{n'-2}/\text{cm.}$$

$$g_c = \text{conversion factor, gm.-cm./dyne-sec.}^2$$

A sample of the viscometer data reduction program results is presented in Table VI. The curve fit giving the value of n' was based on the viscometer data at speeds giving shear rates comparable to the shear rates existing in the tube banks. Capillary viscometer results obtained by Randolph (26) for some of the CMC solutions actually used in this research work are in good agreement with the Fann viscometer

TABLE VI

SAMPLE FANN VISCOMETER RAW DATA AND CALCULATED

RHEOLOGICAL PROPERTIES

CMC Solution Sample Number 1

Temperature = 94.7°F

Speed (rpm)	Deflection (deg.)	Shear Stress ($\frac{\text{dyne}}{\text{cm.}^2}$)	Shear Rate (sec.^{-1})	K ($\frac{\text{dyne-sec.}^n}{\text{cm.}^2}$)	K Prime ($\frac{\text{dyne-sec.}^{n'}}{\text{cm.}^2}$)	Gamma ($\frac{\text{gm-sec.}^{n'-2}}{\text{cm.}}$)	Apparent Viscosity Centipoise
300.0	71.2	326	522	3.222	3.431	1.988	62.4
200.0	53.2	243	348	3.247	3.457	2.004	69.9
100.0	31.7	145	174	3.226	3.435	1.991	83.3

N Prime = 0.738

Average Gamma = 1.994 $\frac{\text{gm-sec.}^{n'-2}}{\text{cm.}}$

Spring Constant = 325.0 $\frac{\text{dyne-cm.}}{\text{deg.}}$

results.

The "apparent shear rate" for the flow across the tube bank was calculated using

$$\text{Apparent Shear Rate} = \left(\frac{du}{dy}\right)_{\text{APP}} = \frac{V_{\text{max}}}{\left(\frac{\text{Minimum Clearance}}{2}\right)} \quad (\text{B-10})$$

For the 1.25 pitch ratio of the tube banks used,

$$\left(\frac{du}{dy}\right)_{\text{APP}} = \frac{V_m}{\frac{D_o}{8}} = \frac{8 V_m}{D_o} \quad (\text{B-11})$$

The "true shear rate" by analogy to the case for flow inside a tube is then

$$\text{True Shear Rate} = \left(\frac{du}{dy}\right)_T = \left(\frac{3n' + 1}{4n'}\right)^{n'} \left(\frac{8 V_m}{D_o}\right) \quad (\text{B-12})$$

In order to use the computer for data reduction, it was necessary to develop equations for γ and n' as a function of temperature. A regression analysis was applied to the γ and n' values obtained for a given sample at different temperatures. The resulting equations were

$$\log_e \gamma = \frac{AGAM}{T^*} + BGAM \quad (\text{B-13})$$

$$n' = CNP (T - 80.0) + DNP \quad (\text{B-14})$$

where

T^* = absolute temperature, °R

AGAM, BGAM = regression coefficients

T = temperature

CNP, DNP = regression coefficients

CMC Solution Physical Properties

Based upon results reported by Metzner, Vaughn, and Houghton (22), the heat capacity and density of water were used for the heat capacity and density of the CMC solutions. Boggs and Sibbitt (7) have reported the CMC solutions' thermal conductivities within 1 percent of the thermal conductivity of water; therefore, the thermal conductivity of water was used for the CMC solution calculations. The water thermal conductivities and viscosities were obtained from a chart presented by Clarke (11), and the densities were obtained from a table presented by Albertson (1).

Reduction of Heat Transfer Data

The computer program used to reduce to the heat transfer data is presented in Appendix H.

Heat transfer coefficients, Reynolds numbers, and j-factors were calculated for each of the several (usually four) sets of temperature readings obtained during each run.

The inlet and outlet temperature of the CMC solution and the water were calculated using Equation B-2. The temperature changes of the CMC solution and the water were calculated using Equation B-1 resulting from the differential thermocouple calibrations. The logarithmic mean temperature difference for heat transfer was calculated using

$$-\ (\Delta T)_{\text{lm}} = \frac{(T_{2w} - T_{1\text{CMC}}) - (T_{1w} - T_{2\text{CMC}})}{\log \frac{T_{2w} - T_{1\text{CMC}}}{T_{1w} - T_{2\text{CMC}}}} \quad (\text{B-15})$$

where

$T_{1\text{CMC}}$ = inlet CMC solution temperature, °F

$T_{2\text{CMC}}$ = outlet CMC solution temperature, °F

$T_{1\text{w}}$ = inlet water temperature, °F

$T_{2\text{w}}$ = outlet water temperature, °F

The apparent amounts of heat transferred to the CMC solution and to the water were calculated using the measured temperature changes obtained from the differential thermocouples. A heat capacity of 1.0 Btu per pound-°F was used for all calculations.

$$Q_{\text{CMC}}^* = C_p W_{\text{CMC}} (\Delta T)_{\text{CMC}} \quad (\text{B-16})$$

$$Q_w^* = C_p W_w (\Delta T)_w \quad (\text{B-17})$$

where

Q_{CMC}^* = apparent amount of heat gained by CMC solution, Btu/hr.

Q_w^* = apparent amount of heat gained by water, Btu/hr.

W_{CMC} = CMC solution mass flow rate, lb./hr.

W_w = water mass flow rate, lb./hr.

The pressure losses measured between the differential thermocouple locations were used to correct the apparent heat gains for frictional heating incurred by the CMC solution and water flowing through the test section. The heat corrections were calculated from

$$Q_{\text{CCMC}} = \frac{(\Delta P_{\text{CMC}}) (W_{\text{CMC}})}{(\rho_{\text{CMC}}) (J)} \quad (\text{B-18})$$

$$Q_{\text{cw}} = \frac{(\Delta P_w) (W_w)}{(\rho_w) (J)} \quad (\text{B-19})$$

where

Q_{CCMC} = heat gain of CMC solution due to pressure drop, Btu/hr.

ΔP_{CMC} = pressure drop for CMC solution between the differential thermocouples, lb._f/ft.²

ρ_{CMC} = CMC solution density, lb._m/ft.³

J = mechanical equivalent of heat, ft.-lb._f/Btu

Q_{CW} = heat gain of water due to pressure drop, Btu/hr.

ΔP_{W} = pressure drop for water between the differential thermocouples, lb._f/ft.²

Since the test section was well insulated and the temperature levels were not extreme, the heat losses from the system were assumed to be negligible. The net amounts of heat transferred are, therefore,

$$Q_{\text{CMC}} = Q_{\text{CMC}}^* - Q_{\text{CCMC}} \quad (\text{B-20})$$

$$Q_{\text{W}} = Q_{\text{W}}^* - Q_{\text{CW}} \quad (\text{B-21})$$

Some difficulty was incurred in obtaining satisfactory heat balances. Plots of the outside heat transfer coefficient based on both Q_{CMC} and Q_{W} versus the CMC solution flow rate indicated that use of Q_{W} for calculating h_{O} gave the most reasonable results. The inaccuracy of Q_{CMC} was attributed to an insufficient amount of mixing of the CMC solution. This conclusion was supported by the observed heat balance improvement when mixing blocks were added to the CMC solution system.

The overall heat transfer coefficient was calculated using

$$U_{\text{O}} = \frac{Q_{\text{W}}}{A_{\text{O}} (\Delta T)_{\text{lm}}} \quad (\text{B-22})$$

The heat transfer coefficient for the water flowing through the tubes was calculated using the Lawrence and Sherwood (18) correlation

$$\frac{h_i D_i}{k_i} = 0.058 (Re_w)^{0.7} (Pr_w)^{0.5} \quad (B-23)$$

The water thermal conductivity, $D_i \rho_w / \mu_w$, and Prandtl number were calculated as a function of temperature using equations developed with a linear regression analysis.

$$k_w = AK + BT (T_w - T_B) \quad (B-24)$$

$$\frac{D_i \rho_w}{\mu_w} = AR + BR T_w + CR T_w^2 \quad (B-25)$$

$$Pr_w = APR + BPR T_w + CPR T_w^2 \quad (B-26)$$

where

AK, BK, AR, BR, CR, APR, BPR, CPR = regression coefficients

$T_B = 90.0^\circ\text{F}$ for cooling runs

$T_B = 150.0^\circ\text{F}$ for heating runs

T_w = average water temperature, $^\circ\text{F}$

The heat transfer coefficient for the CMC solution flowing outside the tubes was calculated from

$$\frac{1}{h_o} = \frac{1}{U_o} - \frac{A_o}{h_i A_i} - \frac{(R_o - R_i) R_o}{k_{cu} R_m} \quad (B-27)$$

where

R_o = outside tube radius, ft.

R_i = inside tube radius, ft.

$R_m = (R_o + R_i) (0.5)$, ft.

k_{cu} = thermal conductivity, Btu/hr.-ft.- $^\circ\text{F}$

The wall temperature was calculated using

$$T_{WALL} = T_{AVCMC} + \frac{h_o}{U_o} (\Delta T)_{lm} \quad (B-28)$$

Equations B-13 and B-14 were then used to calculate γ , γ_w , and n' . The apparent viscosity for use in the Prandtl number was calculated using Equation 4-20.

$$\mu_A = \gamma \left(\frac{v_m}{D} \right)^{n'-1} \quad (4-20)$$

The thermal conductivity of the CMC solution was calculated using an equation of the form

$$k_{CMC} = k_{CMC}^o + AKC (T_{AVCMC} - 110.0) \quad (B-29)$$

where

k_{CMC}^o = thermal conductivity of water at 110.0°F, Btu/hr.-ft.-°F

AKC = regression coefficient

T_{AVCMC} = average CMC solution temperature, °F

The modified Reynolds number, Prandtl number, Sieder, Tate factor, and j-factor were calculated using Equations 4-18, 4-21, 4-23, and 4-25.

The values of Re, Pr, j, and the Sieder-Tate factor obtained for each set of temperature readings were then averaged.

Reduction of Pressure Drop Data

The pressure drop was calculated from the tube bank pressure drop manometer using

$$P = (\Delta Z) (\rho^* - \rho_w) (g/g_c) \quad (B-30)$$

where

ΔP = pressure drop, lb._f/ft.²

ΔZ = manometer reading, ft.

ρ^* = density of manometer fluid, lb._m/ft.³

ρ_w = density of water at room temperature, lb._m/ft.³

The friction factor was then calculated using Equation 4-24,

$$f = \frac{2 \Delta P g_c \rho_{CMC}}{4 G_m^2 N} \left(\frac{\gamma}{\gamma_w} \right)^{0.14} \quad (4-24)$$

where

ρ_{CMC} = density of CMC solution at average temperature, lb._m/ft.³

G_m = mass velocity at minimum cross-sectional flow area,
lb._m/ft.²-hr.

N = number of flow contractions

The average $(\gamma/\gamma_w)^{0.14}$ value calculated for the heat transfer data was used to calculate the friction factor for the non-isothermal runs.

APPENDIX C

THERMOCOUPLE CALIBRATION
RESULTS

DIFFERENTIAL THERMOCOUPLE CALIBRATION

RESULTS

Differential Thermocouple Set Number 1

CMC Solution Differential Thermocouple

For $(\Delta T)_{\text{CMC}} > 0$:

$$(\Delta T)_{\text{CMC}} = (5.69) (\Delta E)_{\text{CMC}}$$

$$\text{Standard Error} = 0.04^{\circ}\text{F}$$

For $(\Delta T)_{\text{CMC}} < 0$:

$$(\Delta T)_{\text{CMC}} = (5.66) (\Delta E)_{\text{CMC}}$$

$$\text{Standard Error} = 0.02^{\circ}\text{F}$$

Water Differential Thermocouple

For $(\Delta T)_{\text{w}} < 0$:

$$(\Delta T)_{\text{w}} = (-5.61) (\Delta E)_{\text{w}}$$

$$\text{Standard Error} = 0.03^{\circ}\text{F}$$

No water differential thermocouple calibration data at the proper temperature level were obtained for application to cooling runs. The constant for the conversion of $(\Delta E)_{\text{w}}$ to $(\Delta T)_{\text{w}}$ for cooling runs was estimated from the CMC differential thermocouple results. Later

thermocouple calibration data indicated that the estimated constant, 5.71°F per millivolt response, was quite reasonable.

Differential Thermocouple Set Number 2--

First Calibration

CMC Solution Differential Thermocouple

For $(\Delta T)_{\text{CMC}} > 0$:

$$(\Delta T)_{\text{CMC}} = (5.44) (\Delta E)$$

$$\text{Standard Error} = 0.16^\circ\text{F}$$

For $(\Delta T)_{\text{CMC}} < 0$:

$$(\Delta T)_{\text{CMC}} = (5.76) (\Delta E)$$

$$\text{Standard Error} = 0.02^\circ\text{F}$$

Water Differential Thermocouple

For $(\Delta T)_w < 0$:

$$(\Delta T)_w = (-5.45) (\Delta E)_w$$

$$\text{Standard Error} = 0.18$$

For $(\Delta T)_w > 0$:

$$(\Delta T)_w = (-5.91) (\Delta E)_w$$

$$\text{Standard Error} = 0.06^\circ\text{F}$$

The undesirably large standard errors obtained for the calibration of these thermocouples were attributed to discrepancies between

individual thermometers used to measure bath temperatures. Use of one thermometer to measure both bath temperatures gave much smaller standard errors for the next calibration of the differential thermocouples.

Differential Thermocouple Set Number 2--

Second Calibration

CMC Solution Differential Thermocouple

For $(\Delta T)_{\text{CMC}} > 0$:

$$(\Delta T)_{\text{CMC}} = 5.60 (\Delta E)_{\text{CMC}}$$

$$\text{Standard Error} = 0.03^\circ\text{F}$$

For $(\Delta T)_{\text{CMC}} < 0$:

$$(\Delta T)_{\text{CMC}} = 5.74 (\Delta E)_{\text{CMC}}$$

$$\text{Standard Error} = 0.04^\circ\text{F}$$

Water Differential Thermocouple

For $(\Delta T)_w < 0$:

$$(\Delta T)_w = (-5.47) (\Delta E)_w$$

$$\text{Standard Error} = 0.04^\circ\text{F}$$

For $(\Delta T)_w > 0$:

$$(\Delta T)_w = (-5.75) (\Delta E)_w$$

$$\text{Standard Error} = 0.06^\circ\text{F}$$

SINGLE THERMOCOUPLE CALIBRATION RESULTS

Single Thermocouple Set Number 1

CMC Solution Single Thermocouples

$$T_{\text{CMC}} = (29.6) (E)_{\text{CMC}} + 32.2$$

Standard Error = 0.02°F

Water Single Thermocouples

For 80 < T_w < 100:

$$T_w = (29.6) (E)_w + 32.2$$

Standard Error = 0.12°F

For 140 < T_w < 165:

$$T_w = (27.0) (E)_w + 40.3$$

Standard Error = 0.08°F

A single straight line was found to adequately express the temperature-thermocouple response relationship for both the CMC solution and water single thermocouples.

$$T = (28.0) (E) + 36.8$$

This relationship gives a standard error of 0.1°F.

APPENDIX D
RAW DATA FROM HEAT
TRANSFER RUNS

RUN NUMBER DESIGNATION PROCEDURE

Consider the run designated as Run Number 1-1.0-H1. The first number, 1, represents the tube bank model number. The second number, 1.0, represents the weight percent sodium carboxymethylcellulose (CMC) in the CMC solution. The letter, H, indicates that the run was a heating run; that is, the CMC solution was heated while passing through the test section. The letters, C and I, indicate cooling heat transfer runs and isothermal pressure drop runs, respectively. The last number, 1, indicates that the run was the first heating run using 1.0 percent CMC solution and Tube Bank Model Number 1.

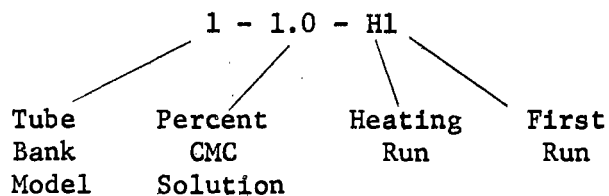


TABLE VII

HEAT TRANSFER RUN THERMOCOUPLE DATA

<u>Run Number</u>	<u>CMC Solution Inlet Thermocouple (Millivolts)</u>	<u>CMC Solution Outlet Thermocouple (Millivolts)</u>	<u>Water Inlet Thermocouple (Millivolts)</u>	<u>Water Outlet Thermocouple (Millivolts)</u>	<u>CMC Solution Differential Thermocouple (Millivolts)</u>	<u>Water Differential Thermocouple (Millivolts)</u>
3-1.0-H1	2.448	x	4.067	4.067	2.301	0.133
3-1.0-H2	2.686	x	4.071	4.066	1.070	0.074
3-1.0-H3	2.427	x	4.061	4.053	2.330	0.145
3-1.0-H4	2.644	x	4.023	4.011	1.065	0.182
3-1.0-H5	2.720	x	4.076	4.065	0.787	0.197
3-1.0-H6	2.376	x	3.984	3.980	2.252	0.143
3-1.0-C1	2.657	x	1.970	2.005	-0.166	-0.139
3-1.0-C2	2.660	x	1.994	2.027	-0.234	-0.123
3-1.0-C3	2.650	x	1.972	1.999	-0.358	-0.114
3-1.0-C4	2.616	x	1.948	1.974	-0.701	-0.090
3-1.0-C5	2.544	x	1.948	1.982	-0.158	-0.118
3-1.5-H1	3.174	3.242	4.268	4.195	0.223	0.168

TABLE VII (Continued)

<u>Run Number</u>	<u>CMC Solution Inlet Thermocouple (Millivolts)</u>	<u>CMC Solution Outlet Thermocouple (Millivolts)</u>	<u>Water Inlet Thermocouple (Millivolts)</u>	<u>Water Outlet Thermocouple (Millivolts)</u>	<u>CMC Solution Differential Thermocouple (Millivolts)</u>	<u>Water Differential Thermocouple (Millivolts)</u>
3-1.5-H2	3.098	3.186	4.166	4.089	0.297	0.156
3-1.5-H3	3.026	3.117	4.109	4.029	0.477	0.146
3-1.5-H4	3.043	3.160	4.200	4.115	0.556	0.145
3-1.5-H5	2.899	3.113	4.242	4.183	0.895	0.104
3-1.5-H6	3.035	3.037	4.238	4.349	x	0.166
3-1.5-H7	2.672	2.997	4.017	4.023	0.748	0.108
3-1.5-H8	2.979	3.206	4.270	4.243	0.503	0.142
3-1.5-H9	3.093	3.378	4.415	4.390	0.611	0.142
3-1.5-H10	2.970	3.413	4.567	4.572	0.888	0.136
3-1.5-H11	2.953	3.410	4.613	4.599	0.816	0.195
3-1.5-H12	3.222	3.389	4.653	4.643	0.353	0.302
2-1.0-H1	2.652	2.950	4.122	4.093	1.260	0.123
2-1.0-H2	2.861	2.997	4.112	4.075	0.576	0.149

TABLE VII (Continued)

Run Number	CMC Solution Inlet Thermocouple (Millivolts)	CMC Solution Outlet Thermocouple (Millivolts)	Water Inlet Thermocouple (Millivolts)	Water Outlet Thermocouple (Millivolts)	CMC Solution Differential Thermocouple (Millivolts)	Water Differential Thermocouple (Millivolts)
2-1.0-H3	2.517	2.852	4.121	4.093	1.377	0.137
2-1.0-H4	2.811	2.926	4.097	4.054	0.509	0.189
2-1.0-H5	2.645	2.864	4.207	4.162	0.909	0.179
2-1.0-H6	2.719	2.862	4.096	4.052	0.538	0.203
2-1.0-H7	2.390	2.788	4.261	4.222	1.333	0.172
2-1.0-C1	2.903	2.777	1.765	1.798	-0.373	-0.126
2-1.0-C2	3.085	2.847	1.783	1.810	-0.705	-0.100
2-1.0-C3	2.835	2.747	1.871	1.901	-0.231	-0.124
2-1.0-C4	3.017	2.922	1.827	1.865	-0.272	-0.173
2-1.0-C5	3.217	3.042	1.898	1.930	-0.524	-0.134
2-1.0-C6	3.082	2.858	1.897	1.917	-0.652	-0.095
2-0.5-H1	2.232	2.648	4.189	4.152	1.303	0.173
2-0.5-H2	2.400	2.673	4.155	4.107	0.801	0.208

TABLE VII (Continued)

Run Number	CMC Solution Inlet Thermocouple (Millivolts)	CMC Solution Outlet Thermocouple (Millivolts)	Water Inlet Thermocouple (Millivolts)	Water Outlet Thermocouple (Millivolts)	CMC Solution Differential Thermocouple (Millivolts)	Water Differential Thermocouple (Millivolts)
2-0.5-H3	2.520	2.719	4.196	4.147	0.653	0.225
2-0.5-H4	2.555	2.742	4.222	4.163	0.588	0.249
2-0.5-H5	2.593	2.753	4.187	4.127	0.516	0.278
2-0.5-H6	2.179	2.628	4.309	4.266	1.418	0.193
2-0.5-C1	3.044	2.820	1.752	1.784	-0.742	-0.107
2-1.0-H8	2.478	2.827	4.131	4.100	1.720	0.140
2-1.0-H9	2.663	2.848	4.065	4.026	0.922	0.160
2-1.0-H10	2.842	2.982	4.227	4.188	0.695	0.190
2-1.0-H11	2.862	2.977	4.202	4.162	0.573	0.194
2-1.0-H12	2.450	2.828	4.286	4.252	1.877	0.157
2-1.0-H13	2.382	2.747	4.325	4.258	1.818	0.305
2-1.0-H14	2.372	2.742	4.313	4.242	1.814	0.309
2-1.0-H15	2.497	2.740	4.316	4.237	1.190	0.361

TABLE VII (Continued)

<u>Run Number</u>	<u>CMC Solution Inlet Thermocouple (Millivolts)</u>	<u>CMC Solution Outlet Thermocouple (Millivolts)</u>	<u>Water Inlet Thermocouple (Millivolts)</u>	<u>Water Outlet Thermocouple (Millivolts)</u>	<u>CMC Solution Differential Thermocouple (Millivolts)</u>	<u>Water Differential Thermocouple (Millivolts)</u>
2-1.0-H16	2.539	2.696	4.283	4.188	0.790	0.404
2-1.0-H17	2.654	2.758	4.186	4.101	0.587	0.397
2-1.0-H18	2.508	2.750	4.303	4.230	1.200	0.348
1-1.0-H1	2.156	2.723	4.239	4.133	2.839	0.567
1-1.0-H2	2.221	2.572	4.064	3.973	1.741	0.567
1-1.0-H3	2.381	2.635	4.118	4.021	1.216	0.596
1-1.0-H4	2.397	2.587	4.152	4.032	0.948	0.632
1-1.0-H5	2.382	2.558	4.162	4.044	0.818	0.678
1-1.0-H6	2.312	2.542	4.202	4.072	1.159	0.663
1-1.0-H7	2.217	2.571	4.265	4.146	1.762	0.641
1-1.0-H8	2.043	2.656	4.362	4.247	3.032	0.607
1-1.0-C1	2.817	2.518	1.752	1.768	-1.317	-0.133
1-1.0-C2	2.851	2.647	1.798	1.828	-0.877	-0.154

TABLE VII (Continued)

<u>Run Number</u>	<u>CMC Solution Inlet Thermocouple (Millivolts)</u>	<u>CMC Solution Outlet Thermocouple (Millivolts)</u>	<u>Water Inlet Thermocouple (Millivolts)</u>	<u>Water Outlet Thermocouple (Millivolts)</u>	<u>CMC Solution Differential Thermocouple (Millivolts)</u>	<u>Water Differential Thermocouple (Millivolts)</u>
1-1.0-C3	2.817	2.677	1.829	1.860	-0.563	-0.168
1-1.0-C4	2.813	2.697	1.825	1.858	-0.460	-0.180
1-1.0-C5	2.735	2.640	1.805	1.837	-0.358	-0.178
1-1.0-C6	3.011	2.694	1.857	1.886	-1.402	-0.137
1-0.5-H1	2.045	2.632	4.143	4.032	2.928	0.569
1-0.5-H2	2.174	2.574	4.196	4.072	2.045	0.639
1-0.5-H3	2.363	2.627	4.206	4.084	1.377	0.644
1-0.5-H4	2.354	2.565	4.180	4.050	1.101	0.671
1-0.5-H5	2.338	2.520	4.132	4.002	0.937	0.678
1-0.5-H6	1.987	2.592	4.262	4.147	3.047	0.602
1-0.5-C1	2.959	2.656	1.842	1.872	-1.477	-0.141
1-0.5-C2	2.815	2.618	1.805	1.837	-0.902	-0.152
1-0.5-C3	2.767	2.626	1.812	1.848	-0.640	-0.159

TABLE VII (Concluded)

<u>Run Number</u>	<u>CMC Solution Inlet Thermocouple (Millivolts)</u>	<u>CMC Solution Outlet Thermocouple (Millivolts)</u>	<u>Water Inlet Thermocouple (Millivolts)</u>	<u>Water Outlet Thermocouple (Millivolts)</u>	<u>CMC Solution Differential Thermocouple (Millivolts)</u>	<u>Water Differential Thermocouple (Millivolts)</u>
1-0.5-C4	2.781	2.672	1.863	1.898	-0.486	-0.171
1-0.5-C5	2.757	2.667	1.879	1.916	-0.403	-0.172
1-0.5-C6	3.019	2.682	1.777	1.811	-1.627	-0.150

TABLE VIII

HEAT TRANSFER RUN FLOW RATE AND MANOMETER DATA

Run Number	CMC Solution Flow Rate (lb./hr.)	Water Flow Rate (lb./hr.)	Tube Bank Manometer Fluid	Tube Bank Manometer Differential (in.)	CMC Solution Orifice Manometer Differential (in.)	Water Orifice Manometer Differential (in.)	CMC Solution Sample Number
3-1.0-H1	2494	27000	CCl ₄	8.62	0.70	24.4	1
3-1.0-H2	6857	27000	CCl ₄	18.10	4.10	24.4	1
3-1.0-H3	2523	27000	CCl ₄	5.18	0.70	24.4	1
3-1.0-H4	7027	27000	CCl ₄	14.68	3.90	24.4	1
3-1.0-H5	10980	27000	CCl ₄	20.46	9.24	24.4	1
3-1.0-H6	2567	27000	CCl ₄	5.91	0.99	24.4	1
3-1.0-C1	10657	27000	CCl ₄	17.10	8.79	24.4	2
3-1.0-C2	7917	27000	CCl ₄	12.51	4.50	24.4	2
3-1.0-C3	5455	27000	CCl ₄	8.57	2.33	24.4	2
3-1.0-C4	2569	27000	CCl ₄	4.53	0.82	24.4	2
3-1.0-C5	10831	27000	CCl ₄	16.42	8.85	24.4	2
3-1.5-H1	13490	27000	CCl ₄	x	13.70	24.4	12

TABLE VIII (Continued)

<u>Run Number</u>	<u>CMC Solution Flow Rate (lb./hr.)</u>	<u>Water Flow Rate (lb./hr.)</u>	<u>Tube Bank Manometer Fluid</u>	<u>Tube Bank Manometer Differential (in.)</u>	<u>CMC Solution Orifice Manometer Differential (in.)</u>	<u>Water Orifice Manometer Differential (in.)</u>	<u>CMC Solution Sample Number</u>
3-1.5-H2	11370	27000	CCl ₄	x	9.68	24.4	13
3-1.5-H3	9746	27000	CCl ₄	48.85	7.17	24.4	14
3-1.5-H4	7007	27000	CCl ₄	38.80	3.54	24.4	15
3-1.5-H5	2593	27000	CCl ₄	x	0.45	24.4	16
3-1.5-H6	10619	27000	TBE	11.88	8.42	24.4	1819
3-1.5-H7	2586	27000	TBE	4.17	0.44	24.4	1819
3-1.5-H8	4966	27000	TBE	6.09	1.85	24.4	20
3-1.5-H9	3744	27000	TBE	6.65	0.93	24.4	21
3-1.5-H10	2569	27000	TBE	5.06	0.39	24.4	22
3-1.5-H11	2570	22400	TBE	5.27	0.41	15.6	2324
3-1.5-H12	6517	19050	TBE	10.16	3.30	9.9	2324
2-1.0-H1	2610	27000	CCl ₄	x	0.35	22.3	25
2-1.0-H2	7520	27000	CCl ₄	18.85	3.90	21.5	26

TABLE VIII (Continued)

<u>Run Number</u>	<u>CMC Solution Flow Rate (lb./hr.)</u>	<u>Water Flow Rate (lb./hr.)</u>	<u>Tube Bank Manometer Fluid</u>	<u>Tube Bank Manometer Differential (in.)</u>	<u>CMC Solution Orifice Manometer Differential (in.)</u>	<u>Water Orifice Manometer Differential (in.)</u>	<u>CMC Solution Sample Number</u>
2-1.0-H3	2600	27000	CCl ₄	6.60	0.44	21.6	27
2-1.0-H4	9750	27000	CCl ₄	19.55	6.72	22.1	28
2-1.0-H5	4990	27000	CCl ₄	8.88	1.94	20.8	29
2-1.0-H6	8470	27000	CCl ₄	13.88	5.13	21.1	3031
2-1.0-H7	2590	27000	CCl ₄	5.40	0.59	21.1	3031
2-1.0-C1	5730	27000	CCl ₄	10.25	2.20	20.9	3235
2-1.0-C2	2550	27000	CCl ₄	5.06	0.49	20.9	3235
2-1.0-C3	8220	27000	CCl ₄	13.97	4.65	20.9	3235
2-1.0-C4	9970	27000	CCl ₄	15.64	7.25	20.6	3235
2-1.0-C5	4380	27000	CCl ₄	5.61	1.29	20.8	3637
2-1.0-C6	2540	27000	CCl ₄	3.25	0.50	20.7	3637
2-0.5-H1	2590	27000	CCl ₄	3.89	0.17	20.7	3941
2-0.5-H2	4991	27000	CCl ₄	7.11	1.50	20.7	3941

TABLE VIII (Continued)

<u>Run Number</u>	<u>CMC Solution Flow Rate (lb./hr.)</u>	<u>Water Flow Rate (lb./hr.)</u>	<u>Tube Bank Manometer Fluid</u>	<u>Tube Bank Manometer Differential (in.)</u>	<u>CMC Solution Orifice Manometer Differential (in.)</u>	<u>Water Orifice Manometer Differential (in.)</u>	<u>CMC Solution Sample Number</u>
2-0.5-H3	6788	27000	CCl ₄	8.91	3.17	20.7	3941
2-0.5-H4	8136	27000	CCl ₄	7.83	4.76	22.9	42
2-0.5-H5	10670	27000	CCl ₄	9.89	8.33	22.8	4344
2-0.5-H6	2556	27000	CCl ₄	2.18	0.49	22.8	4344
2-0.5-C1	2490	27000	CCl ₄	1.69	0.60	22.8	45
2-1.0-H8	2615	27000	CCl ₄	10.10	0.43	22.6	4647
2-1.0-H9	5511	27000	CCl ₄	17.87	2.03	22.6	4647
2-1.0-H10	8546	27000	CCl ₄	21.72	4.77	22.8	4850
2-1.0-H11	10490	27000	CCl ₄	24.60	7.64	22.8	4850
2-1.0-H12	2599	27000	CCl ₄	6.95	0.80	22.8	4850
2-1.0-H13	2600	14750	CCl ₄	5.90	0.86	6.6	51
2-1.0-H14	2610	13940	CCl ₄	5.63	0.85	6.0	5256
2-1.0-H15	4385	13940	CCl ₄	8.81	1.70	6.0	5256

TABLE VIII (Continued)

<u>Run Number</u>	<u>CMC Solution Flow Rate (lb./hr.)</u>	<u>Water Flow Rate (lb./hr.)</u>	<u>Tube Bank Manometer Fluid</u>	<u>Tube Bank Manometer Differential (in.)</u>	<u>CMC Solution Orifice Manometer Differential (in.)</u>	<u>Water Orifice Manometer Differential (in.)</u>	<u>CMC Solution Sample Number</u>
2-1.0-H16	7552	13940	CCl ₄	14.86	4.05	6.0	5256
2-1.0-H17	10040	13940	CCl ₄	18.97	6.89	6.0	5256
2-1.0-H18	4278	13940	CCl ₄	8.09	1.68	6.0	5256
1-1.0-H1	2619	13400	CCl ₄	10.87	0.48	6.0	5860
1-1.0-H2	4274	13400	CCl ₄	14.57	1.40	5.9	5860
1-1.0-H3	6480	13400	CCl ₄	19.58	3.02	5.9	5860
1-1.0-H4	8969	13400	CCl ₄	22.83	5.86	5.7	6163
1-1.0-H5	11120	13400	CCl ₄	25.85	9.16	5.7	6163
1-1.0-H6	7428	13400	CCl ₄	18.42	4.24	5.7	6163
1-1.0-H7	4764	13400	CCl ₄	12.07	2.00	5.7	6465
1-1.0-H8	2613	13400	CCl ₄	7.13	0.56	5.7	6465
1-1.0-C1	2555	27000	CCl ₄	5.70	0.68	23.2	6667
1-1.0-C2	4257	27000	CCl ₄	8.15	1.50	23.2	6667

TABLE VIII (Continued)

<u>Run Number</u>	<u>CMC Solution Flow Rate (lb./hr.)</u>	<u>Water Flow Rate (lb./hr.)</u>	<u>Tube Bank Manometer Fluid</u>	<u>Tube Bank Manometer Differential (in.)</u>	<u>CMC Solution Orifice Manometer Differential (in.)</u>	<u>Water Orifice Manometer Differential (in.)</u>	<u>CMC Solution Sample Number</u>
1-1.0-C3	6572	27000	CCl ₄	12.24	3.20	23.2	6869
1-1.0-C4	8394	27000	CCl ₄	15.70	5.10	23.2	6869
1-1.0-C5	10240	27000	CCl ₄	18.55	7.42	23.2	7071
1-1.0-C6	2542	27000	CCl ₄	4.79	0.80	23.2	7071
1-0.5-H1	2607	13400	CCl ₄	8.38	0.60	6.0	73
1-0.5-H2	4143	13400	CCl ₄	12.50	1.38	6.0	74
1-0.5-H3	6410	13400	CCl ₄	14.99	3.06	6.0	7576
1-0.5-H4	8502	13400	CCl ₄	18.86	5.34	6.0	7576
1-0.5-H5	10080	13400	CCl ₄	20.44	7.42	5.9	7778
1-0.5-H6	2571	13400	CCl ₄	6.38	0.72	5.9	7778
1-0.5-C1	2525	27000	CCl ₄	3.48	0.70	23.3	8081
1-0.5-C2	4334	27000	CCl ₄	5.38	1.50	23.3	8081
1-0.5-C3	6204	27000	CCl ₄	7.73	3.04	23.3	8283

TABLE VIII (Concluded)

<u>Run Number</u>	<u>CMC Solution Flow Rate (lb./hr.)</u>	<u>Water Flow Rate (lb./hr.)</u>	<u>Tube Bank Manometer Fluid</u>	<u>Tube Bank Manometer Differential (in.)</u>	<u>CMC Solution Orifice Manometer Differential (in.)</u>	<u>Water Orifice Manometer Differential (in.)</u>	<u>CMC Solution Sample Number</u>
1-0.5-C4	8410	27000	CCl ₄	10.70	5.34	23.3	8283
1-0.5-C5	10162	27000	CCl ₄	12.66	7.60	23.3	8485
1-0.5-C6	2514	27000	CCl ₄	3.13	0.84	23.3	8485

x - Reading not obtained due to manometer difficulties

CCl₄ - Carbontetrachloride

TBE - Tetrabromoethane

APPENDIX E

CALCULATED RESULTS FOR
HEAT TRANSFER RUNS

TABLE IX

CALCULATED TEMPERATURE DATA FOR HEAT TRANSFER RUNS

Run Number	CMC Solution Inlet Temperature (°F)	CMC Solution Outlet Temperature (°F)	Water Inlet Temperature (°F)	Water Outlet Temperature (°F)	CMC Solution Temperature Change (°F)	Water Temperature Change (°F)
3-1.0-H1	104.6	117.7	150.0	150.2	13.1	-0.747
3-1.0-H2	111.6	117.7	150.1	149.9	6.09	-0.977
3-1.0-H3	103.9	117.2	149.8	149.6	13.3	-0.814
3-1.0-H4	110.4	116.4	148.8	148.5	6.06	-1.022
3-1.0-H5	112.6	117.1	150.2	149.9	4.48	-1.106
3-1.0-H6	102.4	115.2	148.8	147.7	12.8	-0.803
3-1.0-C1	110.7	109.8	90.4	91.4	-0.940	0.795
3-1.0-C2	110.8	109.5	91.1	92.1	-1.32	0.704
3-1.0-C3	110.5	108.5	90.5	91.3	-2.03	0.652
3-1.0-C4	109.5	105.6	89.8	90.5	-3.97	0.515
3-1.0-C5	107.4	106.5	89.8	90.8	-0.894	0.675
3-1.5-H1	126.0	128.0	155.4	153.4	1.27	-0.943

TABLE IX (Continued)

Run Number	CMC Solution Inlet Temperature (°F)	CMC Solution Outlet Temperature (°F)	Water Inlet Temperature (°F)	Water Outlet Temperature (°F)	CMC Solution Temperature Change (°F)	Water Temperature Change (°F)
3-1.5-H2	123.4	126.0	152.2	150.2	1.69	-0.876
3-1.5-H3	121.6	124.3	151.1	149.0	2.54	-0.820
3-1.5-H4	122.1	125.6	153.6	151.3	3.17	-0.814
3-1.5-H5	117.9	124.2	154.7	153.1	5.10	-0.584
3-1.5-H6	121.9	122.0	154.6	157.6	x	-0.932
3-1.5-H7	111.2	120.8	148.6	148.8	4.26	-0.606
3-1.5-H8	120.2	127.0	155.5	154.7	2.86	-0.797
3-1.5-H9	123.6	132.0	159.4	158.7	3.48	-0.797
3-1.5-H10	120.0	133.1	163.5	163.6	5.06	-0.764
3-1.5-H11	119.5	133.0	164.7	164.3	4.65	-1.09
3-1.5-H12	127.4	132.4	165.8	165.5	2.01	-1.70
2-1.0-H1	111.1	119.4	152.2	151.4	7.14	-0.674
2-1.0-H2	116.9	120.7	151.9	150.9	3.27	-0.817

TABLE IX (Continued)

Run Number	CMC Solution Inlet Temperature (°F)	CMC Solution Outlet Temperature (°F)	Water Inlet Temperature (°F)	Water Outlet Temperature (°F)	CMC Solution Temperature Change (°F)	Water Temperature Change (°F)
2-1.0-H3	107.3	116.7	152.2	15.14	7.81	-0.751
2-1.0-H4	115.5	118.7	151.5	150.3	2.89	-1.04
2-1.0-H5	110.9	117.0	154.6	153.3	5.15	-0.981
2-1.0-H6	112.9	116.9	151.5	150.3	3.05	-1.11
2-1.0-H7	103.7	114.9	156.1	155.0	7.56	-0.943
2-1.0-C1	118.1	114.6	86.2	87.1	-2.11	0.743
2-1.0-C2	123.3	116.5	86.7	87.5	-4.00	0.590
2-1.0-C3	116.2	113.7	89.2	90.0	-1.31	0.732
2-1.0-C4	121.3	118.6	88.0	89.0	-1.54	1.02
2-1.0-C5	126.9	122.0	89.9	90.8	-2.97	0.791
2-1.0-C6	123.1	116.8	89.9	90.5	-3.70	0.561
2-0.5-H1	99.3	110.9	154.0	153.1	7.39	-0.948
2-0.5-H2	104.0	111.6	153.1	151.8	4.54	-1.14

TABLE IX (Continued)

Run Number	CMC Solution Inlet Temperature (°F)	CMC Solution Outlet Temperature (°F)	Water Inlet Temperature (°F)	Water Outlet Temperature (°F)	CMC Solution Temperature Change (°F)	Water Temperature Change (°F)
2-0.5-H3	107.4	112.9	154.3	152.9	3.70	-1.23
2-0.5-H4	108.3	113.6	155.0	153.4	3.33	-1.36
2-0.5-H5	109.4	113.9	154.0	152.4	2.93	-1.52
2-0.5-H6	97.8	110.4	157.5	156.2	8.04	-1.06
2-0.5-C1	122.0	115.8	85.9	86.8	-4.21	0.631
2-1.0-H8	106.2	116.0	152.5	151.6	9.75	-0.767
2-1.0-H9	111.4	116.5	150.6	149.5	5.23	-0.877
2-1.0-H10	116.4	120.3	155.2	154.1	3.94	-1.04
2-1.0-H11	116.9	120.2	154.5	153.3	3.25	-1.06
2-1.0-H12	105.4	116.0	156.8	155.9	10.6	-0.860
2-1.0-H13	103.5	113.7	157.9	156.0	10.3	-1.67
2-1.0-H14	103.2	113.6	157.6	155.6	10.3	-1.69
2-1.0-H15	106.7	113.5	157.6	155.4	6.75	-1.98

TABLE IX (Continued)

Run Number	CMC Solution Inlet Temperature (°F)	CMC Solution Outlet Temperature (°F)	Water Inlet Temperature (°F)	Water Outlet Temperature (°F)	CMC Solution Temperature Change (°F)	Water Temperature Change (°F)
2-1.0-H16	107.9	112.3	156.7	154.1	4.48	-2.21
2-1.0-H17	111.1	114.0	154.0	151.6	3.33	-2.18
2-1.0-H18	107.0	113.8	157.3	155.2	6.80	-1.91
1-1.0-H1	97.2	113.0	155.5	152.5	16.1	-3.10
1-1.0-H2	99.0	108.8	150.6	148.0	9.87	-3.10
1-1.0-H3	103.5	110.6	152.1	149.4	6.89	-3.26
1-1.0-H4	103.9	109.2	153.1	149.7	5.38	-3.46
1-1.0-H5	103.5	108.4	153.3	150.0	4.64	-3.71
1-1.0-H6	101.5	108.0	154.5	150.8	6.57	-3.63
1-1.0-H7	98.9	108.8	156.2	152.9	9.99	-3.51
1-1.0-H8	94.0	111.2	158.9	155.7	17.2	-3.32
1-1.0-C1	115.7	107.3	85.6	86.3	-7.56	0.765
1-1.0-C2	116.6	110.9	87.1	88.0	-5.03	0.886

TABLE IX (Continued)

Run Number	CMC Solution Inlet Temperature (°F)	CMC Solution Outlet Temperature (°F)	Water Inlet Temperature (°F)	Water Outlet Temperature (°F)	CMC Solution Temperature Change (°F)	Water Temperature Change (°F)
1-1.0-C3	115.7	111.8	88.0	88.9	-3.23	0.966
1-1.0-C4	115.6	112.3	87.9	88.8	-2.64	1.04
1-1.0-C5	113.4	110.7	87.3	88.2	-2.05	1.02
1-1.0-C6	121.1	112.2	88.8	89.6	-8.05	0.788
1-0.5-H1	94.1	110.5	152.8	149.7	16.6	-3.11
1-0.5-H2	97.7	108.9	154.3	150.8	11.6	-3.50
1-0.5-H3	103.0	110.4	154.6	151.2	7.81	-3.52
1-0.5-H4	102.7	108.6	153.8	150.2	6.24	-3.67
1-0.5-H5	102.3	107.4	152.5	148.9	5.31	-3.71
1-0.5-H6	92.4	109.4	156.1	152.9	17.3	-3.29
1-0.5-C1	119.7	111.2	88.4	89.2	-8.48	0.811
1-0.5-C2	115.6	110.1	87.3	88.2	-5.18	0.874
1-0.5-C3	114.3	110.3	87.5	88.5	-3.67	0.914

TABLE IX (Concluded)

Run Number	CMC Solution Inlet Temperature (°F)	CMC Solution Outlet Temperature (°F)	Water Inlet Temperature (°F)	Water Outlet Temperature (°F)	CMC Solution Temperature Change (°F)	Water Temperature Change (°F)
1-0.5-C4	114.7	111.6	89.0	90.0	-2.79	0.983
1-0.5-C5	114.0	111.5	89.4	90.4	-2.31	0.989
1-0.5-C6	121.3	111.9	86.6	87.5	-9.34	0.863

x - CMC solution differential thermocouple was not operating

TABLE X
CALCULATED HEAT TRANSFER COEFFICIENTS AND PRESSURE DROP
FOR HEAT TRANSFER RUNS

Run Number	Maximum Velocity, V_m (ft./sec.)	Q Based on CMC Sol. T (Btu/hr.)	Q Based on Water T (Btu/hr.)	Log Mean Delta T ($^{\circ}F$)	Overall Heat Transfer Coefficient (Btu/hr. ft. ² $^{\circ}F$)	Water Heat Transfer Coefficient (Btu/hr. ft. ² $^{\circ}F$)	CMC Solution Heat Transfer Coefficient (Btu/hr. ft. ² $^{\circ}F$)	Tube Bank Pressure Drop (lb. _f /ft. ²)
3-1.0-H1	0.318	32700	-20700	-38.6	174	1632	151	26.4
3-1.0-H2	0.874	41500	-26900	-35.3	247	1631	204	39.0
3-1.0-H3	0.322	33400	-22500	-38.8	188	1631	162	15.9
3-1.0-H4	0.896	42300	-28100	-35.2	259	1627	212	45.0
3-1.0-H5	1.400	48300	-30400	-35.2	280	1632	226	62.7
3-1.0-H6	0.327	32900	-22200	-38.5	187	1621	161	18.1
3-1.0-C1	1.36	-10800	20900	19.3	350	1409	261	52.4
3-1.0-C2	1.01	-10900	18500	18.6	322	1411	245	38.3
3-1.0-C3	0.695	-11200	17100	18.6	296	1409	229	26.3
3-1.0-C4	0.328	-10200	13400	17.3	249	1406	200	13.9
3-1.0-C5	1.38	-10600	17700	16.7	343	1406	256	50.3
3-1.5-H1	1.72	15600	-26000	-27.4	307	1647	244	x
3-1.5-H2	1.45	18200	-24200	-26.5	295	1637	236	x
3-1.5-H3	1.24	24100	-22700	-27.0	271	1632	220	150

TABLE X (Continued)

Run Number	Maximum Velocity, V_m (ft./sec.)	Q Based on CMC Sol. T (Btu/hr.)	Q Based on Water T (Btu/hr.)	Log Mean Delta T ($^{\circ}$ F)	Overall Heat Transfer Coefficient (Btu/hr. ft. ² $^{\circ}$ F)	Water Heat Transfer Coefficient (Btu/hr. ft. ² $^{\circ}$ F)	CMC Solution Heat Transfer Coefficient (Btu/hr. ft. ² $^{\circ}$ F)	Tube Bank Pressure Drop (lb. _f /ft. ²)
3-1.5-H4	0.893	21900	-22500	-28.5	255	1639	210	119
3-1.5-H5	0.331	13200	-16300	-32.8	161	1645	142	x
3-1.5-H6	1.36	xx	-25700	-34.1	244	1653	202	121
3-1.5-H7	0.330	11000	-16900	-32.5	168	1628	147	42.3
3-1.5-H8	0.633	14100	-22100	-31.4	227	1649	191	61.8
3-1.5-H9	0.477	13000	-22100	-31.0	230	1665	193	67.5
3-1.5-H10	0.328	13000	-21200	-36.6	187	1685	162	51.3
3-1.5-H11	0.328	11900	-25000	-37.8	213	1483	158	53.5
3-1.5-H12	0.831	12900	-32700	-35.7	296	1328	226	103
2-1.0-H1	0.501	18300	-18700	-36.5	175	1641	152	x
2-1.0-H2	1.44	24500	-22600	-32.6	236	1640	197	57.8
2-1.0-H3	0.499	20300	-20800	-39.7	178	1641	155	20.2
2-1.0-H4	1.87	27500	-28500	-33.8	287	1638	231	59.9
2-1.0-H5	0.957	25600	-27000	-40.0	230	1649	193	27.2
2-1.0-H6	1.62	25400	-30600	-35.9	290	1638	232	42.5
2-1.0-H7	0.497	19600	-26000	-46.1	192	1655	165	16.6
2-1.0-C1	1.10	-12300	19500	29.6	224	1395	183	31.4

TABLE X (Continued)

Run Number	Maximum Velocity, V_m (ft./sec.)	Q Based on CMC Sol. T (Btu/hr.)	Q Based on Water T (Btu/hr.)	Log Mean Delta T ($^{\circ}F$)	Overall Heat Transfer Coefficient (Btu/hr. ft. ² $^{\circ}F$)	Water Heat Transfer Coefficient (Btu/hr. ft. ² $^{\circ}F$)	CMC Solution Heat Transfer Coefficient (Btu/hr. ft. ² $^{\circ}F$)	Tube Bank Pressure Drop (lb. _f /ft. ²)
2-1.0-C2	0.489	-10200	15400	32.7	160	1396	138	15.5
2-1.0-C3	1.58	-11200	19200	25.3	258	1407	206	42.8
2-1.0-C4	1.91	-16000	27000	31.5	292	1402	227	47.9
2-1.0-C5	0.840	-13100	20800	34.0	208	1410	173	17.2
2-1.0-C6	0.487	-9400	14600	29.7	167	1409	144	9.96
2-0.5-H1	0.497	19000	-26100	-48.3	184	1647	159	11.9
2-0.5-H2	0.957	22600	-31300	-44.6	239	1644	199	21.8
2-0.5-H3	1.30	24900	-33800	-43.4	265	1648	217	27.3
2-0.5-H4	1.56	26700	-37400	-43.2	294	1650	236	24.0
2-0.5-H5	2.05	30500	-41700	-41.5	341	1646	265	30.3
2-0.5-H6	0.490	20500	-29100	-52.5	188	1660	163	6.68
2-0.5-C1	0.478	-10500	16500	32.5	173	1393	147	5.18
2-1.0-H8	0.501	25500	-21300	-40.8	177	1642	154	31.0
2-1.0-H9	1.06	28700	-24200	-36.1	228	1636	191	54.8
2-1.0-H10	1.64	33200	-28700	-36.3	269	1651	219	66.6
2-1.0-H11	2.01	33200	-29200	-35.3	281	1649	228	75.4
2-1.0-H12	0.498	27600	-23800	-45.5	178	1658	155	21.3

TABLE X (Continued)

Run Number	Maximum Velocity, V_m (ft./sec.)	Q Based on CMC Sol. T (Btu/hr.)	Q Based on Water T (Btu/hr.)	Log Mean Delta T ($^{\circ}$ F)	Overall Heat Transfer Coefficient (Btu/hr. ft. ² $^{\circ}$ F)	Water Heat Transfer Coefficient (Btu/hr. ft. ² $^{\circ}$ F)	CMC Solution Heat Transfer Coefficient (Btu/hr. ft. ² $^{\circ}$ F)	Tube Bank Pressure Drop (lb. _f /ft. ²)
2-1.0-H13	0.336	26800	-24800	-48.2	175	1087	143	18.1
2-1.0-H14	0.337	26800	-23800	-48.1	168	1044	138	17.3
2-1.0-H15	0.566	29500	-27800	-46.4	204	1044	161	27.0
2-1.0-H16	0.976	33500	-31000	-45.3	233	1041	178	45.6
2-1.0-H17	1.30	32700	-30500	-40.2	258	1035	192	58.2
2-1.0-H18	0.553	29000	-26800	-45.8	199	1044	157	24.8
1-1.0-H1	0.463	42100	-41700	-48.6	258	1010	191	33.3
1-1.0-H2	0.755	42100	-41700	-45.3	276	1000	200	44.7
1-1.0-H3	1.14	44500	-43800	-43.7	301	1003	213	60.0
1-1.0-H4	1.58	47600	-46500	-44.8	312	1004	218	70.0
1-1.0-H5	1.96	50600	-49800	-45.7	327	1005	226	79.2
1-1.0-H6	1.31	48500	-48700	-47.9	306	1007	216	56.5
1-1.0-H7	0.842	47500	-47100	-50.7	279	1011	202	37.0
1-1.0-H8	0.462	44900	-44600	-54.4	246	1018	185	21.9
1-1.0-C1	0.451	-19300	20100	25.2	240	1392	194	17.5
1-1.0-C2	0.752	-21500	23400	26.1	269	1399	212	25.0
1-1.0-C3	1.16	-21500	25600	25.2	304	1402	234	37.5
1-1.0-C4	1.48	-22600	27400	25.6	322	1402	244	48.1

TABLE X (Concluded)

Run Number	Maximum Velocity, V_m (ft./sec.)	Q Based on CMC Sol. T (Btu/hr.)	Q Based on Water T (Btu/hr.)	Log Mean Delta T ($^{\circ}$ F)	Overall Heat Transfer Coefficient (Btu/hr. ft. ² $^{\circ}$ F)	Water Heat Transfer Coefficient (Btu/hr. ft. ² $^{\circ}$ F)	CMC Solution Heat Transfer Coefficient (Btu/hr. ft. ² $^{\circ}$ F)	Tube Bank Pressure Drop (lb. _f /ft. ²)
1-1.0-C5	1.81	-21800	27100	24.3	336	1399	252	56.9
1-1.0-C6	0.449	-20500	20800	27.3	228	1405	186	14.7
1-0.5-H1	0.461	43300	-41900	-48.7	258	1004	191	25.7
1-0.5-H2	0.732	48000	-47000	-49.2	287	1007	206	38.3
1-0.5-H3	1.13	49800	-47400	-46.2	308	1007	217	46.0
1-0.5-H4	1.50	52600	-49300	-46.3	320	1006	222	57.8
1-0.5-H5	1.78	52800	-49800	-45.9	326	1003	225	62.7
1-0.5-H6	0.454	44400	-44300	-53.3	249	1011	186	19.6
1-0.5-C1	0.446	-21400	21400	26.4	243	1404	196	10.7
1-0.5-C2	0.766	-22500	23100	25.0	277	1399	218	16.5
1-0.5-C3	1.10	-23000	24200	24.2	300	1401	231	23.7
1-0.5-C4	1.49	-23900	26000	23.7	330	1406	249	32.8
1-0.5-C5	1.80	-24300	26200	22.8	345	1408	258	38.8
1-0.5-C6	0.444	-23500	22800	29.4	233	1396	189	9.59

x - Pressure drop not measured due to manometer failure

xx - Temperature change not measured due to thermocouple failure

TABLE XI
RHEOLOGICAL PROPERTIES AND REYNOLDS NUMBERS FOR
HEAT TRANSFER RUNS

<u>Run Number</u>	<u>Average CMC Solution Temperature (°F)</u>	<u>Apparent Shear Rate (sec.⁻¹)</u>	<u>True Shear Rate (sec.⁻¹)</u>	<u>N Prime</u>	<u>Gamma ($\frac{\text{gm.} \cdot \text{sec.} \cdot \text{n}^{-2}}{\text{cm}}$)</u>	<u>Apparent Viscosity (Centipoise)</u>	<u>Modified Reynolds Number</u>
3-1.0-H1	111.8	81.4	87.9	0.758	1.49	85.1	10.8
3-1.0-H2	114.6	224	241	0.763	1.41	63.7	39.5
3-1.0-H3	110.6	82.3	89.0	0.757	1.51	85.5	10.8
3-1.0-H4	113.4	229	247	0.761	1.44	64.3	40.2
3-1.0-H5	114.8	358	386	0.763	1.40	56.8	70.9
3-1.0-H6	108.8	83.8	90.6	0.754	1.55	87.2	10.9
3-1.0-C1	110.3	348	368	0.815	0.854	42.4	91.8
3-1.0-C2	110.2	258	273	0.814	0.856	44.9	64.6
3-1.0-C3	109.5	178	188	0.813	0.868	48.6	41.3
3-1.0-C4	107.5	83.8	88.7	0.809	0.908	57.9	16.7
3-1.0-C5	107.0	353	375	0.807	0.921	44.4	89.8

TABLE XI (Continued)

Run Number	Average CMC Solution Temperature (°F)	Apparent Shear Rate (sec. ⁻¹)	True Shear Rate (sec. ⁻¹)	N Prime	Gamma ($\frac{\text{gm.} \cdot \text{sec.} \cdot \text{n}'^{-2}}{\text{cm}}$)	Apparent Viscosity (Centipoise)	Modified Reynolds Number
3-1.5-H1	127.0	440	509	0.615	6.26	134	36.7
3-1.5-H2	125.1	371	432	0.605	6.70	147	28.4
3-1.5-H3	123.0	318	370	0.603	6.89	160	22.5
3-1.5-H4	123.9	229	264	0.615	6.43	177	14.5
3-1.5-H5	121.0	84.6	98.0	0.613	6.80	273	3.47
3-1.5-H6	122.0	347	385	0.693	3.65	115	33.7
3-1.5-H7	116.0	84.4	94.3	0.681	4.18	197	4.80
3-1.5-H8	123.6	162	180	0.693	3.63	144	12.5
3-1.5-H9	127.8	122	139	0.642	5.75	217	6.22
3-1.5-H10	126.5	83.8	95.3	0.649	5.88	258	3.58
3-1.5-H11	126.2	83.9	95.1	0.651	5.88	259	3.66
3-1.5-H12	129.9	213	240	0.659	5.43	177	13.4
2-1.0-H1	115.2	128	140	0.722	1.34	61.9	23.2

TABLE XI (Continued)

Run Number	Average CMC Solution Temperature (°F)	Apparent Shear Rate (sec. ⁻¹)	True Shear Rate (sec. ⁻¹)	N Prime	Gamma ($\frac{\text{gm.-sec. n}^{-2}}{\text{cm}}$)	Apparent Viscosity (Centipoise)	Modified Reynolds Number
2-1.0-H2	118.8	369	397	0.765	1.08	43.9	96.2
2-1.0-H3	112.0	128	136	0.787	0.983	54.5	26.3
2-1.0-H4	117.1	479	510	0.794	0.875	35.7	142
2-1.0-H5	113.9	245	259	0.808	0.786	40.7	68.2
2-1.0-H6	114.9	416	438	0.826	0.697	35.0	134
2-1.0-H7	109.3	127	134	0.818	0.773	46.7	30.7
2-1.0-C1	116.3	281	295	0.841	0.604	34.2	93.7
2-1.0-C2	119.8	125	131	0.844	0.570	37.1	37.7
2-1.0-C3	114.9	404	423	0.839	0.617	32.9	138
2-1.0-C4	119.9	489	512	0.844	0.569	29.9	183
2-1.0-C5	124.4	215	222	0.880	0.444	29.9	79.6
2-1.0-C6	120.0	125	129	0.875	0.480	34.1	41.1
2-0.5-H1	105.1	127	134	0.821	0.393	24.0	59.8

TABLE XI (Continued)

<u>Run Number</u>	<u>Average CMC Solution Temperature (°F)</u>	<u>Apparent Shear Rate (sec.⁻¹)</u>	<u>True Shear Rate (sec.⁻¹)</u>	<u>N Prime</u>	<u>Gamma ($\frac{\text{gm.} \cdot \text{sec.} \cdot \text{n}'^{-2}}{\text{cm}}$)</u>	<u>Apparent Viscosity (Centipoise)</u>	<u>Modified Reynolds Number</u>
2-0.5-H2	107.8	245	258	0.826	0.373	20.6	133
2-0.5-H3	110.1	333	350	0.830	0.357	19.0	197
2-0.5-H4	111.0	399	417	0.849	0.323	17.9	252
2-0.5-H5	111.6	524	540	0.890	0.212	13.4	439
2-0.5-H6	104.1	125	130	0.885	0.235	17.1	82.5
2-0.5-C1	118.9	122	124	0.939	0.149	12.6	110
2-1.0-H8	111.1	128	140	0.726	1.77	82.5	17.5
2-1.0-H9	114.0	271	296	0.729	1.69	65.0	46.7
2-1.0-H10	118.3	420	454	0.754	1.26	47.4	98.8
2-1.0-H11	118.5	515	557	0.754	1.25	45.0	129
2-1.0-H12	110.7	128	138	0.745	1.42	70.0	30.6
2-1.0-H13	108.6	86.0	91.8	0.788	1.02	61.9	23.1
2-1.0-H14	108.4	86.3	92.4	0.779	1.05	62.3	23.2

TABLE XI (Continued)

Run Number	Average CMC Solution Temperature (°F)	Apparent Shear Rate (sec. ⁻¹)	True Shear Rate (sec. ⁻¹)	N Prime	Gamma ($\frac{\text{gm.-sec. n}^{\prime-2}}{\text{cm}}$)	Apparent Viscosity (Centipoise)	Modified Reynolds Number
2-1.0-H15	110.1	145	155	0.781	1.02	54.1	44.7
2-1.0-H16	110.1	250	267	0.781	1.02	48.1	85.5
2-1.0-H17	112.6	332	355	0.784	0.976	43.6	126
2-1.0-H18	110.4	141	151	0.781	1.01	54.2	43.5
1-1.0-H1	105.1	118	126	0.796	1.01	58.4	22.3
1-1.0-H2	103.9	193	206	0.794	1.04	53.9	40.4
1-1.0-H3	107.0	293	312	0.799	0.973	47.2	69.2
1-1.0-H4	106.6	406	428	0.818	0.791	38.6	118
1-1.0-H5	106.0	503	531	0.817	0.800	37.5	151
1-1.0-H6	104.8	336	355	0.815	0.818	41.0	92.2
1-1.0-H7	103.8	215	219	0.802	0.960	50.1	48.3
1-1.0-H8	102.6	118	126	0.801	0.985	57.6	22.9
1-1.0-C1	111.5	116	120	0.862	0.535	36.9	35.7

TABLE XI (Continued)

<u>Run Number</u>	<u>Average CMC Solution Temperature (°F)</u>	<u>Apparent Shear Rate (sec.⁻¹)</u>	<u>True Shear Rate (sec.⁻¹)</u>	<u>N Prime</u>	<u>Gamma $\left(\frac{\text{gm.-sec.}^{n'-2}}{\text{cm}}\right)$</u>	<u>Apparent Viscosity (Centipoise)</u>	<u>Modified Reynolds Number</u>
1-1.0-C2	113.8	193	200	0.865	0.510	33.2	65.5
1-1.0-C3	113.7	297	310	0.856	0.534	31.7	105
1-1.0-C4	113.9	380	396	0.856	0.532	30.5	139
1-1.0-C5	112.1	463	479	0.877	0.448	27.2	192
1-1.0-C6	116.7	115	119	0.883	0.409	29.9	42.6
1-0.5-H1	102.3	118	125	0.809	0.600	35.9	37.5
1-0.5-H2	103.3	187	204	0.737	1.11	48.4	43.4
1-0.5-H3	106.7	290	311	0.774	0.786	34.9	93.6
1-0.5-H4	105.7	385	413	0.772	0.800	33.1	131
1-0.5-H5	104.8	456	490	0.767	0.803	31.3	164
1-0.5-H6	100.9	116	125	0.761	0.864	45.6	28.6
1-0.5-C1	115.4	114	120	0.838	0.343	22.3	56.7
1-0.5-C2	112.9	196	206	0.835	0.359	21.2	104

TABLE XI (Concluded)

<u>Run Number</u>	<u>Average CMC Solution Temperature (°F)</u>	<u>Apparent Shear Rate (sec.⁻¹)</u>	<u>True Shear Rate (sec.⁻¹)</u>	<u>N Prime</u>	<u>Gamma ($\frac{\text{gm.} \cdot \text{sec.}^{n'-2}}{\text{cm}}$)</u>	<u>Apparent Viscosity (Centipoise)</u>	<u>Modified Reynolds Number</u>
1.0.5-C3	112.3	281	288	0.900	0.208	14.6	216
1-0.5-C4	113.4	380	391	0.901	0.205	14.0	303
1-0.5-C5	112.7	460	477	0.868	0.287	16.8	307
1-0.5-C6	116.6	114	118	0.874	0.267	19.1	66.3

TABLE XII

SEIDER-TATE NONISOTHERMAL CORRECTION FACTORS FOR
HEAT TRANSFER RUNS

Run Number	Wall Temperature (°F)	CMC Sol. Gamma at Wall Temperature $\left(\frac{\text{gm.} \cdot \text{sec.} \cdot n^{\prime-2}}{\text{cm}}\right) \gamma_w$	CMC Sol. Gamma at Average Temperature $\left(\frac{\text{gm.} \cdot \text{sec.} \cdot n^{\prime-2}}{\text{cm}}\right)$	$\left(\frac{\gamma_w}{\gamma}\right)^{0.14}$
3-1.0-H1	144.7	0.862	1.49	0.926
3-1.0-H2	143.8	0.875	1.41	0.936
3-1.0-H3	144.0	0.872	1.51	0.926
3-1.0-H4	142.2	0.897	1.44	0.936
3-1.0-H5	143.3	0.882	1.40	0.937
3-1.0-H6	142.0	0.899	1.55	0.926
3-1.0-C1	96.0	1.19	0.854	1.048
3-1.0-C2	96.1	1.19	0.856	1.047
3-1.0-C3	95.1	1.22	0.868	1.048
3-1.0-C4	93.6	1.26	0.908	1.047
3-1.0-C5	94.5	1.23	0.921	1.042

TABLE XII (Continued)

Run Number	Wall Temperature (°F)	CMC Sol. Gamma at Wall Temperature $(\frac{\text{gm.} \cdot \text{sec.} \cdot \text{n}^{-2}}{\text{cm}}) \gamma_w$	CMC Sol. Gamma at Average Temperature $(\frac{\text{gm.} \cdot \text{sec.} \cdot \text{n}^{-2}}{\text{cm}})$	$(\frac{\gamma_w}{\gamma})^{0.14}$
3-1.5-H1	148.8	4.62	6.26	0.958
3-1.5-H2	146.3	4.65	6.70	0.951
3-1.5-H3	145.0	4.56	6.89	0.944
3-1.5-H4	147.3	4.51	6.43	0.952
3-1.5-H5	149.9	3.93	6.80	0.926
3-1.5-H6	150.3	1.98	3.65	0.918
3-1.5-H7	144.4	2.24	4.18	0.916
3-1.5-H8	149.9	2.02	3.63	0.921
3-1.5-H9	153.9	3.43	5.75	0.930
3-1.5-H10	158.2	2.95	5.88	0.908
3-1.5-H11	157.8	3.05	5.88	0.912
3-1.5-H12	157.2	3.09	5.43	0.924
2-1.0-H1	147.0	0.798	1.34	0.930

TABLE XII (Continued)

Run Number	Wall Temperature (°F)	CMC Sol. Gamma at Wall Temperature $\left(\frac{\text{gm.-sec. } n^{l-2}}{\text{cm}}\right) \gamma_w$	CMC Sol. Gamma at Average Temperature $\left(\frac{\text{gm.-sec. } n^{l-2}}{\text{cm}}\right)$	$\left(\frac{\gamma_w}{\gamma}\right)^{0.14}$
2-1.0-H2	146.0	0.629	1.08	0.927
2-1.0-H3	146.4	0.588	0.983	0.931
2-1.0-H4	144.3	0.542	0.875	0.935
2-1.0-H5	147.4	0.399	0.786	0.909
2-1.0-H6	143.8	0.423	0.697	0.933
2-1.0-H7	149.0	0.389	0.773	0.908
2-1.0-C1	92.1	0.916	0.604	1.060
2-1.0-C2	91.7	0.923	0.570	1.070
2-1.0-C3	94.7	0.873	0.617	1.050
2-1.0-C4	95.5	0.861	0.569	1.060
2-1.0-C5	96.2	0.749	0.444	1.076
2-1.0-C6	94.5	0.775	0.480	1.069
2-0.5-H1	146.9	0.185	0.393	0.899

TABLE XII (Continued)

Run Number	Wall Temperature (°F)	CMC Sol. Gamma at Wall Temperature $\left(\frac{\text{gm.} \cdot \text{sec.} \cdot n^{1-2}}{\text{cm}}\right) \gamma_w$	CMC Sol. Gamma at Average Temperature $\left(\frac{\text{gm.} \cdot \text{sec.} \cdot n^{1-2}}{\text{cm}}\right)$	$\left(\frac{\gamma_w}{\gamma}\right)^{0.14}$
2-0.5-H2	144.9	0.191	0.373	0.910
2-0.5-H3	145.6	0.189	0.357	0.914
2-0.5-H4	145.6	0.205	0.323	0.849
2-0.5-H5	143.9	0.140	0.212	0.944
2-0.5-H6	149.5	0.131	0.235	0.921
2-0.5-C1	91.1	0.196	0.149	1.039
2-1.0-H8	146.6	1.03	1.77	0.927
2-1.0-H9	144.2	1.06	1.69	0.938
2-1.0-H10	147.9	0.808	1.26	0.940
2-1.0-H11	147.1	0.817	1.25	0.942
2-1.0-H12	150.3	0.781	1.42	0.920
2-1.0-H13	148.1	0.582	1.02	0.924
2-1.0-H14	147.7	0.536	1.05	0.910

TABLE XII (Continued)

Run Number	Wall Temperature (°F)	CMC Sol. Gamma at Wall Temperature $\left(\frac{\text{gm.} \cdot \text{sec.} \cdot n^{1-2}}{\text{cm}}\right) \gamma_w$	CMC Sol. Gamma at Average Temperature $\left(\frac{\text{gm.} \cdot \text{sec.} \cdot n^{1-2}}{\text{cm}}\right)$	$\left(\frac{\gamma_w}{\gamma}\right)^{0.14}$
2-1.0-H15	146.7	0.545	1.02	0.916
2-1.0-H16	144.7	0.562	1.02	0.920
2-1.0-H17	142.5	0.583	0.976	0.930
2-1.0-H18	146.7	0.544	1.01	0.917
1-1.0-H1	141.1	0.503	1.01	0.907
1-1.0-H2	136.7	0.545	1.04	0.914
1-1.0-H3	137.9	0.533	0.973	0.919
1-1.0-H4	138.0	0.454	0.791	0.925
1-1.0-H5	137.5	0.458	0.800	0.925
1-1.0-H6	138.5	0.450	0.818	0.920
1-1.0-H7	140.5	0.473	0.960	0.906
1-1.0-H8	143.4	0.449	0.985	0.896
1-1.0-C1	91.1	0.835	0.535	1.064

TABLE XII (Continued)

Run Number	Wall Temperature (°F)	CMC Sol. Gamma at Wall Temperature $(\frac{\text{gm.} \cdot \text{sec.} \cdot n^{\prime-2}}{\text{cm}}) \gamma_w$	CMC Sol. Gamma at Average Temperature $(\frac{\text{gm.} \cdot \text{sec.} \cdot n^{\prime-2}}{\text{cm}})$	$(\frac{\gamma_w}{\gamma})^{0.14}$
1-1.0-C2	93.1	0.798	0.510	1.065
1-1.0-C3	94.3	0.815	0.534	1.061
1-1.0-C4	94.5	0.811	0.532	1.061
1-1.0-C5	93.8	0.650	0.448	1.053
1-1.0-C6	94.4	0.642	0.409	1.065
1-0.5-H1	138.2	0.324	0.600	0.917
1-0.5-H2	138.6	0.619	1.11	0.922
1-0.5-H3	139.2	0.456	0.786	0.927
1-0.5-H4	137.9	0.465	0.800	0.927
1-0.5-H5	136.5	0.456	0.803	0.924
1-0.5-H6	140.7	0.425	0.864	0.905
1-0.5-C1	94.1	0.499	0.343	1.054
1-0.5-C2	93.2	0.507	0.359	1.050

TABLE XII (Concluded)

<u>Run Number</u>	<u>Wall Temperature (°F)</u>	<u>CMC Sol. Gamma at Wall Temperature ($\frac{\text{gm.} \cdot \text{sec.} \cdot \text{n}^{\text{t}-2}}{\text{cm}}$) γ_w</u>	<u>CMC Sol. Gamma at Average Temperature ($\frac{\text{gm.} \cdot \text{sec.} \cdot \text{n}^{\text{t}-2}}{\text{cm}}$)</u>	<u>$(\frac{\gamma_w}{\gamma})^{0.14}$</u>
1-0.5-C3	93.6	0.287	0.208	1.046
1-0.5-C4	95.3	0.278	0.205	1.044
1-0.5-C5	95.7	0.399	0.287	1.047
1-0.5-C6	92.7	0.423	0.267	1.067

TABLE XIII

CALCULATED DIMENSIONLESS GROUPS FOR HEAT TRANSFER RUNS

<u>Run Number</u>	$\left(\frac{3n' + 1}{4n'}\right)^{1/3}$	<u>Prandtl Number</u>	<u>j-Factor</u>	<u>Friction Factor</u>	<u>Modified Reynolds Number</u>
3-1.0-H1	1.026	560	0.133	5.65	10.8
3-1.0-H2	1.025	418	0.0544	1.55	39.5
3-1.0-H3	1.026	563	0.135	3.32	10.8
3-1.0-H4	1.026	422	0.0538	1.20	40.2
3-1.0-H5	1.025	372	0.0347	0.684	70.9
3-1.0-H6	1.026	576	0.139	3.66	10.9
3-1.0-C1	1.019	280	0.0383	0.543	91.8
3-1.0-C2	1.019	296	0.0501	0.721	64.6
3-1.0-C3	1.019	321	0.0714	1.04	41.3
3-1.0-C4	1.019	383	0.144	2.47	16.7
3-1.0-C5	1.019	294	0.0376	0.508	89.8
3-1.5-H1	1.050	866	0.0536	x	36.7
3-1.5-H2	1.052	952	0.0641	x	28.4

TABLE XIII (Continued)

<u>Run Number</u>	<u>$(\frac{3n' + 1}{4n'})^{1/3}$</u>	<u>Prandtl Number</u>	<u>j-Factor</u>	<u>Friction Factor</u>	<u>Modified Reynolds Number</u>
3-1.5-H3	1.052	1036	0.0730	2.06	22.5
3-1.5-H4	1.050	1148	0.105	3.14	14.5
3-1.5-H5	1.050	1774	0.250	x	3.47
3-1.5-H6	1.036	746	0.0496	1.44	33.7
3-1.5-H7	1.038	1291	0.218	8.50	4.81
3-1.5-H8	1.036	934	0.118	3.35	12.5
3-1.5-H9	1.044	1401	0.195	6.39	6.22
3-1.5-H10	1.043	1668	0.266	10.6	3.58
3-1.5-H11	1.043	1674	0.296	11.0	3.66
3-1.5-H12	1.041	1140	0.119	3.24	13.4
2-1.0-H1	1.031	405	0.0668	x	23.2
2-1.0-H2	1.025	287	0.0239	0.780	96.2
2-1.0-H3	1.022	358	0.0639	2.28	26.3
2-1.0-H4	1.021	247	0.0197	0.478	142

TABLE XIII (Continued)

<u>Run Number</u>	<u>$\left(\frac{3n' + 1}{4n'}\right)^{1/3}$</u>	<u>Prandtl Number</u>	<u>j-Factor</u>	<u>Friction Factor</u>	<u>Modified Reynolds Number</u>
2-1.0-H5	1.019	267	0.0331	0.852	68.2
2-1.0-H6	1.017	230	0.0222	0.450	134
2-1.0-H7	1.018	308	0.0608	1.92	30.7
2-1.0-C1	1.016	224	0.0284	0.637	93.7
2-1.0-C2	1.015	242	0.0526	1.58	37.7
2-1.0-C3	1.016	216	0.0221	0.428	138
2-1.0-C4	1.015	195	0.0186	0.322	183
2-1.0-C5	1.011	194	0.0332	0.592	79.6
2-1.0-C6	1.012	222	0.0514	1.02	41.5
2-0.5-H1	1.018	159	0.0377	1.40	59.8
2-0.5-H2	1.017	136	0.0222	0.681	133
2-0.5-H3	1.017	125	0.0170	0.459	197
2-0.5-H4	1.015	118	0.0150	0.274	252
2-0.5-H5	1.010	87.9	0.0107	0.200	439

TABLE XIII (Continued)

<u>Run Number</u>	$\left(\frac{3n' + 1}{4n'}\right)^{1/3}$	<u>Prandtl Number</u>	<u>i-Factor</u>	<u>Friction Factor</u>	<u>Modified Reynolds Number</u>
2-0.5-H6	1.011	114	0.0320	0.786	82.5
2-0.5-C1	1.005	82.2	0.0279	0.570	110
2-1.0-H8	1.030	544	0.0822	3.46	17.5
2-1.0-H9	1.030	426	0.0421	1.36	46.7
2-1.0-H10	1.026	310	0.0253	0.688	98.8
2-1.0-H11	1.026	294	0.0209	0.515	129
2-1.0-H12	1.028	461	0.0740	2.43	20.6
2-1.0-H13	1.022	409	0.0647	3.04	23.1
2-1.0-H14	1.023	412	0.0613	2.93	23.2
2-1.0-H15	1.023	357	0.0388	1.61	44.7
2-1.0-H16	1.023	317	0.0232	0.908	85.5
2-1.0-H17	1.022	287	0.0179	0.652	126
2-1.0-H18	1.023	357	0.0388	1.56	43.5
1-1.0-H1	1.021	388	0.0896	4.46	22.3

TABLE XIII (Continued)

<u>Run Number</u>	$\left(\frac{3n^2 + 1}{4n^2}\right)^{1/3}$	<u>Prandtl Number</u>	<u>j-Factor</u>	<u>Friction Factor</u>	<u>Modified Reynolds Number</u>
1-1.0-H2	1.021	358	0.0540	2.23	40.4
1-1.0-H3	1.020	313	0.0347	1.30	69.2
1-1.0-H4	1.018	256	0.0228	0.785	118
1-1.0-H5	1.018	248	0.0186	0.579	151
1-1.0-H6	1.019	272	0.0280	0.928	92.2
1-1.0-H7	1.020	333	0.0461	1.50	48.3
1-1.0-H8	1.020	383	0.0839	2.98	22.9
1-1.0-C1	1.013	243	0.0780	2.10	35.7
1-1.0-C2	1.013	218	0.0485	1.08	65.5
1-1.0-C3	1.014	208	0.0334	0.684	105
1-1.0-C4	1.014	200	0.0267	0.538	139
1-1.0-C5	1.012	179	0.0206	0.430	192
1-1.0-C6	1.011	196	0.0674	1.78	42.6
1-0.5-H1	1.019	239	0.0644	3.43	37.5

TABLE XIII (Concluded)

<u>Run Number</u>	<u>$\left(\frac{3n' + 1}{4n'}\right)^{1/3}$</u>	<u>Prandtl Number</u>	<u>j-Factor</u>	<u>Friction Factor</u>	<u>Modified Reynolds Number</u>
1-0.5-H2	1.029	321	0.0534	2.02	43.4
1-0.5-H3	1.024	231	0.0293	1.01	93.6
1-0.5-H4	1.024	220	0.0220	0.720	131
1-0.5-H5	1.025	208	0.0180	0.557	164
1-0.5-H6	1.025	304	0.0738	2.73	28.6
1-0.5-C1	1.016	146	0.0573	1.33	56.7
1-0.5-C2	1.016	139	0.0354	0.698	104
1-0.5-C3	1.010	95.8	0.0207	0.491	216
1-0.5-C4	1.009	91.8	0.0160	0.371	303
1-0.5-C5	1.012	111	0.0155	0.300	307
1-0.5-C6	1.012	125	0.0514	1.19	66.3

APPENDIX F

RAW DATA AND CALCULATED RESULTS
FOR ISOTHERMAL PRESSURE
DROP RUNS

TABLE XIV

RAW DATA FROM ISOTHERMAL PRESSURE DROP RUNS

<u>Run Number</u>	<u>Solution Flow Rate lb./hr.</u>	<u>CMC Solution Thermocouple (Millivolts)</u>	<u>Tube Bank Manometer Fluid</u>	<u>Tube Bank Manometer Differential (in.)</u>	<u>CMC Solution Orifice Differential (in.)</u>	<u>CMC Solution Sample Number</u>
3-1.0-I1	7470	2.524	CCl ₄	12.98	4.47	1
3-1.0-I2	13580	2.837	CCl ₄	20.28	15.55	1
3-1.0-I3	4930	2.282	CCl ₄	9.18	3.95	1
3-1.0-I4	2580	2.176	CCl ₄	5.30	0.81	1
3-1.0-I5	10750	2.658	CCl ₄	14.37	9.01	4
3-1.0-I6	7600	2.618	CCl ₄	10.25	4.73	4
3-1.0-I7	5030	2.553	CCl ₄	6.73	2.03	4
3-1.0-I8	2450	2.475	CCl ₄	3.69	0.94	4
3-1.0-I9	10690	2.632	CCl ₄	13.82	8.93	4
3-1.0-I10	2660	1.474	CCl ₄	6.25	0.87	5
3-1.0-I11	6720	1.474	CCl ₄	13.3	3.16	5
3-1.0-I12	9490	1.499	CCl ₄	17.56	6.02	5

TABLE XIV (Continued)

<u>Run Number</u>	<u>Solution Flow Rate lb./hr.</u>	<u>CMC Solution Thermocouple (Millivolts)</u>	<u>Tube Bank Manometer Fluid</u>	<u>Tube Bank Manometer Differential (in.)</u>	<u>CMC Solution Orifice Differential (in.)</u>	<u>CMC Solution Sample Number</u>
3-1.0-I13	11360	1.518	CCl ₄	20.81	9.36	5
3-1.0-I14	13050	1.565	CCl ₄	23.02	12.46	5
3-1.5-I1	2586	2.300	TBE	4.47	0.38	19
3-1.5-I2	10870	1.787	TBE	26.15	8.60	24
3-1.5-I3	5160	1.679	TBE	17.69	1.54	24
3-1.5-I4	9366	1.740	TBE	24.08	5.95	24
3-1.5-I5	2687	1.624	TBE	12.68	0.58	24
2-1.0-I1	7520	3.047	CCl ₄	18.75	3.90	26
2-1.0-I2	2600	2.719	CCl ₄	7.16	0.45	27
2-1.0-I3	7480	2.692	CCl ₄	18.30	3.86	27
2-1.0-I4	9743	2.878	CCl ₄	20.23	6.66	28
2-1.0-I5	4990	2.791	CCl ₄	9.42	1.95	29
2-1.0-I6	8470	2.860	CCl ₄	14.40	5.13	3031

TABLE XIV (Continued)

<u>Run Number</u>	<u>Solution Flow Rate lb./hr.</u>	<u>CMC Solution Thermocouple (Millivolts)</u>	<u>Tube Bank Manometer Fluid</u>	<u>Tube Bank Manometer Differential (in.)</u>	<u>CMC Solution Orifice Differential (in.)</u>	<u>CMC Solution Sample Number</u>
2-1.0-I7	2590	2.766	CCl ₄	4.75	0.42	3031
2-1.0-I8	5577	2.873	CCl ₄	8.43	2.2	3235
2-1.0-I9	8220	2.864	CCl ₄	12.66	4.66	3235
2-1.0-I10	9954	3.090	CCl ₄	13.83	7.25	3235
2-1.0-I11	4298	3.099	CCl ₄	5.61	1.29	3637
2-1.0-I12	2540	3.171	CCl ₄	3.25	0.50	3637
2-1.0-I13	2651	1.352	CCl ₄	7.60	0.54	38
2-1.0-I14	3784	1.318	CCl ₄	10.51	1.10	38
2-1.0-I15	5304	1.305	CCl ₄	13.97	2.11	38
2-1.0-I16	7247	1.328	CCl ₄	18.46	3.60	38
2-1.0-I17	10290	1.362	CCl ₄	25.49	7.54	38
2-1.0-I18	8572	1.356	CCl ₄	21.44	5.03	38
2-1.0-I19	2533	2.948	CCl ₄	3.31	0.57	38

TABLE XIV (Continued)

<u>Run Number</u>	<u>Solution Flow Rate lb./hr.</u>	<u>CMC Solution Thermocouple (Millivolts)</u>	<u>Tube Bank Manometer Fluid</u>	<u>Tube Bank Manometer Differential (in.)</u>	<u>CMC Solution Orifice Differential (in.)</u>	<u>CMC Solution Sample Number</u>
2-1.0-I20	10020	2.894	CCl ₄	14.04	7.23	38
2-0.5-I1	2598	2.418	CCl ₄	3.12	0.40	3941
2-0.5-I2	4789	2.422	CCl ₄	6.12	1.50	3941
2-0.5-I3	6780	2.511	CCl ₄	8.81	3.14	3941
2-0.5-I4	7901	2.612	CCl ₄	7.15	4.78	4413
2-0.5-I5	10530	2.607	CCl ₄	9.92	8.34	4413
2-0.5-I6	2557	2.428	CCl ₄	2.29	0.50	4413
2-1.0-I21	2557	2.440	CCl ₄	7.66	0.91	4850
1-1.0-I1	2730	1.078	CCl ₄	31.26	0.56	5712
1-1.0-I2	3890	0.897	CCl ₄	36.55	1.00	5712
1-1.0-I3	2620	2.337	CCl ₄	7.48	0.68	5865
1-1.0-I4	4315	2.313	CCl ₄	10.34	1.40	5865
1-1.0-I5	6301	2.457	CCl ₄	14.40	3.00	5865

TABLE XIV (Continued)

<u>Run Number</u>	<u>Solution Flow Rate lb./hr.</u>	<u>CMC Solution Thermocouple (Millivolts)</u>	<u>Tube Bank Manometer Fluid</u>	<u>Tube Bank Manometer Differential (in.)</u>	<u>CMC Solution Orifice Differential (in.)</u>	<u>CMC Solution Sample Number</u>
1-1.0-I6	8779	2.452	CCl ₄	19.01	5.78	5865
1-1.0-I7	7483	2.419	CCl ₄	16.06	4.26	5865
1-1.0-I8	4774	2.372	CCl ₄	10.35	1.96	5865
1-1.0-I9	2577	2.622	CCl ₄	4.43	0.78	6671
1-1.0-I10	4266	2.680	CCl ₄	6.76	1.50	6671
1-1.0-I11	6383	2.683	CCl ₄	9.70	3.20	6671
1-1.0-I12	8085	2.717	CCl ₄	12.56	5.06	6671
1-1.0-I13	10080	2.688	CCl ₄	15.80	7.48	6671
1-1.0-I14	2657	1.552	CCl ₄	6.96	0.76	72
1-1.0-I15	4920	1.553	CCl ₄	11.55	1.90	72
1-1.0-I16	7047	1.568	CCl ₄	16.12	3.66	72
1-1.0-I17	8772	1.610	CCl ₄	19.90	5.72	72
1-0.5-I1	2597	2.268	CCl ₄	4.78	0.56	7912

TABLE XIV (Continued)

<u>Run Number</u>	<u>Solution Flow Rate lb./hr.</u>	<u>CMC Solution Thermocouple (Millivolts)</u>	<u>Tube Bank Manometer Fluid</u>	<u>Tube Bank Manometer Differential (in.)</u>	<u>CMC Solution Orifice Differential (in.)</u>	<u>CMC Solution Sample Number</u>
1-0.5-I2	4583	2.339	CCl ₄	7.55	1.48	7912
1-0.5-I3	6580	2.426	CCl ₄	10.06	3.04	7935
1-0.5-I4	8458	2.432	CCl ₄	13.02	5.40	7935
1-0.5-I5	9960	2.428	CCl ₄	14.80	7.46	7935
1-0.5-I6	2522	2.739	CCl ₄	2.62	0.80	8613
1-0.5-I7	4168	2.644	CCl ₄	4.31	1.50	8613
1-0.5-I8	6235	2.701	CCl ₄	6.47	3.12	8613
1-0.5-I9	8265	2.679	CCl ₄	8.83	5.34	8645
1-0.5-I10	10150	2.678	CCl ₄	10.89	7.68	8645
1-0.5-I11	2587	1.555	CCl ₄	3.76	0.94	87
1-0.5-I12	4169	1.531	CCl ₄	5.95	1.58	87
1-0.5-I13	6283	1.527	CCl ₄	8.92	3.18	87
1-0.5-I14	2640	1.469	CCl ₄	4.13	0.96	87

TABLE XIV (Concluded)

<u>Run Number</u>	<u>Solution Flow Rate lb./hr.</u>	<u>CMC Solution Thermocouple (Millivolts)</u>	<u>Tube Bank Manometer Fluid</u>	<u>Tube Bank Manometer Differential (in.)</u>	<u>CMC Solution Orifice Differential (in.)</u>	<u>CMC Solution Sample Number</u>
1-0.5-I15	8555	1.528	CCl ₄	12.27	5.42	87
1-0.5-I16	10296	1.612	CCl ₄	14.56	7.96	87

TABLE XV

CALCULATED DATA FROM ISOTHERMAL PRESSURE DROP RUNS

<u>Run Number</u>	<u>Maximum Velocity, V_m (ft./sec.)</u>	<u>CMC Solution Temperature (°F)</u>	<u>Tube Bank Pressure Drop (lb._f/ft.²)</u>	<u>Friction Factor</u>
3-1.0-I1	0.952	106.8	39.8	0.879
3-1.0-I2	1.73	116.1	62.2	0.416
3-1.0-I3	0.627	99.7	28.1	1.43
3-1.0-I4	0.328	96.5	16.2	3.01
3-1.0-I5	1.37	110.8	44.1	0.469
3-1.0-I6	0.970	109.6	31.4	0.670
3-1.0-I7	0.641	107.7	20.6	1.01
3-1.0-I8	0.312	105.4	11.3	2.32
3-1.0-I9	1.36	110.0	42.4	0.457
3-1.0-I10	0.337	75.8	19.2	3.37
3-1.0-I11	0.851	75.8	40.8	1.12
3-1.0-I12	1.20	76.5	53.8	0.741

TABLE XV (Continued)

<u>Run Number</u>	<u>Maximum Velocity, V_m (ft./sec.)</u>	<u>CMC Solution Temperature (°F)</u>	<u>Tube Bank Pressure Drop (lb. f/ft.²)</u>	<u>Friction Factor</u>
3-1.0-II3	1.44	77.1	63.8	0.612
3-1.0-II4	1.66	78.4	70.6	0.513
3-1.5-I1	0.329	100.2	56.8	10.5
3-1.5-I2	1.38	85.0	267	2.80
3-1.5-I3	0.655	81.8	181	8.40
3-1.5-I4	1.19	83.6	246	3.47
3-1.5-I5	0.341	80.2	129	22.2
2-1.0-I1	1.45	122.1	57.5	0.718
2-1.0-I2	0.499	112.9	21.9	2.30
2-1.0-I3	1.44	112.2	56.1	0.709
2-1.0-I4	1.87	117.4	62.0	0.461
2-1.0-I5	0.960	120.0	28.9	0.819
2-1.0-I6	1.63	116.9	44.1	0.435
2-1.0-I7	0.498	114.3	14.6	1.54

TABLE XV (Continued)

<u>Run Number</u>	<u>Maximum Velocity, V_m (ft./sec.)</u>	<u>CMC Solution Temperature (°F)</u>	<u>Tube Bank Pressure Drop (lb._f/ft.²)</u>	<u>Friction Factor</u>
2-1.0-I8	1.07	117.2	25.8	0.587
2-1.0-I9	1.58	117.0	38.8	0.406
2-1.0-I10	1.92	123.3	43.4	0.302
2-1.0-I11	0.827	123.6	17.2	0.657
2-1.0-I12	0.489	125.6	9.96	1.09
2-1.0-I13	0.505	74.7	23.3	2.36
2-1.0-I14	0.721	73.7	32.2	1.60
2-1.0-I15	1.01	73.3	42.8	1.09
2-1.0-I16	1.38	74.0	56.6	0.768
2-1.0-I17	1.96	74.9	78.1	0.526
2-1.0-I18	1.63	74.8	65.7	0.638
2-1.0-I19	0.487	119.3	10.1	1.12
2-1.0-I20	1.93	117.8	43.0	0.302
2-0.5-I1	0.498	104.5	9.56	1.00

TABLE XV (Continued)

Run Number	Maximum Velocity, V_m (ft./sec.)	CMC Solution Temperature (°F)	Tube Bank Pressure Drop (lb. _f /ft. ²)	Friction Factor
2-0.5-I2	0.918	104.6	18.8	0.579
2-0.5-I3	1.30	107.1	27.0	0.416
2-0.5-I4	1.52	109.9	21.9	0.249
2-0.5-I5	2.02	109.8	30.4	0.194
2-0.5-I6	0.490	104.8	7.02	0.761
2-1.0-I21	0.490	105.1	23.5	2.54
1-1.0-I1	0.479	67.0	95.8	10.8
1-1.0-I2	0.682	61.9	112.0	6.23
1-1.0-I3	0.462	102.2	22.9	2.79
1-1.0-I4	0.759	101.6	31.7	1.73
1-1.0-I5	1.11	105.6	44.1	0.928
1-1.0-I6	1.55	105.5	58.3	0.631
1-1.0-I7	1.32	104.5	49.2	0.734
1-1.0-I8	0.843	103.2	31.7	1.16

TABLE XV (Continued)

<u>Run Number</u>	<u>Maximum Velocity, V_m (ft./sec.)</u>	<u>CMC Solution Temperature (°F)</u>	<u>Tube Bank Pressure Drop (lb._f/ft.²)</u>	<u>Friction Factor</u>
1-1.0-I9	0.455	110.2	13.6	1.71
1-1.0-I10	0.755	111.8	20.7	0.949
1-1.0-I11	1.13	111.9	29.7	0.608
1-1.0-I12	1.43	112.9	38.5	0.491
1-1.0-I13	1.78	112.1	48.4	0.398
1-1.0-I14	0.467	80.3	21.3	2.53
1-1.0-I15	0.865	80.3	21.3	2.53
1-1.0-I16	1.24	80.7	49.4	0.835
1-1.0-I17	1.54	81.9	61.0	0.665
1-0.5-I1	0.458	100.3	14.7	1.82
1-0.5-I2	0.808	102.3	23.1	0.921
1-0.5-I3	1.16	104.7	30.8	0.594
1-0.5-I4	1.49	104.9	39.9	0.466
1-0.5-I5	1.76	104.8	45.4	0.382

TABLE XV (Concluded)

<u>Run Number</u>	<u>Maximum Velocity, V_m (ft./sec.)</u>	<u>CMC Solution Temperature (°F)</u>	<u>Tube Bank Pressure Drop (lb._f/ft.²)</u>	<u>Friction Factor</u>
1-0.5-I6	0.446	113.5	8.03	1.05
1-0.5-I7	0.736	110.8	13.2	0.635
1-0.5-I8	1.10	112.4	19.8	0.425
1-0.5-I9	1.46	111.8	27.1	0.330
1-0.5-I10	1.80	111.8	33.4	0.270
1-0.5-I11	0.455	80.3	11.5	1.44
1-0.5-I12	0.733	79.7	18.2	0.880
1-0.5-I13	1.10	79.6	27.3	0.581
1-0.5-I14	0.464	77.9	12.7	1.52
1-0.5-I15	1.50	79.6	37.6	0.431
1-0.5-I16	1.81	81.9	44.6	0.353

TABLE XVI

RHEOLOGICAL PROPERTIES FOR ISOTHERMAL PRESSURE DROP RUNS

<u>Run Number</u>	<u>CMC Solution Temperature (°F)</u>	<u>Apparent Shear Rate (sec.⁻¹)</u>	<u>True Shear Rate (sec.⁻¹)</u>	<u>N Prime</u>	<u>Gamma n'⁻² ($\frac{\text{gm.} \cdot \text{sec.}}{\text{cm}}$)</u>	<u>Apparent Viscosity (Centipoise)</u>
3-1.0-I1	106.8	244	259	0.752	1.61	68.8
3-1.0-I2	116.1	443	469	0.764	1.37	53.3
3-1.0-I3	99.7	161	171	0.742	1.83	84.1
3-1.0-I4	96.5	84.1	89.5	0.737	1.93	84.1
3-1.0-I5	110.8	351	365	0.849	0.621	35.0
3-1.0-I6	109.6	248	258	0.846	0.638	37.6
3-1.0-I7	107.7	164	171	0.842	0.667	41.3
3-1.0-I8	105.4	80.0	83.2	0.836	0.704	48.3
3-1.0-I9	110.0	349	362	0.847	0.632	35.5
3-1.0-I10	75.8	86.3	89.0	0.761	1.52	112
3-1.0-I11	75.8	218	225	0.871	1.52	99.2
3-1.0-I12	76.5	308	318	0.872	1.50	93.8
3-1.0-I13	77.1	369	381	0.873	1.48	91.0

TABLE XVI (Continued)

<u>Run Number</u>	<u>CMC Solution Temperature (°F)</u>	<u>Apparent Shear Rate (sec.⁻¹)</u>	<u>True Shear Rate (sec.⁻¹)</u>	<u>N Prime</u>	<u>Gamma ($\frac{\text{gm.} \cdot \text{sec.} \cdot \text{n}^{\prime-2}}{\text{cm}}$)</u>	<u>Apparent Viscosity (Centipoise)</u>
3-1.0-I14	78.4	424	437	0.876	1.44	87.6
3-1.5-I1	100.2	84.3	92.1	0.619	6.09	248
3-1.5-I2	85.0	353	389	0.583	12.9	266
3-1.5-I3	81.8	168	185	0.574	13.9	379
3-1.5-I4	83.6	305	336	0.579	13.3	287
3-1.5-I5	80.2	87.3	96.3	0.570	14.4	514
2-1.0-I1	122.1	370	391	0.771	1.01	42.0
2-1.0-I2	112.9	128	135	0.788	1.28	53.8
2-1.0-I3	112.2	368	387	0.787	0.979	43.4
2-1.0-I4	117.4	480	504	0.795	0.871	37.6
2-1.0-I5	120.0	246	257	0.821	0.692	37.5
2-1.0-I6	116.9	417	434	0.829	0.673	34.2
2-1.0-I7	114.3	127	133	0.825	0.706	43.5
2-1.0-I8	117.2	275	286	0.842	0.595	33.9

TABLE XVI (Continued)

<u>Run Number</u>	<u>CMC Solution Temperature (°F)</u>	<u>Apparent Shear Rate (sec.⁻¹)</u>	<u>True Shear Rate (sec.⁻¹)</u>	<u>N Prime</u>	<u>Gamma ($\frac{\text{gm.} \cdot \text{sec.} \cdot \text{n}'^{-2}}{\text{cm}}$)</u>	<u>Apparent Viscosity (Centipoise)</u>
2-1.0-I9	117.0	405	421	0.841	0.597	32.0
2-1.0-I10	123.3	490	509	0.847	0.539	28.7
2-1.0-I11	123.6	212	218	0.879	0.450	30.3
2-1.0-I12	125.6	125	129	0.882	0.435	31.4
2-1.0-I13	74.7	129	134	0.862	0.771	52.6
2-1.0-I14	73.7	185	191	0.862	0.787	51.0
2-1.0-I15	73.3	259	268	0.861	0.793	49.0
2-1.0-I16	74.0	354	366	0.862	0.782	46.3
2-1.0-I17	74.9	502	519	0.862	0.767	43.4
2-1.0-I18	74.8	418	432	0.862	0.769	44.6
2-1.0-I19	119.3	125	128	0.894	0.327	25.2
2-1.0-I20	117.8	494	507	0.892	0.336	21.5
2-0.5-I1	104.5	128	133	0.820	0.398	24.2
2-0.5-I2	104.6	235	246	0.820	0.397	21.6

TABLE XVI (Continued)

<u>Run Number</u>	<u>CMC Solution Temperature (°F)</u>	<u>Apparent Shear Rate (sec.⁻¹)</u>	<u>True Shear Rate (sec.⁻¹)</u>	<u>N Prime</u>	<u>Gamma ($\frac{\text{gm.} \cdot \text{sec.}^{n'-2}}{\text{cm}}$)</u>	<u>Apparent Viscosity (Centipoise)</u>
2-0.5-I3	107.1	333	347	0.825	0.379	19.7
2-0.5-I4	109.9	388	396	0.889	0.217	14.1
2-0.5-I5	109.8	517	528	0.889	0.217	13.7
2-0.5-I6	104.8	126	128	0.886	0.233	17.0
2-1.0-I21	105.1	126	134	0.738	1.55	75.6
1-1.0-I1	67.0	123	132	0.680	3.31	138
1-1.0-I2	61.9	175	189	0.670	3.68	133
1-1.0-I3	102.2	118	122	0.869	0.509	35.7
1-1.0-I4	101.6	177	183	0.868	0.517	34.3
1-1.0-I5	105.6	285	294	0.874	0.473	30.2
1-1.0-I6	105.5	397	410	0.874	0.474	29.0
1-1.0-I7	104.5	338	349	0.872	0.484	30.0
1-1.0-I8	103.2	216	223	0.870	0.498	32.5
1-1.0-I9	110.2	117	120	0.890	0.388	28.9

TABLE XVI (Continued)

Run Number	CMC Solution Temperature (°F)	Apparent Shear Rate (sec. ⁻¹)	True Shear Rate (sec. ⁻¹)	N Prime	Gamma ($\frac{\text{gm.} \cdot \text{sec.} \cdot \text{n}^{\prime-2}}{\text{cm}}$)	Apparent Viscosity (Centipoise)
1-1.0-I10	111.8	193	198	0.893	0.375	26.6
1-1.0-I11	111.9	289	297	0.893	0.374	25.5
1-1.0-I12	112.9	366	376	0.894	0.367	24.5
1-1.0-I13	112.1	456	469	0.893	0.373	24.2
1-1.0-I14	80.3	120	124	0.866	0.641	44.6
1-1.0-I15	80.3	221	229	0.866	0.641	41.0
1-1.0-I16	80.7	317	328	0.867	0.634	38.8
1-1.0-I17	81.9	395	408	0.869	0.616	37.0
1-0.5-I1	100.3	117	123	0.810	0.503	30.2
1-0.5-I2	102.3	207	217	0.814	0.483	26.3
1-0.5-I3	104.7	298	313	0.798	0.540	26.0
1-0.5-I4	104.9	383	402	0.798	0.539	24.7
1-0.5-I5	104.8	450	473	0.798	0.540	23.9
1-0.5-I6	113.5	114	117	0.898	0.214	16.3

TABLE XVI (Concluded)

<u>Run Number</u>	<u>CMC Solution Temperature (°F)</u>	<u>Apparent Shear Rate (sec.⁻¹)</u>	<u>True Shear Rate (sec.⁻¹)</u>	<u>N Prime</u>	<u>Gamma $\frac{\text{gm.-sec. } n'-2}{\text{cm}}$</u>	<u>Apparent Viscosity (Centipoise)</u>
1-0.5-I7	110.8	189	193	0.897	0.223	16.1
1-0.5-I8	112.4	282	290	0.898	0.217	15.1
1-0.5-I9	111.8	374	384	0.894	0.225	15.0
1-0.5-I10	111.8	460	472	0.894	0.225	14.7
1-0.5-I11	80.3	116	120	0.870	0.343	24.3
1-0.5-I12	79.7	188	194	0.870	0.349	23.1
1-0.5-I13	79.6	283	292	0.870	0.349	22.0
1-0.5-I14	77.9	119	123	0.868	0.363	25.4
1-0.5-I15	79.6	385	398	0.870	0.349	21.1
1-0.5-I16	81.9	463	478	0.872	0.331	19.7

TABLE XVII
 FRICTION FACTORS AND REYNOLDS NUMBERS FOR
 ISOTHERMAL PRESSURE DROP RUNS

<u>Run Number</u>	<u>Friction Factor</u>	<u>Modified Reynolds Number</u>
3-1.0-I1	0.879	39.8
3-1.0-I2	0.416	93.5
3-1.0-I3	1.43	21.5
3-1.0-I4	3.01	9.09
3-1.0-I5	0.469	113
3-1.0-I6	0.670	74.2
3-1.0-I7	1.01	44.6
3-1.0-I8	2.32	18.6
3-1.0-I9	0.457	111
3-1.0-I10	3.37	8.73
3-1.0-I11	1.12	24.9
3-1.0-I12	0.741	37.1
3-1.0-I13	0.612	45.8
3-1.0-I14	0.513	54.7
3-1.5-I1	10.5	3.82
3-1.5-I2	2.80	15.0
3-1.5-I3	8.40	5.00
3-1.5-I4	3.47	12.0
3-1.5-I5	22.2	1.92
2-1.0-I1	0.718	98.9
2-1.0-I2	2.30	26.7

TABLE XVII (Continued)

<u>Run Number</u>	<u>Friction Factor</u>	<u>Modified Reynolds Number</u>
2-1.0-I3	0.709	95.2
2-1.0-I4	0.461	143
2-1.0-I5	0.819	73.5
2-1.0-I6	0.435	137
2-1.0-I7	1.54	32.9
2-1.0-I8	0.587	90.7
2-1.0-I9	0.406	142
2-1.0-I10	0.302	192
2-1.0-I11	0.657	78.2
2-1.0-I12	1.09	44.7
2-1.0-I13	2.36	27.8
2-1.0-I14	1.60	41.0
2-1.0-I15	1.09	59.8
2-1.0-I16	0.768	86.3
2-1.0-I17	0.526	131
2-1.0-I18	0.638	106
2-1.0-I19	1.12	57.4
2-1.0-I20	0.302	257
2-0.5-I1	1.00	59.3
2-0.5-I2	0.579	122.2
2-0.5-I3	0.416	190
2-0.5-I4	0.249	310
2-0.5-I5	0.194	425

TABLE XVII (Continued)

<u>Run Number</u>	<u>Friction Factor</u>	<u>Modified Reynolds Number</u>
2-0.5-I6	0.761	83.1
2-1.0-I21	2.54	18.7
1-1.0-I1	10.8	10.1
1-1.0-I2	6.23	14.9
1-1.0-I3	2.79	37.3
1-1.0-I4	1.73	58.0
1-1.0-I5	0.928	106
1-1.0-I6	0.631	154
1-1.0-I7	0.734	127
1-1.0-I8	1.16	74.7
1-1.0-I9	1.71	45.3
1-1.0-I10	0.949	81.5
1-1.0-I11	0.608	127
1-1.0-I12	0.491	168
1-1.0-I13	0.398	212
1-1.0-I14	2.53	30.3
1-1.0-I15	1.23	61.0
1-1.0-I16	0.835	92.3
1-1.0-I17	0.665	121
1-0.5-I1	1.82	43.8
1-0.5-I2	0.921	88.5
1-0.5-I3	0.594	129
1-0.5-I4	0.466	174

TABLE XVII (Concluded)

<u>Run Number</u>	<u>Friction Factor</u>	<u>Modified Reynolds Number</u>
1-0.5-I5	0.382	212
1-0.5-I6	1.05	78.6
1-0.5-I7	0.635	132
1-0.5-I8	0.425	210
1-0.5-I9	0.330	280
1-0.5-I10	0.270	351
1-0.5-I11	1.44	54.2
1-0.5-I12	0.880	91.8
1-0.5-I13	0.581	146
1-0.5-I14	1.52	52.9
1-0.5-I15	0.431	206
1-0.5-I16	0.353	266

APPENDIX G
RHEOLOGICAL PROPERTIES
CALCULATED FROM FANN
VISCOMETER DATA

TABLE XVIII
 CMC SOLUTIONS' RHEOLOGICAL PROPERTIES FROM
 FANN VISCOMETER DATA

<u>CMC Solution Sample Number</u>	<u>Percent CMC</u>	<u>Temperature (°F)</u>	<u>N Prime</u>	<u>Gamma $\left(\frac{\text{gm.} \cdot \text{sec.} \cdot \text{n}^{-2}}{\text{cm}}\right)$</u>
1	1.0	94.7	0.738	1.99
1	1.0	109.0	0.752	1.56
1	1.0	133.4	0.792	1.03
2	1.0	99.8	0.796	1.07
2	1.0	113.2	0.814	0.827
2	1.0	134.1	0.869	0.501
3	1.0	103.0	0.803	0.928
3	1.0	119.0	0.860	0.595
3	1.0	134.0	0.836	0.536
4	1.0	96.3	0.814	0.874
4	1.0	112.0	0.850	0.604
5	1.0	72.0	0.865	0.672
5	1.0	79.7	0.881	0.558
5	1.0	84.3	0.881	0.518
5	1.0	89.0	0.894	0.453
12	1.5	125.0	0.614	6.42
12	1.5	132.8	0.619	5.81
12	1.5	139.7	0.632	5.20
13	1.5	141.0	0.631	5.06
13	1.5	136.9	0.620	5.51
13	1.5	130.9	0.616	5.98

TABLE XVIII (Continued)

<u>CMC Solution Sample Number</u>	<u>Percent CMC</u>	<u>Temperature (°F)</u>	<u>N Prime</u>	<u>Gamma ($\frac{\text{gm.} \cdot \text{sec.} \cdot n^{-2}}{\text{cm}}$)</u>
13	1.5	125.8	0.603	6.64
14	1.5	140.9	0.636	4.87
14	1.5	136.0	0.625	5.41
14	1.5	128.5	0.613	6.22
14	1.5	120.9	0.603	7.14
15	1.5	120.3	0.611	6.75
15	1.5	127.0	0.614	6.16
15	1.5	136.9	0.628	5.36
15	1.5	141.5	0.645	4.83
16	1.5	141.6	0.647	4.55
16	1.5	136.2	0.634	5.12
16	1.5	132.1	0.633	5.45
16	1.5	124.7	0.617	6.32
19	1.5	139.1	0.729	2.48
19	1.5	134.0	0.715	2.83
19	1.5	129.5	0.706	3.10
19	1.5	124.6	0.700	3.41
20	1.5	140.9	0.730	2.44
20	1.5	135.5	0.717	2.77
20	1.5	130.4	0.705	3.15
20	1.5	124.6	0.696	3.51
21	1.5	144.7	0.674	4.08
21	1.5	138.0	0.661	4.69

TABLE XVIII (Continued)

<u>CMC Solution Sample Number</u>	<u>Percent CMC</u>	<u>Temperature (°F)</u>	<u>N Prime</u>	<u>Gamma ($\frac{\text{gm.} \cdot \text{sec.} \cdot n'^{-2}}{\text{cm}}$)</u>
21	1.5	131.6	0.649	5.37
21	1.5	127.9	0.646	5.71
22	1.5	140.9	0.679	4.26
22	1.5	136.4	0.671	4.72
22	1.5	132.2	0.663	5.16
22	1.5	125.2	0.645	6.07
23	1.5	142.8	0.690	4.03
23	1.5	138.1	0.671	4.63
23	1.5	130.7	0.652	5.49
23	1.5	123.8	0.650	6.06
24	1.5	143.9	0.653	4.90
24	1.5	136.7	0.652	5.41
24	1.5	131.9	0.642	6.05
24	1.5	124.4	0.628	6.98
24	1.5	88.0	0.595	11.9
24	1.5	87.3	0.585	12.4
24	1.5	86.3	0.583	12.7
24	1.5	78.9	0.562	15.1
24	1.5	75.8	0.563	15.5
24	1.5	74.1	0.553	16.6
25	1.0	112.7	0.759	1.21
25	1.0	122.1	0.766	1.04
25	1.0	134.0	0.780	0.874

TABLE XVIII (Continued)

<u>CMC Solution Sample Number</u>	<u>Percent CMC</u>	<u>Temperature (°F)</u>	<u>N Prime</u>	<u>Gamma ($\frac{\text{gm.} \cdot \text{sec.} \cdot \text{n}'^{-2}}{\text{cm}}$)</u>
26	1.0	136.2	0.800	0.755
26	1.0	124.9	0.775	0.967
26	1.0	115.0	0.759	1.16
27	1.0	112.0	0.784	0.982
27	1.0	129.7	0.803	0.749
27	1.0	119.7	0.800	0.871
28	1.0	113.8	0.791	0.928
28	1.0	121.2	0.801	0.815
28	1.0	131.9	0.820	0.669
29	1.0	112.6	0.802	0.818
29	1.0	117.3	0.820	0.719
29	1.0	120.7	0.824	0.683
29	1.0	129.4	0.841	0.571
3031	1.0	108.9	0.812	0.808
3031	1.0	119.5	0.850	0.598
3031	1.0	129.6	0.846	0.547
3031	1.0	134.7	0.856	0.500
3234	1.0	92.1	0.824	0.892
3235	1.0	88.0	0.806	1.02
3235	1.0	102.8	0.834	0.738
3235	1.0	113.7	0.837	0.629
3235	1.0	120.5	0.839	0.574
3637	1.0	92.5	0.844	0.796

TABLE XVIII (Continued)

<u>CMC Solution Sample Number</u>	<u>Percent CMC</u>	<u>Temperature (°F)</u>	<u>N Prime</u>	<u>Gamma ($\frac{\text{gm.} \cdot \text{sec.} \cdot \text{n}^{-1} \cdot \text{cm}^{-2}}{\text{cm}}$)</u>
3637	1.0	107.3	0.852	0.623
3637	1.0	118.9	0.876	0.482
38	1.0	80.0	0.866	0.685
38	1.0	75.0	0.857	0.776
38	1.0	70.0	0.859	0.844
3941	0.5	106.5	0.823	0.384
3941	0.5	117.9	0.847	0.307
3941	0.5	130.3	0.867	0.247
42	0.5	110.3	0.862	0.308
42	0.5	119.9	0.833	0.310
42	0.5	130.0	0.849	0.256
42	0.5	137.5	0.869	0.217
4344	0.5	109.5	0.891	0.215
4344	0.5	118.0	0.886	0.200
4344	0.5	128.4	0.901	0.167
4413	0.5	111.7	0.915	0.0691
4413	0.5	108.0	0.915	0.0724
4413	0.5	103.8	0.921	0.0741
45	0.5	91.7	0.911	0.198
45	0.5	109.2	0.914	0.156
45	0.5	118.7	0.893	0.153
4647	1.0	110.1	0.722	1.80
4647	1.0	118.4	0.734	1.56

TABLE XVIII (Continued)

<u>CMC Solution Sample Number</u>	<u>Percent CMC</u>	<u>Temperature (°F)</u>	<u>N Prime</u>	<u>Gamma ($\frac{\text{gm.} \cdot \text{sec.} \cdot n'^{-2}}{\text{cm}}$)</u>
4647	1.0	131.0	0.745	1.30
4850	1.0	107.4	0.741	1.48
4850	1.0	115.8	0.746	1.33
4850	1.0	129.9	0.767	1.05
51	1.0	99.2	0.779	1.19
51	1.0	109.6	0.792	0.996
51	1.0	129.5	0.800	0.755
5256	1.0	130.7	0.804	0.711
5256	1.0	120.4	0.794	0.847
5256	1.0	98.0	0.768	1.28
5712	1.0	76.2	0.698	2.74
5712	1.0	70.2	0.687	3.07
5712	1.0	67.0	0.679	3.32
5860	1.0	137.3	0.848	0.538
5860	1.0	115.1	0.811	0.833
5860	1.0	105.9	0.798	0.991
5865	1.0	111.2	0.884	0.420
5865	1.0	105.3	0.876	0.473
5865	1.0	102.3	0.869	0.511
6163	1.0	105.1	0.817	0.810
6163	1.0	110.7	0.822	0.737
6163	1.0	133.6	0.853	0.488
6465	1.0	133.7	0.843	0.542

TABLE XVIII (Continued)

CMC Solution Sample Number	Percent CMC	Temperature (°F)	N Prime	Gamma $\left(\frac{\text{gm.} \cdot \text{sec.} \cdot \text{n}^{-2}}{\text{cm}}\right)$
6465	1.0	115.2	0.825	0.743
6465	1.0	107.7	0.806	0.893
6465	1.0	103.1	0.799	0.986
6667	1.0	110.7	0.861	0.541
6667	1.0	102.9	0.846	0.648
6667	1.0	93.0	0.831	0.798
6671	1.0	110.7	0.893	0.383
6671	1.0	107.0	0.886	0.417
6671	1.0	102.1	0.880	0.461
6869	1.0	113.0	0.856	0.542
6869	1.0	104.2	0.843	0.655
6869	1.0	94.2	0.825	0.817
7071	1.0	118.6	0.882	0.395
7071	1.0	107.6	0.872	0.487
7071	1.0	103.7	0.864	0.532
72	1.0	83.7	0.874	0.588
72	1.0	81.5	0.868	0.622
72	1.0	78.4	0.862	0.672
73	0.5	132.4	0.848	0.357
73	0.5	114.1	0.828	0.480
73	0.5	103.2	0.808	0.594
74	0.5	133.2	0.778	0.673
74	0.5	110.4	0.747	0.982

TABLE XVIII (Continued)

<u>CMC Solution Sample Number</u>	<u>Percent CMC</u>	<u>Temperature (°F)</u>	<u>N Prime</u>	<u>Gamma ($\frac{\text{gm.} \cdot \text{sec.} \cdot \text{n}^{-2}}{\text{cm}}$)</u>
74	0.5	102.9	0.738	1.11
7576	0.5	135.1	0.809	0.488
7576	0.5	112.9	0.784	0.698
7576	0.5	103.5	0.767	0.837
7778	0.5	133.8	0.811	0.477
7778	0.5	112.7	0.780	0.692
7778	0.5	103.2	0.765	0.828
7912	0.5	106.0	0.820	0.447
7912	0.5	104.0	0.815	0.468
7912	0.5	100.3	0.809	0.502
7935	0.5	107.3	0.802	0.514
7935	0.5	104.9	0.796	0.543
7935	0.5	101.3	0.794	0.572
8081	0.5	113.2	0.839	0.355
8081	0.5	105.2	0.826	0.413
8081	0.5	95.9	0.819	0.481
8283	0.5	113.2	0.900	0.205
8283	0.5	105.0	0.895	0.234
8283	0.5	93.5	0.883	0.288
8485	0.5	114.9	0.873	0.275
8485	0.5	105.5	0.858	0.330
8485	0.5	95.7	0.843	0.398
8613	0.5	115.7	0.896	0.209

TABLE XVIII (Concluded)

<u>CMC Solution Sample Number</u>	<u>Percent CMC</u>	<u>Temperature (°F)</u>	<u>N Prime</u>	<u>Gamma ($\frac{\text{gm.} \cdot \text{sec.} \cdot n'^{-2}}{\text{cm}}$)</u>
8613	0.5	110.8	0.901	0.218
8613	0.5	107.1	0.892	0.239
8645	0.5	115.8	0.898	0.210
8645	0.5	112.6	0.892	0.224
8645	0.5	107.8	0.891	0.240
87	0.5	84.0	0.880	0.315
87	0.5	80.0	0.870	0.349
87	0.5	77.0	0.868	0.368

TABLE XIX
REGRESSION COEFFICIENTS FOR CALCULATING GAMMA AND
N PRIME AS A FUNCTION OF TEMPERATURE

$$\log_e [\gamma \times 100] = \frac{AGAM}{T + 460} + BGAM$$

$$n' = CNP (T - 80.0) + DNP$$

CMC Solution Sample Number	<u>AGAM</u>	<u>BGAM</u>	<u>CNP</u>	<u>DNP</u>
1	5635.1	-4.8610	0.0014	0.714
2	7376.6	-8.4882	0.0022	0.748
3	5990.1	-6.1577	0.0011	0.792
4	7510.5	-9.0301	0.0023	0.778
5	5990.1	-6.1577	0.0016	0.878
12	4996.5	-2.0724	0.0012	0.559
13	6110.8	-3.9369	0.0017	0.528
14	6638.5	-4.8519	0.0016	0.534
15	5362.2	-2.7176	0.0016	0.545
16	6740.8	-5.0794	0.0017	0.543
19	7661.2	-7.2649	0.0020	0.609
20	7922.3	-7.6804	0.0021	0.601
21	7171.4	-5.8445	0.0017	0.561
22	7885.2	-7.0667	0.0022	0.547
23	7526.2	-6.4620	0.0021	0.554
24 (Low Temp.)	6540.0	-4.8360	0.0024	0.556
24 (High Temp.)	6494.7	-4.5703	0.0014	0.570

TABLE XIX (Continued)

<u>CMC Solution Sample Number</u>	<u>AGAM</u>	<u>BGAM</u>	<u>CNP</u>	<u>DNP</u>
25	5164.7	-4.2241	0.0010	0.726
26	7001.6	-7.4126	0.0019	0.691
27	5170.3	-4.4518	0.0010	0.755
28	6140.9	-6.1692	0.0016	0.735
29	7053.9	-7.9263	0.0022	0.733
3031	6007.0	-6.2040	0.0015	0.777
3235	5475.7	-5.4010	0.0009	0.808
3637	6032.1	-6.5289	0.0012	0.827
38	5955.3	-6.7932	0.0007	0.866
3941	6215.0	-7.3253	0.0018	0.776
42	4531.0	-4.4604	0.0004	0.837
4344	4433.8	-4.7040	0.0006	0.871
4413	2630.8	-2.6631	0.0007	0.937
45	3168.0	-2.7730	0.0005	0.920
4647	5271.4	-4.0574	0.0011	0.692
4850	5258.3	-4.2584	0.0012	0.708
51	4940.5	-4.0606	0.0007	0.768
5256	6295.5	-7.0538	0.0012	0.825
5712	5815.0	-5.2334	0.0020	0.706
5860	6593.9	-7.0510	0.0016	0.756
5865	6986.5	-8.4958	0.0016	0.833
6163	5986.7	-6.1957	0.0013	0.783
6465	6527.4	-7.0120	0.0014	0.769

TABLE XIX (Concluded)

<u>CMC Solution Sample Number</u>	<u>AGAM</u>	<u>BGAM</u>	<u>CNP</u>	<u>DNP</u>
6667	6894.3	-8.0846	0.0017	0.808
6671	6905.6	-8.4519	0.0014	0.848
6869	6921.0	-8.0852	0.0016	0.802
7071	6460.5	-7.4912	0.0013	0.835
72	7329.8	-9.4062	0.0023	0.865
73	5774.4	-6.1757	0.0014	0.778
74	5550.5	-5.1469	0.0013	0.707
7576	5688.6	-5.6742	0.0013	0.739
7778	6016.9	-6.2677	0.0015	0.730
7912	6474.1	-7.6366	0.0020	0.769
7935	5569.9	-5.8734	0.0014	0.763
8081	5588.4	-6.1755	0.0011	0.799
8283	5449.2	-6.4872	0.0009	0.871
8485	6149.7	-7.3809	0.0015	0.819
8613	5060.9	-5.7618	0.0004	0.885
8645	5339.2	-6.2229	0.0008	0.869
87	6568.6	-8.6203	0.0025	0.870

APPENDIX H

COMPUTER PROGRAMS FOR REDUCTION
OF HEAT TRANSFER, PRESSURE
DROP, AND FANN VISCOMETER
DATA

COMPUTER PROGRAM FOR REDUCTION OF
FANN VISCOMETER DATA

```

DIMENSION YY(10),XX(10),Y(10),X(10),XSQ(10),XY(10)
DIMENSION VV(10),GA(10)
DIMENSION TAU(10)
DIMENSION APVIS(10)
DIMENSION P(10),PP(10),PPP(10),SHR(10),SHRT(10)
402 FORMAT(//3X,5HSPEED,2X,10HDEFLECTION,3X,5HSHEAR,5X,5HSHEAR,
17X,1HK,6X,7HK PRIME,5X,5HGAMMA,4X,8HAPPARENT)
353 FORMAT(1X,45HLOG GAMMA VS. RECIP. ABS. TEMPERATURE-SAMPLE ,I4)
354 FORMAT(1X,34HN PRIME VS. T MINUS EIGHTY-SAMPLE ,I4)
350 FORMAT(2E14.8)
300 FORMAT(3I4,3F10.5)
301 FORMAT(2F10.5)
302 FORMAT(2F10.5)
400 FORMAT(1H1/8X,24HVISCOMETER DATA ANALYSIS)
401 FORMAT(//14X,13HSAMPLE NUMBER,I4)
405 FORMAT(1X,9HN PRIME =,F10.5)
406 FORMAT(1X,22HENTER NEXT SET OF DATA)
408 FORMAT(1X,7HGAMMA =,F10.5,5HPOISE)
403 FORMAT(23X,6HSTRESS,4X,4HRATE,33X,9HVISCOSITY)
410 FORMAT(//14X,13HTEMPERATURE =,F10.5)
404 FORMAT(7F10.4,F10.5)
455 FORMAT(1X,18HSPRING CONSTANT =,F10.5)
421 FORMAT(1X,25HRECIPROCAL TEMPERATURE =,F10.7)
420 FORMAT(1X,12HLOG GAMMA =,F10.5)
1 READ(5,300)K,M,N,ON,SPCON,T
  READ(5,302)RA,RB
  SUMX=0.0
  SUMY=0.0
  SUMXY=0.0
  SUMXS=0.0
  DO 2 I=1,N
    READ(5,301)YY(I),XX(I)
C   XX IS DEFLECTION. YY IS SPEED,RPM.
  2 CONTINUE
    DO 6 I=M,N
      Y(I)=ALOG(YY(I))
      X(I)=ALOG(XX(I))
      XSQ(I)=(X(I))**(2.0)
      XY(I)=(X(I))*(Y(I))
      SUMX=SUMX+X(I)
      SUMY=SUMY+Y(I)
      SUMXY=SUMXY+XY(I)

```

```

SUMXS=SUMXS+XSQ(I)
6 CONTINUE
DELTA=((ON)*(SUMXS))-((SUMX)**(2.0))
DEL=(1.0)/(DELTA)
DOG=((ON)*(SUMXY))-((SUMX)*(SUMY))
ENP=(DEL)*(DOG)
R=(2.0)/(ENP)
R1NP=(RA)**(R)
R2NP=(RB)**(R)
R2=(RA)**(2.0)
AA=(6.28)*(R2)*(3.8)
A=(SPCON)/(AA)
R3NP=(R2NP-R1NP)/(R2NP)
BB=(ENP)*(R3NP)*(30.0)
B=(BB)**(ENP)
C=(A)*(B)
SP=0.0
DO 3 I=1,N
P(I)=(C)*(YY(I))
PP(I)=((XX(I))*(6.28))**(ENP)
PPP(I)=(P(I))/(PP(I))
SHR(I)=(BB)/((XX(I))*(6.28))
SHRT(I)=(1.0)/(SHR(I))
3 CONTINUE
DO 7 I=M,N
SP=PPP(I)+SP
7 CONTINUE
SPAV=(SP)/(ON)
F=(3.0)*(ENP)
FF=(F)+(1.0)
FFF=(4.0)*(ENP)
FACT=(FF)/(FFF)
FAC=(FACT)**(ENP)
VIS=(SPAV)*(FAC)
V=(ENP)-(1.0)
VI=(8.0)**(V)
GAMMA=(VIS)*(VI)
DO 5 I=1,N
TAU(I)=(A)*(YY(I))
VV(I)=(PPP(I))*(FAC)
GA(I)=(VV(I))*(VI)
APVIS(I)=(TAU(II))/(SHRT(I))
5 CONTINUE
TABS=460.0+T
TT=T-80.0
RCIPT=(1.0)/(TABS)
GAM=ALOG((GAMMA)*(100.0))
WRITE(6,400)
WRITE(6,401)K
WRITE(6,410)T
WRITE(6,402)
WRITE(6,403)
WRITE(7,353)K

```

```
WRITE(7,350)GAM,RCIPT
WRITE(7,354)K
WRITE(7,350)ENP,TT
DO 4 I=1,N
WRITE(6,404)XX(I),YY(I),TAU(I),SHRT(I),PPP(I),VV(I),GA(I),
APVIS(I)
4 CONTINUE
WRITE(6,405)ENP
WRITE(6,408)GAMMA
WRITE(6,420)GAM
WRITE(6,421)RCIPT
WRITE(6,455)SPCON
WRITE(6,406)
GO TO 1
END
```

COMPUTER PROGRAM FOR REDUCTION OF
EXPERIMENTAL DATA

```
DIMENSION TMCE(10),TMCL(10),TMWL(10),TMWE(10),DMC(10),DMW(10)
DIMENSION DTC(10),DTW(10),TCE(10),TCL(10),TWE(10),TWL(10),TAV(10)
DIMENSION TWAX(10),QG(10),Q(10),QGW(10),QW(10),DETT(10),U(10)
DIMENSION UDEL(10),PRW(10),REW(10),THCON(10),HW(10),H(10),TW(10)
DIMENSION GAMMA(10),GAMWA(10),ENP(10),REMOD(10),GAMF(10),GMOD(10)
DIMENSION PRMOD(10),VISC(10),VISC(10)
DIMENSION DELFC(10),THKCM(10),VISCW(10),USELT(10)
DIMENSION FVISF(10)
100 FORMAT(2I4,F10.5)
101 FORMAT(2F10.3)
102 FORMAT(4F10.5)
103 FORMAT(4F10.5)
104 FORMAT(I2,4F10.5)
105 FORMAT(4F10.5)
106 FORMAT(F10.2)
107 FORMAT(4F10.6)
108 FORMAT(2F10.5,F10.7,F10.2,F10.5,F10.6)
109 FORMAT(F10.2,3F10.5)
110 FORMAT(I4,2F10.6,F10.3,F10.5)
111 FORMAT(6F10.5)
115 FORMAT(1X,2F10.6,F10.3,F10.5)
200 FORMAT(1H1/14X,33HNON-NEWTONIAN FLUID HEAT TRANSFER)
201 FORMAT(//25X,10HRUN NUMBER,I4)
202 FORMAT(//26X,8HRAW DATA)
203 FORMAT(//,1X,3HCMC,6X,3HCMC,7X,5HWATER,5X,5HWATER,5X,3HCMC,7X,
15HWATER)
204 FORMAT(1X,4HT IN,5X,5HT OUT,5X,4HT IN,6X,5HT OUT,5X,7HDELTA T,
3X,17HDELTA T)
205 FORMAT(6F10.5)
206 FORMAT(1H1)
207 FORMAT(/45X,27HNON-NEWTONIAN HEAT TRANSFER)
208 FORMAT(//45X,10HRUN NUMBER,I4)
209 FORMAT(//45X,12HMODEL NUMBER,I4)
210 FORMAT(//45X,15HCALCULATED DATA)
211 FORMAT(//1X,3HCMC,6X,3HCMC,7X,3HCMC,7X,5HWATER,5X,5HWATER,5X,
15HWATER)
212 FORMAT(1X,4HT IN,5X,5HT OUT,5X,5HT AVG,5X,4HT IN,6X,5HT OUT,5X,
15HT AVG)
213 FORMAT(6F10.4)
214 FORMAT(//1X,3HCMC,6X,5HWATER,5X,1HQ,9X,1HQ,9X,4HMEAN,6X,
7HVERALL)
215 FORMAT(1X,7HDELTA T,2X,7HDELTA T,3X,3HCMC,7X,5HWATER,5X,
7HDELTA T,13X,6HCOEFF.)
```

216 FORMAT(2F10.5,2F10.2,F10.5,F10.4)
 217 FORMAT(//1X,5HWATER,4X,5HWATER,5X,5HWATER,5X,3HCMC,7X,4HWALL)
 218 FORMAT(1X,7HPRANDTL,2X,8HREYNOLDS,2X,6HCOEFF.,4X,6HCOEFF.,4X,
 111HTEMPERATURE)
 219 FORMAT(F10.5,F10.2,F10.3,F10.4,F10.4)
 220 FORMAT(//1X,5HGAMMA,4X,5HGAMMA,5X,7HN PRIME,3X,5HGAMMA,5X,
 17HPRANDTL,3X,8HREYNOLDS,2X,1HJ)
 221 FORMAT(10X,4HWALL,16X,4HCORR,6X,6HNUMBER,4X,6HNUMBER,4X,6HFACTOR)
 222 FORMAT(2F10.4,2F10.5,F10.4,F10.5,F10.5)
 223 FORMAT(//1X,8HAPPARENT,1X,8HAPPARENT,2X,9HVISCOSITY)
 224 FORMAT(1X,6HVISCOS,3X,9HVISC-WALL,1X,4HCORR)
 225 FORMAT(3F10.5)
 226 FORMAT(1H1)
 227 FORMAT(//)
 249 FORMAT(//1X,5HWATER,5X,3HCMC,7X,5HDELTA,5X,3HCMC)
 250 FORMAT(1X,8HTH. CON.,1X,8HTH. CON.,2X,6HFACTOR,4X,7HNUSSELT)
 251 FORMAT(3F10.6,F10.5)
 228 FORMAT(5X,44HAVERAGE OVERALL HEAT TRANSFER COEFFICIENT = ,F10.3)
 229 FORMAT(5X,32HAVERAGE COEFFICIENT VARIATION = ,F10.5)
 230 FORMAT(5X,30HSHELL SIDE MAXIMUM VELOCITY = ,F10.5,2X,6HFT/SEC)
 234 FORMAT(5X,29HTUBE SIDE AVERAGE VELOCITY = ,F10.5,2X,6HFT/SEC)
 233 FORMAT(5X,23HTUBE WALL RESISTANCE = ,F11.8)
 231 FORMAT(5X,21HCMC MASS FLOW RATE = ,F10.3,2X,5HLB/HR)
 232 FORMAT(5X,20HCMC MASS VELOCITY = ,F10.2,2X,11HLB/HR-SQ FT)
 235 FORMAT(5X,19HCMC Q CORRECTION = ,F10.4,2X,6HBTU/HR)
 236 FORMAT(5X,21HWATER Q CORRECTION = ,F10.4,2X,6HBTU/HR)
 237 FORMAT(5X,22HAPPARENT SHEAR RATE = ,F10.4,2X,14HRECIPROCAL SEC)
 238 FORMAT(5X,22HTUBE BANK MANOMETER = ,F10.2,6HINCHES)
 239 FORMAT(5X,20HORIFICE MANOMETER = ,F10.2,6HINCHES)
 240 FORMAT(5X,18HWATER MANOMETER = ,F10.2,6HINCHES)
 241 FORMAT(5X,26HTUBE BANK PRESSURE DROP = F10.5,2X,8HLB/SQ FT)
 242 FORMAT(5X,18HFRICITION FACTOR = ,F10.5)
 243 FORMAT(5X,35HAVERAGE MODIFIED REYNOLDS NUMBER = ,F10.5)
 244 FORMAT(5X,28HAVERAGE MODIFIED J FACTOR = ,F10.6)
 247 FORMAT(5X,44HAVERAGE OUTSIDE HEAT TRANSFER COEFFICIENT = ,F10.5)
 248 FORMAT (5X,22HENTER NEXT SET OF DATA)
 260 FORMAT(5X,24HBASE TEMPERATURE = 110 F)
 261 FORMAT(5X,28HGAMMA AT BASE TEMPERATURE = ,F10.4)
 262 FORMAT(5X,30HN PRIME AT BASE TEMPERATURE = ,F7.4)
 263 FORMAT(5X,41HAPPARENT VISCOSITY AT BASE TEMPERATURE = ,F10.4,2X,
 110HCENTIPOISE)
 264 FORMAT(5X,18HTRUE SHEAR RATE = ,F10.4,2X,14HRECIPROCAL SEC)
 265 FORMAT(5X,26HCMC SOLUTION SAMPLE NUMBER,2X,I4)
 400 FORMAT(2F10.5,I4)
 C NR IS RUN NUMBER.N IS NUMBER OF POINTS.ON=N.O.
 C A=CMC Q CORR.QCW=WATER Q CORR.
 C TCA,TCB,TWA,TWB CONVERT EMF TO DELTA T.
 C TTCA,TTCB,TTWA,TTWB CONVERT EMF TO TEMPERATURE.
 C MN=MODEL NUMBER.AF=MIN. FLOW AREA.AH=SHELL H.T. AREA.
 C AFT=TUBE SIDE FLOW AREA.CNON=NO. OF CONTRACTIONS.
 C RHOMF=MANOMETER FLUID DENSITY.RHO=WATER DENSITY INSIDE TUBES.
 C RHO=CMC DENSITY.RHOMW=WATER DENSITY IN MANOMETER.
 C WW=WATER RATE , LB/HR.

```

C   TKCA,TKCB GIVE CMC K AS F(TEMP.).
C   TKWA,TKWA,TKWB GIVE WATER K AS F(TEMP.).
C   RA,RB,RC GIVE WATER (D) (RHO)/(MU)AS F(TEMP.).
C   PRA,PRB,PRC GIVE WATER PRANDTL NUMBERAS F(TEMP.).
C   WCMC=CMC FLOW RATE ,LB/HR.TBMAN=TUBE BANK MANOM. READ.
C   ORF=CMC ORIFICE MNOM.READ. WSMAN=WATER ORIFICE MANOM. READ.
C   AA,BBGIVE N PRIME AS F(T-80.0).
C   CVISA,CVISB GIVE LOG(GAMMA)AS F(U)/ABS.TEMP..
C   CVISA,CVISB GIVE LOG(GAMMA)AS F(1.0/ABS. TEMP.).
C   THCON(I) IS DIFFERENT FOR HEATING AND COOLING RUNS.
777 READ(5,100)NR,N,ON
    READ(5,101)A,QCW
    READ(5,102)TCA,TCB,TWA,TWB
    READ(5,103)TTCA,TTCB,TTWA,TTWB
    READ(5,104)MN,AF,AH,AFT,CNON
    READ(5,105)RHOMF,RHOW,RHO,RHOMW
    READ(5,106)WW
    READ(5,107)TKCA,TKCB,TKWA,TKWB
    READ(5,108)PRA,PRB,PRC,RA,RB,RC
    READ(5,109)WCMC,TBMAN,ORF,WSMAN
    READ(5,110)NS,AA,BB,CVISA,CVISB
    VCMC=(WCMC)/((AF)*(RHO)*(3600.0))
    GCMC=(VCMC)*(RHO)*(3600.0)
    GCMCC=(VCMC)*(RHO)
    WCMC2=(WCMC)**(2.0)
    SHRT=(VCMC)*(256.0)
    QC=A
    HT=0.0
    RETMD=0.0
    GTMD=0.0
    UT=0.0
    AVT=0.0
    ENPT=0.0
    DO 10 I=1,N
      READ(5,111)TMCE(I),TMCL(I),TMWE(I),TMWEL(I),DMC(I),DMW(I)
      DTC(I)=(TCA)*(DMC(I))+TCB
      DTW(I)=(TWA)*(DMW(I))+TWB
      TCE(I)=(TTCA)*(TMCE(I))+TTCB
      TCL(I)=TCE(I)+DTC(I)
      TWE(I)=(TTWA)*(TMWE(I))+TTWB
      TWL(I)=(TTWA)*(TMWL(I))+TTWB
      BUG=TWL(I)-TCE(I)-TWE(I)+TCL(I)
      BUM=ALOG((TWL(I)-TCE(I))/(TWE(I)-TCL(I)))
      DETT(I)=(BUG)/(BUM)
      TAV(I)=(0.5)*(TCE(I)+TCL(I))
      TWAV(I)=(0.5)*(TWE(I)+TWL(I))
      QG(I)=(WCMC)*(DTC(I))
      Q(I)=QG(I)-QC
      QGW(I)=(WW)*(DTW(I))
      QW(I)=QGW(I)-QCW
      U(I)=(QW(I))/(DETT(I)*(AH))
      U(I)=(U(I))*(-1.0)
      UT=UT+U(I)

```

```

10 CONTINUE
  UOAV=(UT)/(ON)
  UDELL=0.0
  DO 11 I=1,N
    UDEL(I)=ABS(UOAV-U(I))
    UDELL=UDELL+(UDEL(I))**(2.0)
11 CONTINUE
  SIGMA=((UDELL)**(0.5))/(ON)
  RTW=0.0000213
  VW=(VW)/((AFT)*(RHOW)*(3600.0))
  DO 12 I=1,N
    TWWAV=(TWAV(I))**(2.0)
    PRW(I)=PRA+(PRB)*(TWAV(I))+(PRC)*(TWWAV)
    RESUB=RA+(RB)*(TWAV(I))+(RC)*(TWWAV)
    REW(I)=(VW)*(RESUB)
    CON=(0.058)*(12.0)/(0.277)
    REX=(REW(I))**(0.700)
    PREX=(PRW(I))**(0.50)
    THCON(I)=TKWA+(TKWB)*(TWAV(I)-150.0)
    HW(I)=(THCON(I))*(REX)*(PREX)*(CON)
    R1=(1.0)/(U(I))
    R2=(1.354)/(HW(I))
    HOIN=R1+R2+RTW
    H(I)=(1.0)/(HOIN)
    HT=HT+H(I)
    RAT=(H(I))/(U(I))
    TW(I)=(TAV(I))+((RAT)*(DETT(I)))
    TWABS=(TW(I))+460.0
    RTAW=(1.0)/(TWABS)
    TABS=(TAV(I))+460.0
    RTAAV=(1.0)/(TABS)
    GAMMA(I)=EXP((CVISA)*(RTAAV)+CVISB)
    GAMWA(I)=EXP((CVISA)*(RTAW)+CVISB)
    TTAV=TAV(I)-80.0
    TTAVV=(TTAV)**(2.0)
    ENP(I)=(AA)*(TTAV)+BB
    ENPT=ENPT+ENP(I)
    DENP=(0.0312)**(ENP(I))
    TENP=2.0-ENP(I)
    TOENP=1.0-ENP(I)
    VCENP=(VCMC)**(TENP)
    ARE=(DENP)*(VCENP)*(RHO)
    DRE=(GAMMA(I))*(0.000672)
    REMOD(I)=(ARE)/(DRE)
    DELNU=(3.0)*(ENP(I))+1.0
    DELDE=(4.0)*(ENP(I))
    DEL=(DELNU)/(DELDE)
    DELFC(I)=(DEL)**(0.333)
    CCF=(H(I))/(DELFC(I))
    CCFF=(CCF)/(GCMC)
    THKCM(I)=TKCA+(TKCB)*(TAV(I)-110.0)
    P=(VCMC)*(12.0)/(0.375)
    PP=(P)**(ENP(I)-1.0)

```

```

PRMOD(I)=((2.42)*(GAMMA(I))*(PP))/(THKCM(I))
PRFFF=(PRMOD(I)**(0.667))
GARAT=(GAMWA(I))/(GAMMA(I))
GAMF(I)=(GARAT)**(0.14)
GMOD(I)=(CCFF)*(PRFFF)*(GAMF(I))
RETMD=RETMD+REMOD(I)
GTMD=GTMD+GMOD(I)
YY=(ENP(I))-1.0
Y=(8.0)**(YY)
CFEX=(DEL)**(ENP(I))
CK=(GAMMA(I))/((100.0)*(Y))
S=(SHRT)**(ENP(I))
VISC(I)=(CK)*(S)*(100.0)/(SHRT)
CKW=(GAMWA(I))/((100.0)*(Y))
VISCW(I)=(CKW)*(S)*(100.0)/(SHRT)
VISR=(VISCW(I))/(VISC(I))
RVISR=(1.0)/(VISR)
FVISF(I)=(RVISR)**(0.14)
AVT=AVT+FVISF(I)
VISCF(I)=(VISR)**(0.14)
USELT(I)=((H(I))*(0.0313))/(THKCM(I))
12 CONTINUE
HDAV=(HT)/(ON)
GMDAV=(GTMD)/(ON)
RMDAV=(RETMD)/(ON)
AV=(AVT)/(ON)
ENPAV=(ENPT)/(ON)
COW=((3.0)*(ENPAV)+1.0)/((4.0)*(ENPAV))
SHRTR=(COW)*(SHRT)
TWC=(1.0)/(RTW)
RTBAS=(1.0)/(570.0)
GGG=EXP((CVISA)*(RTBAS)+CVISB)
ENBAS=(AA*(30.0)+BB)
YYBAS=ENBAS-1.0
YBAS=(8.0)**(YYBAS)
SBAS=(SHRT)**(ENBAS)
CKBAS=(GGG)/((100.0)*(YBAS))
VIBAS=(CKBAS)*(SBAS)*(100.0)/(SHRT)
PD=(TBMAN)*(RHOMF-RHOMW)*(0.0833)
GGC=(10.0)**(8.0)
GC=(4.18)*(GGC)
PHH=(PD)*(RHO)*(GC)*(0.5)/(CNON)
PH=(PHH)/((GCMC)**(2.0))
PH=(PH)*(AV)
WRITE(6,200)
WRITE(6,201)NR
WRITE(6,202)
WRITE(6,203)
WRITE(6,204)
DO 14 I=1,N
WRITE(6,205)TMCE(I),TMCL(I),TMWE(I),TMWL(I),DMC(I),DMW(I)
14 CONTINUE
WRITE(6,100)NR,N,ON

```



```

WRITE(6,101)A,QCW
WRITE(6,102)TCA,TCB,TWA,TWB
WRITE(6,103)TTCA,TTCB,TTWA,TTWB
WRITE(6,104)MN,AF,AH,AFT,CNON
WRITE(6,105)RHOMF,RHOW,RHO,RHOMW
WRITE(6,106)WW
WRITE(6,107)TKCA,TKCB,TKWA,TKWB
WRITE(6,108)PRA,PRB,PRC,RA,RB,RC
WRITE(6,109)WCMC,TBMAN,ORF,WSMAN
WRITE(6,115)NS,AA,BB,CVISA,CVISB
WRITE(6,206)
WRITE(6,207)
WRITE(6,208)NR
WRITE(6,209)MN
WRITE(6,210)
WRITE(6,211)
WRITE(6,212)
DO 15 I=1,N
WRITE(6,213)TCE(I),TCL(I),TAV(I),TWE(I),TWL(I),TWAV(I)
15 CONTINUE
WRITE(6,214)
WRITE(6,215)
DO 16 I=1,N
WRITE(6,216)DTC(I),DTW(I),Q(I),QW(I),DETT(I),U(I)
16 CONTINUE
WRITE(6,217)
WRITE(6,218)
DO 17 I=1,N
WRITE(6,219)PRW(I),REW(I),HW(I),H(I),TW(I)
17 CONTINUE
WRITE(6,226)
WRITE(6,227)
WRITE(6,208)NR
WRITE(6,220)
WRITE(6,221)
DO 18 I=1,N
WRITE(6,222)GAMMA(I),GAMWA(I),ENP(I),GAMF(I),PRMOD(I),REMOD(I),
1GMOD(I)
18 CONTINUE
WRITE(6,223)
WRITE(6,224)
DO 19 I=1,N
WRITE(6,225)VISC(I),VISCW(I),VISCF(I)
19 CONTINUE
WRITE(6,249)
WRITE(6,250)
DO 20 I=1,N
WRITE(6,251)THCON(I),THKCM(I),DELFC(I),USELT(I)
20 CONTINUE
WRITE(6,231)WCMC
WRITE(6,230)VCMC
WRITE(6,232)GCMC
WRITE(6,237)SHRTR

```

```
WRITE(6,260)
WRITE(6,261)GGG
WRITE(6,265)NS
WRITE(6,262)ENBAS
WRITE(6,263)VIBAS
WRITE(6,234)VW
WRITE(6,235)QC
WRITE(6,236)QCW
WRITE(6,228)UDAV
WRITE(6,229)SIGMA
WRITE(6,233)RTW
WRITE(6,247)HOAV
WRITE(6,238)TBMAN
WRITE(6,239)ORF
WRITE(6,240)WSMAN
WRITE(6,241)PD
WRITE(6,242)PH
WRITE(6,243)RMDAV
WRITE(6,244)GMDAV
WRITE(6,248)
WRITE(7,400)GMDAV,RMDAV,NR
WRITE(7,400)GMDAV,RMDAV,NR
WRITE(7,400)PH,RMDAV,NR
WRITE(7,400)PH,RMDAV,NR
GO TO 777
END
```

VITA

Don Adams

Candidate for the Degree of

Doctor of Philosophy

Thesis: HEAT TRANSFER AND PRESSURE DROP FOR FLOW OF CARBOXYMETHYL-CELLULOSE (CMC) SOLUTIONS ACROSS IDEAL TUBE BANKS

Major Field: Chemical Engineering

Biographical:

Personal Data: Born in Oklahoma City, Oklahoma, April 2, 1940, to Walter D. and Florence Hereford.

Education: Attended first two years of grade school at Lincoln School in Oklahoma City, Oklahoma; completed grade school at Putnam City; graduated from Putnam City High School, Oklahoma City, Oklahoma, in 1958; received degree of Bachelor of Science in Chemical Engineering, May, 1962, from Oklahoma State University; received degree of Master of Science in Chemical Engineering, May, 1964, from Oklahoma State University; completed requirements for the Doctor of Philosophy degree in May, 1968.

Professional Experience: Employed by Humble Oil and Refining Company, Baytown, Texas, during the summer of 1961; employed by Phillips Petroleum Company, Bartlesville, Oklahoma, during the summers of 1962 and 1964; employed by Continental Oil Company, Ponca City, Oklahoma, during the summer of 1965; presently employed by Phillips Petroleum Company, Bartlesville, Oklahoma.

Professional Societies: Associate Member of the American Institute of Chemical Engineers.